EUROPEAN COMMISSION
Innovation and Networks Executive Agency

HORIZON 2020 PROGRAMME
RESEARCH and INNOVATION ACTION
Call Identifier: H2020-LCE-2016-RES-CCS-RIA
Competitive Low-Carbon Energy

GA No. 727600

Flexible Dimethyl ether production from biomass gasification with sorption enhanced processes

Starting date: 1st November 2016
Duration: 48 months

WP 2 – Deliverable D2.5:

Results of the sorption enhanced gasification in CSIC and USTUTT lab-scale testing

Dissemination level	PU Public CO Confidential, only for members of the consortium (including Commission Services)		PU
Written By	Isabel Martínez, M. Soledad Callén, Gemma Grasa, Jose Manuel López, Ramón Murillo (ICB-CSIC) Selina Hafner, Max Schmid (USTUTT)		
Due date	2019-07-31	***Issue date***	2019-07-30

Track changes

Version	DATE	Changes	CHECKED	APPROVED
V1	2019-07-30	First version released	ICB-CSIC, USTUTT	Isabel Martínez
V2	2019-09-13	Second version released (Summary abstract and conclusions modified)	ICB-CSIC, USTUTT	

WP lead institution: CSIC

Authors' contacts

Author name	Organisation	e-mail address
Isabel Martínez	ICB-CSIC	imartinez@icb.csic.es
M. Soledad Callén	ICB-CSIC	marisol@icb.csic.es
Gemma Grasa	ICB-CSIC	gga@icb.csic.es
Jose Manuel López	ICB-CSIC	jmlopez@icb.csic.es
Ramón Murillo	ICB-CSIC	ramon.murillo@csic.es
Selina Hafner	USTUTT	Selina.Hafner@ifk.uni-stuttgart.de
Max Schmid	USTUTT	Max.Schmid@ifk.uni-stuttgart.de

Contents

Executive summary

In this document, all the results and conclusions obtained in the sorption enhanced gasification (SEG) experiments performed at the 30 kW_{th} BFB reactor at ICB-CSIC and at the 20 kW_{th} DFB facility at USTUTT have been reported.

Concerning the 30 kW_{th} BFB reactor at ICB-CSIC, SEG performance has been evaluated for 6 different biomasses as feedstocks. Special attention has been paid to study the influence of the main operating variables of this SEG process in the syngas yield and syngas composition as well as in solids conversion, with the aim of determining the suitability of modifying each variable depending on the desired effect. Concretely, it has been studied the influence of the gasification temperature (between 630 and 740 ºC), the steam-to-biomass ratio (between 0.85 and 3), the sorbent-to-biomass ratio (CaO/C molar ratios between 0.20 and 1.22) and the activity of the CO_2 sorbent used (two different CO_2 sorbents with different textural properties and CO_2 carrying capacities). From this analysis, it has been concluded that:

- *Gasification temperature* has a great impact on the gas yield through char conversion, but also affects syngas composition. Depending on the reactivity of the biomass used, this variable would determine the M-module either by limiting the carbonation reaction and/or by improving char gasification reactions. Concerning light hydrocarbons content in the syngas and tar yield, both increase noticeably when reducing the temperature, affecting the gas conditioning for the subsequent synthesis process.
- *The steam-to-biomass (S/C) ratio* does not influence the permanent gas composition (i.e. the M-module), but affects the content of light hydrocarbons in the syngas (C_2-C_4) as well as tar yield. When increasing the S/C ratio, the content of C_4 hydrocarbons in the syngas diminishes, increasing the content of C_3H_6, C_3H_8, C_2H_4 and C_2H_6. Moreover, the increase of C_2H_4 in the syngas, which is known to be a precursor of aromatic rings formation, promotes tar formation.
- *The sorbent-to-biomass (CaO/C) ratio* influences mainly the C_3-C_4 hydrocarbons content and the tar yield (due to the catalytic effect of CaO towards tar cracking). Moreover, the CaO/C ratio influences the M-module since its variation affects the amount of CO_2 separated and the solid residence time of char particles, and therefore their conversion. Increasing too much the CaO/C ratio reduces significantly the solid residence time of char particles in the gasifier and their conversion, which could limit the M-module fulfilled.

Regarding the performance of the different biomass feedstocks evaluated, it has been possible to operate the facility with all of them without any remarkable problem. The only issue to be highlighted is that during the testing of straw pellets the fraction <1-2 mm collected from the overflow pipe contained (generally) larger char amount than the smaller fraction collected for the other biomasses. The main reason is that the straw pellets were fragile and most of them broke along the BFBR, being the cause of some segregation issues under certain conditions. Main differences observed between the different feedstocks have been linked to the reactivity of the char. For ECOH feedstocks and wood pellets/chips, char gasification kinetics were sufficiently fast as for not being the limiting factor of the M-module. Therefore, CO_2 capture determines the M-module reached for these biomasses. For reducing the M-module, CO_2 capture should be limited by raising the gasification temperature. Lignocellulosic biomasses (i.e. wood pellets and wood chips) resulted the most reactive and so needed a higher temperature to get the desired M-module around 2 through a limited CO_2 capture ratio by the equilibrium (i.e. around 715-720 ºC for wood-based biomass and higher for ECOH feedstock). Alternatively, CO_2 capture could be limited using a CO_2 sorbent with a lower CO_2 carrying capacity (as lime #1 in this document), which will allow reaching M-modules around 2 at a lower temperatures than using more reactive sorbents. On the other hand, straw resulted in the lowest M-modules reached. For this biomass, reactivity of the char was the limiting factor. Therefore, the M-module of 2 is a compromise between having sufficient char reactivity and limited CaO conversion. As seen during SEG testing with straw (section 1.2.5.2), temperature needed for reaching an M-module of 2 was around 700 ºC, slightly lower than for the rest of the biomasses.

Finally, in the 30 kW_{th} BFB reactor at ICB-CSIC combustion/calcination tests have been also performed with the objective of assessing the performance in terms of gas emissions and combustion and calcination efficiencies. Experiments using unconverted char as a fuel from two different biomass feedstocks (i.e. grape seeds and ECOH pellets) have been performed. For each fuel, a parametric study has been carried out comprising different fuel/sorbent ratios, different air excess ratios and different temperatures. Gas contaminants (i.e. NOx, SO_2, PAHs) were analyzed for the experiments performed, and solid samples were taken for characterization to calculate the calcination and combustion efficiencies reached. Char combustion efficiencies between 96.6 and 98.9 % were reached for temperatures ranging from 841 ºC and 894 ºC, respectively, using grape seeds char as fuel. Slightly lower char combustion efficiencies were calculated when using ECOH char as fuel, going from 95.5 to 96.1 % at temperatures around 840-850 ºC and different air excess ratios. Calcination of the carbonated solids that resulted from the SEG tests was fulfilled with an efficiency above 93 %. No SO_2 was detected in the flue gas in any of the combustion/calcination test performed, indicating that CaO resulting from $CaCO_3$ calcination is reacting with it to form $CaSO_4$. Regarding NOx emissions, they came from the N contained in the fuel since the combustion temperatures reached were not as high as for favoring thermal NOx, and therefore they depended mostly on the air/fuel ratio used. Finally, the emission of polycyclic aromatic hydrocarbons (PAHs) was also evaluated for these combustion/calcination tests. A maximum PAHs emission value was found at the intermediate temperature of 856 ºC (609 mg/Nm^3 dry gas) compared to the other temperatures of 841 and 894 ºC (397 and 379 mg/Nm^3 dry gas, respectively). This trend is linked to the combustion conditions and the fuel as already observed in the literature for coal combustion in a fluidized bed reactor at different combustion temperatures.

Concerning the experimental work performed in the 20 kW_{th} DFB facility at USTUTT, gasification pre-tests have been conducted using wood pellets and ECO biomass as feedstocks in order to reduce any risk of delay or additional costs when operating SEG tests at TRL-5 in the 200 kW_{th} pilot scale facility. This facility allows a coupled operation of a bubbling fluidized bed gasifier and a circulating fluidized bed as combustor/calciner, as well as a semi-batch operation of the bubbling fluidized bed reactor. Tests using wood pellets as fuel showed that the process can be operated stably in DFB mode and that the syngas composition can be adjusted flexibly by variation of the gasification temperature for fulfilling the requirements of the downstream DME synthesis process. Results achieved during the tests in the 20 kW_{th} electrically heated DFB facility are comparable to the results from first tests in the not electrically heated 200 kW_{th} pilot scale facility. This leads to the conclusion that the 20 kW_{th} facility is suitable for testing difficult novel fuels prior to their use in the 200 kW_{th} facility.

Semi-batch SEG tests have been successfully conducted in the bubbling fluidized bed reactor of the 20 kW_{th} DFB facility at USTUTT using ECO pellets as biomass. It was possible to operate the facility with ECO-pellets without mentionable problems. During the experiments M-modules between 12.6 and 0.8 were achieved for gasification temperatures between 604 and 754 ºC. This shows that an adjustment of the syngas composition is possible for SEG with ECO-pellets. Due to the outcome of the experiments with ECOH pellets at the 20 kW_{th} facility, it was expected that ECOH pellets are also suitable for gasification at larger scale. In the meantime this has been proven during pilot scale tests with ECOH pellets as fuel.

Finally, in order to validate the results obtained in both gasification facilities, the following table shows the results obtained for two biomass feedstocks tested at ICB-CSIC and USTUTT facilities (i.e. wood chips/pellets and ECOH pellets) under similar conditions of gasifier temperature (i.e. 705-

710 ºC). As appreciated for the woody feedstocks, syngas composition obtained at the ICB-CSIC facility was practically the same concerning permanent gases as in the USTUTT facility operated in dual mode, despite of the differences in the S/C ratio. As for ECOH pellets, this biomass was tested only in semi-batch mode at the 20 kWth DFB facility at USTUTT, which would explain the small differences observed for permanent gas content. Based on this validation table, it can be confirmed that operation under high CaO/C ratios in the BFBR at ICB-CSIC is needed when results obtained in terms of gas composition want to be extrapolated to the performance of a dual fluidized bed system with a high temperature combustor/calciner connected to the gasifier.

Biomass used	*Wood chips (ICB-CSIC) and wood pellets (USTUTT)*		*ECOH pellets*	
Facility	*30 kWth BFBR at ICB-CSIC*	*20 kWth DFB at USTUTT*	*30 kWth BFBR at ICB-CSIC*	*20 kWth at USTUTT (semi-batch)*
Gasifier bed temperature	710ºC	710ºC	707-711ºC	709ºC
S/C ratio	3	1.3	1.3	1.5
Syngas composition [% dry basis and without N_2]				
H_2	72.7-74.3	72.1	60-64	65.1*
CO	8-8.8	7.6	5.4-5.8	5.9*
CO_2	7.6-8.9	10.3	10-11	13.6*
CH_4	6.9-9.3	8.4	11-11.6	9.5*
CxHy	2.1-2.8	No data available	6.9-7.7	5.9*

*extrapolated data (no measurement data at 709 ºC available)

1 Experimental results at the 30 kW_{th} bubbling fluidized bed reactor (BFBR) at ICB-CSIC

1.1 Experimental section

1.1.1 Description of the ICB-CSIC facility

Sorption enhanced gasification (SEG) tests were carried out in the 30 kW_{th} (referred to the thermal input of biomass in LHV-basis) bubbling fluidized bed reactor (BFBR) shown in Figure 1. It consists of a 3 m height stainless steel reactor comprising two zones: a bottom dense zone of 1 m height (0.15 m of internal diameter) and a freeboard zone of 2 m height (0.20 m of ID). The reactor is externally heated through five electrical resistances and insulated with glass wool as shown in the plant scheme in Figure 2. Temperature and pressure distribution along the reactor are monitored through thermocouples and pressure transducers placed as shown in this figure. CO_2 sorbent and biomass are fed separately into the reactor from two independent closed hoppers. As indicated in the figure, these hoppers are placed over two screw feeders that introduce the solids at the bottom of the reactor (right above the gas distribution plate). Both feeders are provided with a regulation system that changes the rotation speed of the electric motor for regulating the mass flow rate. Biomass screw feeder is externally cooled with water in order to prevent its excessive heating due to conduction and so the prompt decomposition of the biomass in the screw. The CO_2 sorbent screw feeder was heated with a tracer up to 400 ºC and insulated with glass wool that allowed increasing the CO_2 sorbent flow rate to the reactor and so rising the CaO/C molar ratio fulfilled (as explained below). This modification was performed while finishing the experimental campaign with ECOH pellets and therefore not all the biomass feedstocks were tested under such high CO_2 sorbent flow rate conditions. Solids ($CaO/CaCO_3$, unconverted char and ashes) leave the reactor through a lateral overflow (shown schematically in the left-hand side of the reactor in Figure 2), and are collected in a hopper that is periodically discharged during operation. This overflow regulates the solid bed inventory in the bottom dense zone of the reactor, which resulted around 5-7 kg depending on the fluidization conditions.

Figure 1 Picture of the 30 kW_{th} BFB gasifier at ICB-CSIC

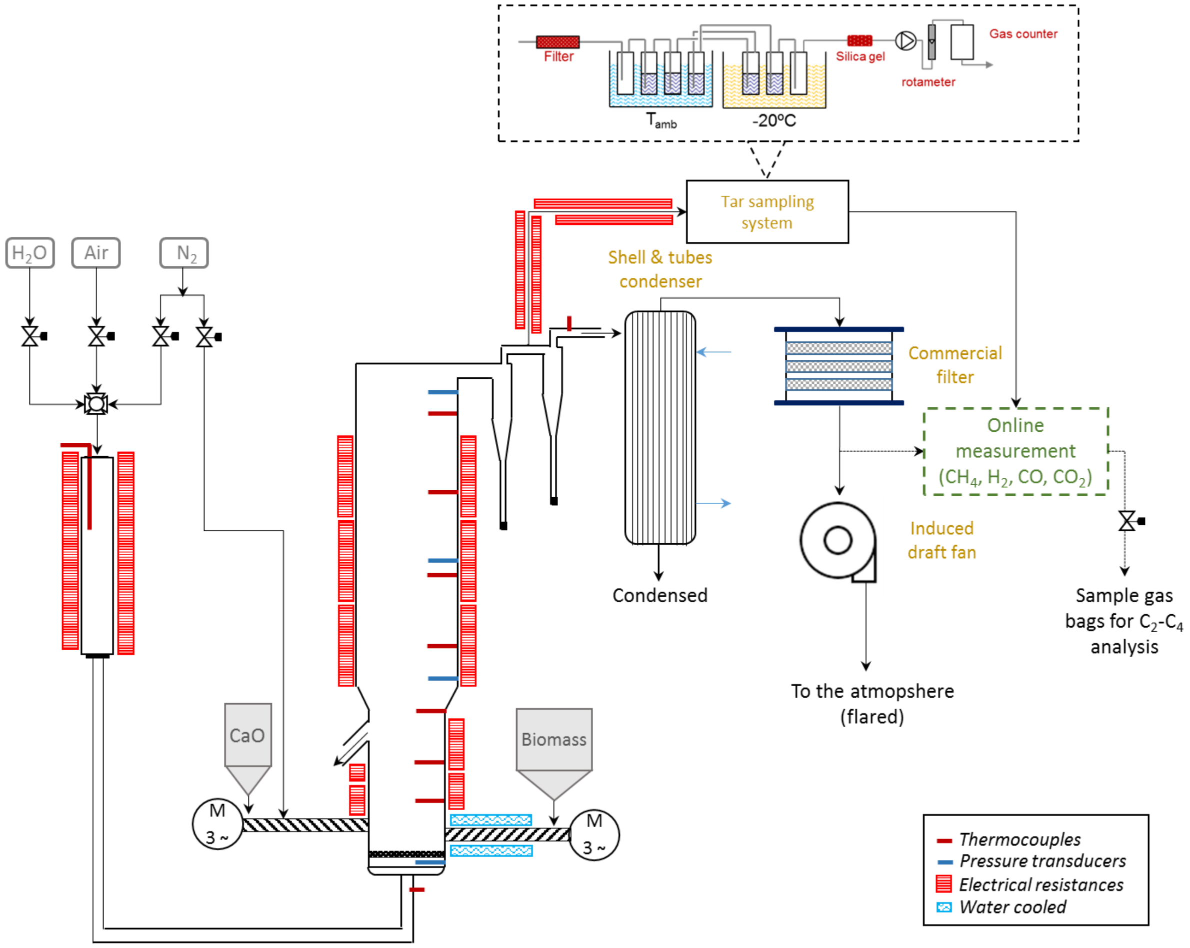

Figure 2 Scheme of the 30 kW_{th} gasification plant at ICB-CSIC (Horizontal red bars indicate the position of thermocouples throughout the main components of the plant)

The flow rate of steam or air fed to the reactor is controlled by means of the corresponding mass flow controllers. Liquid water contained in a pressurized process vessel passes through a tubular evaporator that is externally heated by an electric furnace, producing overheated steam at 160-180 ºC that is fed through the bottom of the reactor. A constant flow rate of N_2 is fed together with the water at the entrance of the evaporator in order to facilitate the flow of H_2O through the evaporation system as well as to serve as an internal standard for calculating the syngas flow rate at gasifier outlet. Moreover, a constant flow rate of N_2 is also fed into the reactor through the screw feeder of the CO_2 sorbent in order to avoid the backflow of rich-H_2O syngas through the sorbent hopper, which would cause operational problems due to the premature hydration of the CaO. Both N_2 flow rates account for 0.0120 Nm^3/min, which has been accounted for in the N balance solved for calculating the syngas yield obtained in the experiments.

Downstream the gasifier, two high efficiency cyclones are placed in order to separate entrained particles of CO_2 sorbent and unconverted char generated during the gasification process. Each cyclone is provided with a hopper where fine particles are accumulated and that can be purged during operation. After passing through the cyclones, syngas is cooled down to around 35 ºC in a shell and tubes condenser, where water at room temperature is used as coolant. Partially dried cooled syngas is then passed through a wet gas scrubber and a commercial dust filter, where fine particles not retained so far are separated. Right after the filter, the gas sampling line connected to the online gas analyser is placed. This sampling line contains a pump, a cooler and the gas analysis racks for determining CH_4, CO, CO_2, H_2 and O_2 concentrations in filtered syngas. Gasbags are also taken from this gas sampling line during steady state operation to be analyzed by gas chromatography, as explained in section 1.1.2.3. An induced drive fan is placed downstream the filter in order to push the syngas produced out of the reactor. Finally, syngas is burnt in a flare and sent out to the atmosphere through the stack.

1.1.2 Materials description and characterization

1.1.2.1 Feedstocks (biomasses and CO_2 sorbents)

Six different fuels have been fully characterized before being tested in the 30 kW_{th} BFBR explained before: A1 wood pellets, grape seeds, two different waste derived fuels delivered by Econward (ECOH pellets and ECOH biomass), straw and pine wood. Table 1 shows the ultimate and proximate analysis, as well as the calorific value of the different fuels tested. For determining the properties shown in this table, representative samples of each biomass were left to stabilize in air until constant weight before being analyzed. Ultimate analysis was determined in a Thermo Flash 111 (UNE-EN-5104) whereas moisture, volatile matter and ash contents were calculated according to standards UNE-EN 18134-3, UNE-EN 14775 and UNE-EN 15148, respectively. Detailed information about each characterization technique used for biomass analysis was detailed in a previous deliverable (i.e. *D2.1. Characterisation of raw materials for sorption enhanced gasification*).

Table 1. Proximate analysis, ultimate analysis and calorific value of the different biomasses tested in the 30 kW_{th} BFB gasifier at ICB-CSIC

PROXIMATE ANALYSIS						
%wt.	Wood pellets	GRAPE SEEDS	ECOH pellets	ECOH biomass	Straw pellets	Pine wood
% moisture	5.55	6.30	5.90	6.56	6.51	8.09
% ash	0.36	4.30	32.20	32.47	4.87	1.30
% volatile matter	78.80	65.12	55.40	53.63	70.28	72.94
% fixed carbon	15.29	24.28	6.60	7.34	18.33	17.67
ULTIMATE ANALYSIS						
% C	49.28	53.92	34.80	36.46	45.08	49.15
% H*	6.30	6.58	4.40	5.19	5.96	5.83
% N	0.10	2.20	1.70	1.36	0.70	0.14
% S**	0.02	0.12	0.66	0.21	0.13	0.05
% O	40.77	32.35	30.9	29.24	38.6	39.53
%Cl**	0.00	0.06	0.43	0.56	0.36	0.01
CALORIFIC VALUE						
HHV (MJ/kg)	19.05	22.07	13.80	14.74	17.37	18.05
LHV (MJ/kg)	17.59	20.51	12.84	13.47	16.06	16.69

**Includes H in the moisture*

***For wood pellets, pine wood, straw and ECOH pellets, this number was determined by ionic chromatography since this technique is able to determine low amounts of S and Cl in the samples*

Most of the biomass feedstocks were introduced in the BFBR in pellet form for the sake of facilitating their dosing through the screw feeders. Figure 3 shows a picture of each biomass feedstock as introduced in the BFBR. As noticed, grape seeds were introduced into the gasifier in their original seed form, corresponding to particles ranging between 4.5 mm and 6.8 mm. Regarding pine wood, it was received as wood chips and it was dried using a warm air flux at 140 ºC before being grinded to get the sawdust feedstock shown in Figure 3.

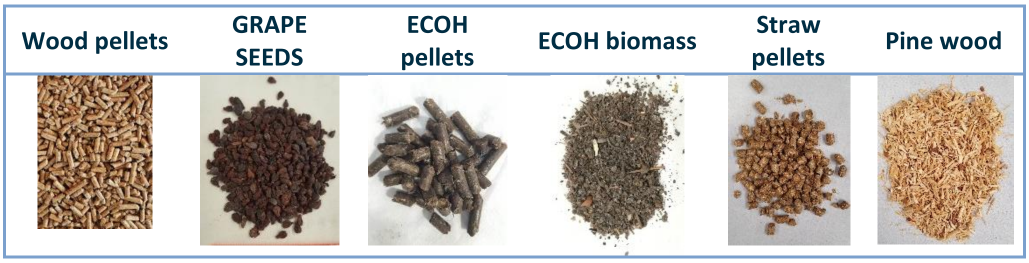

Figure 3 Pictures of each biomass feedstock tested in the 30 kW$_{th}$ BFB gasifier at ICB-CSIC

Ash composition was determined by ICP-OES, obtaining the results given in Table 2. One of the characteristics to be highlighted is the high content of Calcium and Silicon in the biomass ashes from ECOH feedstocks (68264 and 49910 for ECOH pellets and 52214 and 65222 for ECOH biomass), which were in the form of Ca_2SiO_4 as determined by X-ray diffraction (XRD). Moreover, also for these ECOH biomasses and the straw, the content of Potassium and Chlorine was significantly high (14265 and 4300 for ECOH pellets, 9515 and 5600 for ECOH biomass and 11834 and 3600 for straw pellets), which resulted in KCl in the collected solids.

Table 2 Ash chemical composition (in ppm, referred to 'as received' biomass, i.e. in kg of trace element/10^6 kg of biomass) of the different biomasses tested in the 30 kW$_{th}$ BFB gasifier at ICB-CSIC

TRACE ELEMENTS						
	Wood pellets	GRAPE SEEDS	ECOH pellets	ECOH biomass	Straw pellets	Pine wood
F (ppm)	n.d.	n.d.	58	n.d.	<10	n.d.
Al (ppm)	37	357	7696	9984	175	163
Ca (ppm)	741	8313	68264	52214	2805	3367
Fe (ppm)	43	313	4218	3248	131	119
K (ppm)	489	8639	14265	9515	11834	487
Mg (ppm)	136	781	7245	5033	1120	209
Mn (ppm)	37	54	290	164	10	10
Na (ppm)	15	86	8952	13393	40	41
P (ppm)	41	2094	3928	3046	614	60
Si (ppm)	135	1359	49910	65222	8523	782
Ti (ppm)	3	13	805	1129	10	10

Two different natural CaO based sorbents have been selected for the experimental testing in the BFBR at ICB-CSIC. These materials have been characterized and tested in an atmospheric TGA apparatus to determine their CO_2 carrying capacity. Table 3 shows the ICP- OES results those represent the % in weight of representative elements in the calcined sorbents. As it can be seen, the limestone 1 is a high purity material with more than 98 %wt. CaO after calcination. Minor impurities are Al_2O_3, SiO_2 and MgO. With respect to limestone 2, CaO represents 89.83 % wt. after calcination, and SiO_2 seems to be the mayor impurity from the calcined solid. The materials have been also texturally characterized, and their porosity, BET surface area and true density are compiled in Table 4. Comparing both materials, lime #1 presents slightly higher porosity and lower BET surface area than lime #2 and very similar true density. It is important to highlight that the values presented in Table 4, all fall in the typical range expected for CaO-based natural sorbents.

Table 3 Chemical composition of the two limestones used as CaO precursors for SEG tests in the 30 kW$_{th}$ BFB gasifier at ICB-CSIC

	Limestone 1	Limestone 2
% weight loss upon calcination	46.5	47.0
CaO (% wt in residue)	98.25	89.83
Al_2O_3 (% wt in residue)	0.145	0.143
Fe_2O_3 (% wt in residue)	0.002	0.100
K_2O (% wt in residue)	<0.001	0.145
MgO (% wt in residue)	0.183	0.779
Na_2O(% wt in residue)	<0.001	<0.001
SiO_2 (% wt in residue)	0.132	1.091

Table 4 Textural characterization of the calcined materials obtained from the limestones used for SEG tests in the 30 kW$_{th}$ BFB gasifier at ICB-CSIC

	Porosity	S_{BET} (m^2/g)	ρ_{true} (kg/m^3)	dp (μm)
Lime-1	0.52	8.8	3139	450
Lime-2	0.42	11.6	3202	277

The evolution of materials CO_2 carrying capacity with the number of reaction cycles has been assessed in an atmospheric TGA apparatus especially designed for high temperature multi-cycle testing [1]. The experimental cycles consisted of a calcination stage performed at 900 ºC in air (5 minutes stage) and a carbonation stage performed at 650 ºC in a 15 %vol. CO_2 in air for 15 minutes. Figure 4 shows the evolution of CO_2 carrying capacity of both calcined materials expressed as g CO_2/g calcined material. As it can be observed, the materials present the decay in CO_2 carrying capacity that is widely described in the literature when submitting natural CO_2 sorbents to multiple calcination/carbonation cycles. According to the data from TGA both limestones present a very similar behavior, being able to capture about 0.3 g CO_2/g calcined material at the 5th cycle.

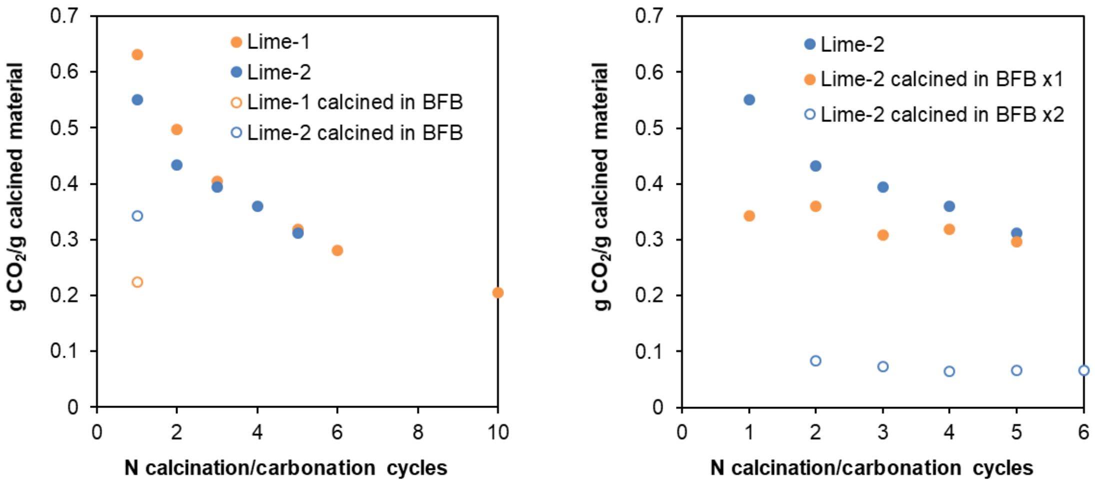

Figure 4 Evolution of calcined materials CO_2 carrying capacity expressed as g CO_2 reacted/g calcined material. (Left) Calcination/carbonation cycles performed in TGA to lime-1 and 2. Hollow symbols correspond to a carbonation step performed in TGA to materials calcined in the BFBR.(Right) TGA carbonation/calcination cycles performed to the fresh limestone-2 (bold blue series), to lime-2 from limestone-2 calcined once in bed (bold orange series) and lime-2 from limestone calcined in bed/carbonated in SEG/calcined in bed (hollow blue series).

To perform the SEG gasification tests, the original limestones 1 and 2 have gone through a calcination step that has been performed in the BFB reactor shown in Figure 1. $CaCO_3$ calcination is a highly endothermic reaction that is favored at high temperatures. In this way the combustion of 1 kg/h grape seeds with 0.12 Nm^3 air/min provided the energy required to reach the calcination temperature in the reactor, that was maintained between 875-900 ºC during the calcination process. As a result of the combustion process and the simultaneous $CaCO_3$ calcination, around 20 %vol. CO_2 (dry basis) was measured on the flue gas stream. Approximately 1 kg calcined sorbent/h was obtained through the bed overflow pipe. Several samples have been taken along the different calcination campaigns, and the calcination efficiency has been determined in muffle oven. It has been consistently observed that 95 %mol. of Ca were in CaO form from the overflow samples. It is well known that the calcination conditions (in terms of calcination temperature, time, calcination atmosphere) have an important impact on sorbent CO_2 carrying capacity. Therefore, several samples of 'in bed' calcined material have been sent to TGA to perform a CaO carbonation step (carbonation for 15 minutes at 650 ºC and 15 %vol. CO_2) to determine the active CaO content of the sorbent introduced during the SEG tests. The experimental data correspond to the hollow points introduced in Figure 4 (left). As it can be observed, the calcination of the limestones in bed has reduced significantly the CO_2 carrying capacity of the sorbents. Lime obtained from limestone-1 resulted in the most deactivated sorbent, being able of capturing about 0.2 g CO_2/g calcined material after one calcination in the reactor. Figure 4 (right) is focused on lime #2 (from calcination of Limestone-2) that has been widely used in the experimental campaigns reported in this deliverable. As it can be observed, the Limestone-2 calcination in bed reduces its CO_2 carrying capacity down to 0.34 g CO_2/g calcined material after one calcination, and the material CO_2 carrying capacity is slightly below 0.1 g CO_2/g calcined material after 2 consecutive cycles of calcination/gasification-carbonation/calcination in bed. Almost the totality of experiments with lime #2 have been performed with the material calcined once in the reactor, and it is specified when using the highly deactivated sorbent in some determined tests.

Different reasons can cause this drastic decay in sorbent CO_2 carrying capacity after being calcined in the reactor, mainly linked to sintering phenomena and/or presence of Sulphur in the sorbent in the form of $CaSO_4$ with higher molar volume than $CaCO_3$ [2]. As described above, grape seeds have been generally used during the calcination of the sorbents, and therefore part of the Sulphur in the fuel (see Table 1) can be retained by the sorbent during the calcination process. Also, the sorbent can capture part of the Sulphur released to the gas phase during the SEG tests, in this way the sorbent that has been reused in several calcination/SEG/calcination tests will be accumulating CaS (transformed to $CaSO_4$ during calcination) that can reduce its CO_2 carrying capacity. To determine the presence of S in the calcined sorbent samples of lime #2 calcined x1 and x2 in the BFBR have been submitted to XRD and ICP analyses. Also N_2 adsorption has been performed to lime #2 calcined in bed (BFBx1). A BET surface area of 4.7 m^2/g has been determined to this material indicating that sorbent calcination in bed has affected its textural properties and reduced its CO_2 carrying capacity with respect to that estimated trough TGA analysis. With respect to the S present in the calcined sorbent, although XRD analysis performed to the materials (BFBx1 and BFBx2) did not revealed the presence of $CaSO_4$, ICP revealed the presence of S in materials taken from the overflow pipe during SEG tests with grape seeds as biomass feedstock. This indicates that the materials those have undergone 2 calcinations in bed (BFBx2) may have up to 0.07 % wt. Sulphur (depending on CaO/C ratio among other variables). In principle, this might be the main reason together with the sintering occurred during calcination x1 BFB to the low CO_2 carrying capacity that has shown lime #2 BFBx2.

1.1.2.2 Solid samples from the BFBR

Solid samples have been taken from the solids collected through the overflow every 15 min during the steady-state period. Coarse particles (>1-2mm) corresponding to unconverted biomass particles are separated and their ultimate composition is determined using a Thermo Flash 111

(UNE-EN-5104), as done also for the biomass fed to the gasifier. Proximate composition (i.e. moisture, volatile matter and ash contents) of these coarse particles is also determined following the same procedures explained in section 1.1.2.1 and deliverable D2.1 for the biomass feedstocks. Smaller particles (<1-2mm) containing char, $CaCO_3$ and CaO are characterized as follows:

- X-ray diffraction (XRD) analysis is done in a Bruker D8 Advance diffractometer to determine the relative amount of the crystalline phases $CaO/CaCO_3$ and so determine the conversion of CaO into $CaCO_3$
- Scanning electron microscopy (SEM) coupled with EDS (Energy Dispersive X-rays spectroscopy) is used for determining the total amount of Ca in the solids that is complemented with XRD information for quantifying the mass fractions of CaO and $CaCO_3$ in the solid fraction <1-2 mm
- Ultimate analysis is done for calculating the total amount of carbon and so calculate the mass fraction of carbon corresponding to char particles.

Based on this information on solid samples characterization, biomass conversion in the gasifier (X_{OM}) is regarded as the conversion of the organic matter of the biomass (i.e. fixed carbon and volatile matter), and it is calculated for the different solid samples taken during the steady-state operation according to equation (1). Based on this expression, X_{OM} is calculated referred to the organic matter fed with the biomass into the gasifier during 15 min and the corresponding organic matter collected from the gasifier overflow in the same period. This organic matter is calculated as the fixed carbon and volatile matter contents of the coarse particles (i.e. >1-2mm) determined by proximate analysis, and the C content associated to the char fraction in the <1-2mm particles, which is determined by subtracting to the total organic carbon the carbon associated to the $CaCO_3$.

$$X_{OM} = \left(1 - \frac{m_{FC+VM,>2mm} + m_{C(char),<2mm}}{m_{FC+VM,biomass}}\right) \cdot 100 \qquad (1)$$

Fixed carbon conversion (X_{FC}) is also calculated according to equation (2), which is similar to X_{OM} but referred exclusively to the fixed carbon of the char contained in the different solid samples collected during the steady-state period. The fixed carbon content contained in the <1-2mm particles (i.e. $m_{FC(char)\,<2mm}$ in equation (2)) is calculated assuming that the char contained in these particles has the same fixed carbon and volatile matter contents as the coarse particles collected at the same time.

$$X_{FC} = \left(1 - \frac{m_{FC,>2mm} + m_{FC(char),<2mm}}{m_{FC,biomass}}\right) \cdot 100 \qquad (2)$$

Finally, solid residence time for the char particles in the BFB gasifier has been also estimated considering the inventory of char particles in the BFB gasifier (m_{char}) and the amount of fixed carbon and ashes fed into the reactor with the biomass, according to equation (3). For the inventory of char particles in the gasifier, it is assumed that the fraction of coarse particles collected from the overflow corresponds to the fraction of char particles within the gasifier, which is reasonable considering the low fraction of C from the char measured in the particles <1-2mm (i.e., below 3%wt. for all the tests included in this work).

$$\tau_{char} = \frac{m_{char}}{\dot{m}_{biomass} \cdot (y_{FC} + y_{ash})} \qquad (3)$$

1.1.2.3 Gas analysis

Permanent gases concentration (e.g. H_2, CH_4, CO and CO_2) during each gasification or combustion/calcination test has been measured online using a SICK GMS810 analyser placed downstream the condenser or downstream the tar sampling system as depicted in Figure 2. In addition to this continuous gas measurement, four sample bags (each one every 15 min) are collected during each gasification test. Subsequently, those bags are analyzed in order to determine the gas composition for permanent gases, light hydrocarbons and sulphur compounds. Permanent gases and light hydrocarbons (up to C_4) have been analyzed in a Varian CP-3800 gas chromatograph

(GC) equipped with both a TCD and a FID detector. Separation has been performed by using three SS packed columns (Molsieve 13X, HayeSep Q and HayeSep T) and a wide bore capillary column (HP Al/KCl). The oven programme used for this GC consisted of an initial oven temperature of 50 ºC, which was maintained for 7 min, and then a heating rate of 25 ºC/min to reach a final oven temperature of 140 ºC. This temperature was maintained for 1.4 min. The carrier gas was Ar at a constant column flow of 2 Nml/min. The injector, TCD and FID temperatures were 120 ºC, 175 ºC and 220 ºC, respectively. Permanent gases analyzed included H_2, CO_2, O_2, N_2 and CO whilst light hydrocarbons analyzed included methane, ethane, ethylene, propane, propylene, isobutane, n-butane, trans-2-butene, 1-butene, isobutene, cis-2-butene and 1,3-butadiene. Certificated gas mixtures (Air Products) were used for identification and quantification purposes. Figure 5 shows typical chromatograms obtained for permanent gases (top) and light hydrocarbons (bottom) respectively.

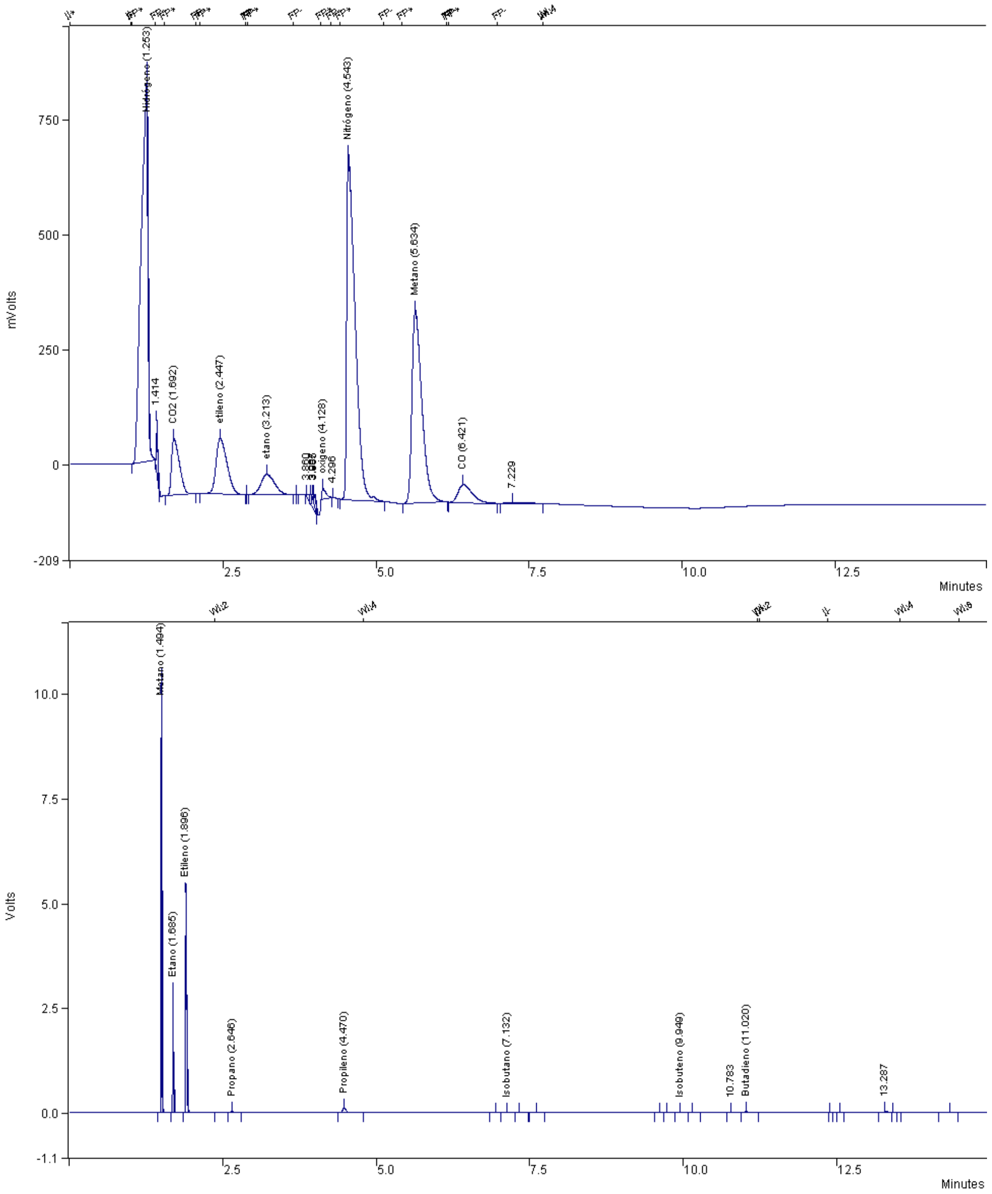

Figure 5 Examples of chromatograms obtained by GC for permanent gases (top) and light hydrocarbons (bottom) in a SEG experiment

Sulphur compounds have been analysed in a Perkin Elmer Clarus 590 gas chromatograph (GC) equipped with a FPD detector. Separation has been performed by using a 30 m Rt-Silica BOND capillary column. An initial oven temperature of 45 ºC was maintained for 4 min. Then, a heating rate of 15 ºC /min was implemented to reach a final oven temperature of 200 ºC. This temperature was maintained for 2 min. The carrier gas was N_2 at a constant column flow of 2 NmL/min. The injector and FPD temperatures were 250 ºC and 300 ºC, respectively. Sulphur compounds analysed included carbonyl sulphide (COS), hydrogen sulphide (H_2S), carbon disulphide (CS_2) and methyl mercaptan (CH_4S). Certificated gas mixtures (Air Products) were used for identification and quantification purposes.

1.1.2.4 Tar sampling

An off-line method for tar sampling is used based on the specific protocol for biomass gasification units described in [3]. This tar sampling method is based on absorbing tars by flowing the gas through a series of 7 impinger bottles filled with isopropanol, which are placed in two different cooling baths as shown in Figure 6: four impingers (1, 2, 3 and 5) at room temperature and three (4, 6 and 7) at -20 ºC. All of them contained 100 ml of isopropanol with the exception of impingers 1 and 7, which were empty. Gas flow rate sampled through the tar system is regulated by a pump and the total volume passed is measured by a gas-meter before sending the gas to the online analyser. In general, the sampling time was around 20 minutes, collecting gas volumes that varied among 0.06 and 0.147 Nm^3 of dry gas.

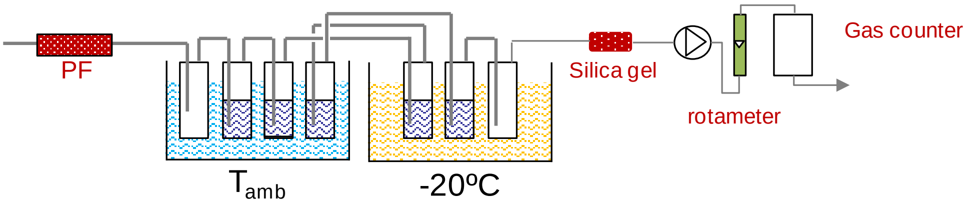

Figure 6 Scheme of the set-up for tar sampling placed at the ICB-CSIC BFB plant

Once finished the tar sampling test, the isopropanol from the impingers (Figure 7) was collected in an amber glass bottle, rinsing the impingers as well as the connection tubes with isopropanol, measuring the final volume collected. This was named as collected tar and the tar content was determined by GC-MS. In addition, from each sample, it was also determined the gravimetric tar. An aliquot of 100 mL of collected tar was concentrated by rotary evaporator (Figure 7) until dryness at controlled temperature and vacuum. Afterwards, the sample was kept in a desiccator for at least 12 hours and weighted in a microbalance of 0.1 mg precision. In this way, the gravimetric tar was determined according to the gas volume that has passed through the sampling system and expressed as g/Nm^3 dry gas. This gravimetric tar was then dissolved in 5 mL of 2-propanol for further injection in the GC-MS obtaining the gravimetric (GC-MS) tar.

Figure 7 Example picture of impingers after tar sampling (left) and rotary evaporator (middle) used to concentrate samples and determine gravimetric tar (right)

Chemical composition of the different tars (collected and gravimetric tars) was determined using a Varian CP-3800 gas chromatograph connected to a Saturn 2200 Ion Trap Mass Spectrometer (GS-MS). A low bleed capillary column, CP-Sil 8 CB: 5% phenyl, 95% dimethylpolysiloxane (60 mx 0.25 mm i.d. x0.25 μm film thickness) was used. One microliter of sample was injected in the split mode with a ratio 25:1. An initial oven temperature of 60 ºC was maintained for 3 minutes keeping a ramp rate of 7 ºC/min until a final temperature of 300 ºC for 15.57 minutes. The carrier gas was He (BIP quality) at a constant column flow of 1 mL/min. The injector, detector and transfer line temperatures were 300 ºC, 200 ºC and 300 ºC, respectively.
The MS was operated in electron ionization mode within 35-550 m/z range. The identification and quantification of compounds was carried out by external standard calibration for a total of 22 compounds according to the quantitation ion. In Figure 9, it is shown three chromatograms obtained by GS-MS corresponding to a standard, collectable tar and gravimetric tar.

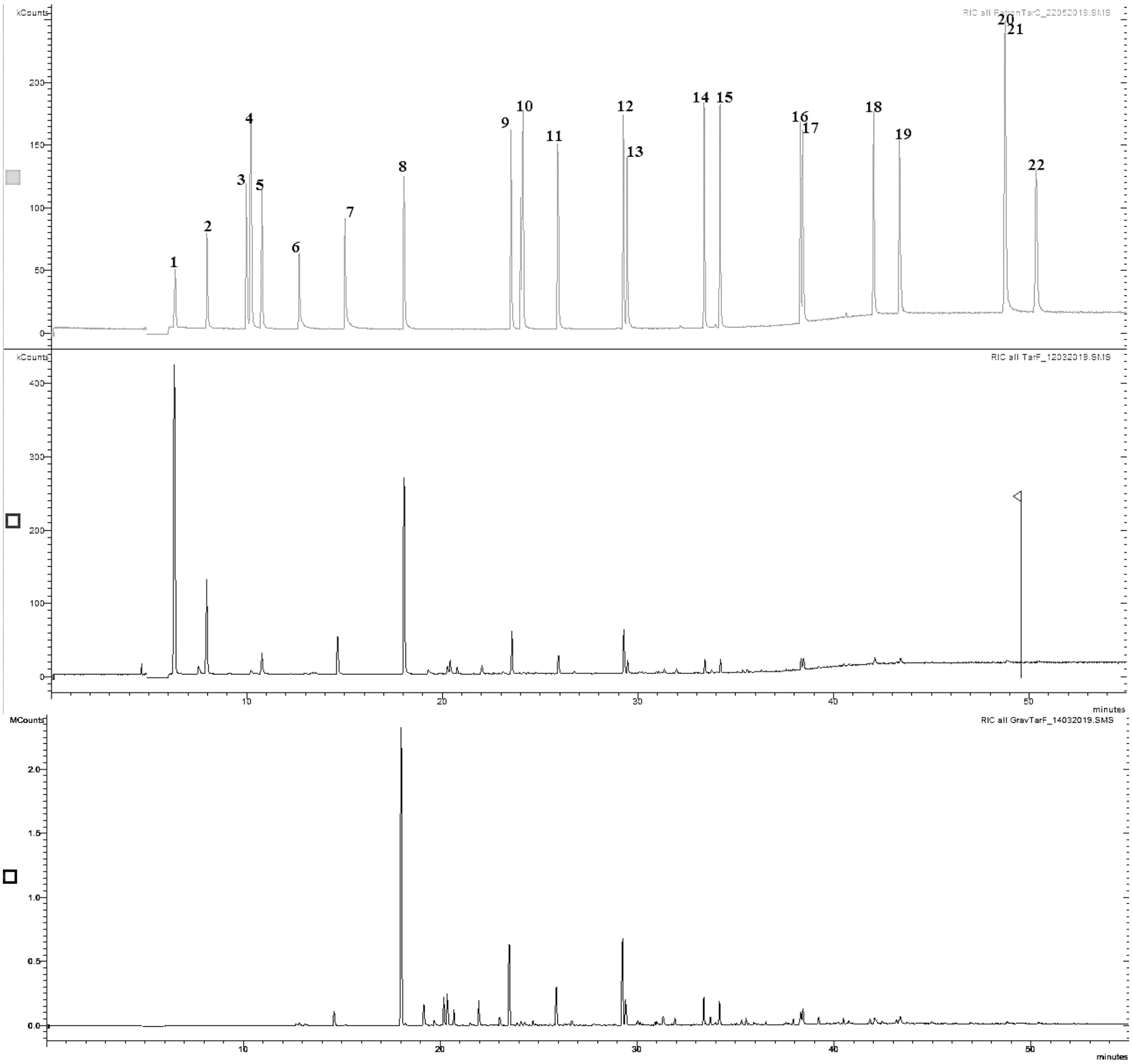

Figure 8 Chromatograms obtained for a standard solution containing a total of 22 compounds (up), collected tar (middle) and gravimetric tar (down) corresponding to a SEG experiment with ECOH pellets. Numbers correspond to: 1=Benzene, 2=Toluene, 3=Ethylbenzene, 4=p+m Xylene, 5= o-Xylene, 6= Phenol, 7= 4-Methyl phenol, 8= Napthalene, 9= Acenaphtylene, 10=Acenapthene, 11=Fluorene, 12=Phenanthrene, 13=Anthracene, 14=Fluoranthene, 15=Pyrene, 16=

Benzo(a)anthracene, 17= Chrysene, 18=Benzo(b)fluoranthene, 19=Benzo(a)pyrene, 20= Indeno(1,2,3-cd)pyrene, 21=Dibenzo(a,h)anthracene, 22=Benzo(g,h,i)perylene.

The main differences regarding both the collected and gravimetric tar were related to the nature of the identified compounds. Whereas in the collectable tar, the most volatile compounds (i.e. hydrocarbons with one aromatic ring like benzene, toluene, (o,m, p-xylenes) and some polycyclic aromatic hydrocarbons like naphthalene) were the dominant hydrocarbons, the concentration of the gravimetric tar (20 times more concentrated) allowed that heavier compounds with retention times higher than 20 minutes, which were negligible in the collected tar due to the low concentrations, were observable with the minimum presence of the most volatile compounds due to evaporation in the rotary evaporator. These results were also reported by different authors in the literature [4–6]. It is also worth mentioning that styrene was present in some collected tars but this compound was not quantified.

1.1.2.5 Polycyclic aromatic hydrocarbons (PAHs) determination

The same off-line sampling procedure as for tar sampling described in section 1.1.2.4 was used during combustion/calcination experiments to determine the concentrations of emitted polycyclic aromatic hydrocarbons (PAHs). Similarly to tar sampling, the seven impingers used contained 100 ml of isopropanol with the exception of impingers 1 and 7, which were empty. Because the final solution was not concentrated enough to determine the composition of the different aromatic compounds directly by injection in the gas chromatograph, an aliquot of the final solution (150 ml) was concentrated in a rotary evaporator and taken to a final volume of 5 ml.

The analysis was performed with a Varian CP-3800 gas chromatograph connected to a Saturn 2200 Ion Trap Mass Spectrometer (GS-MS). The identification and quantification of compounds was carried out as explained in section 1.1.2.4 for the tars analysis by injecting 1 microliter of sample in split mode (25:1).

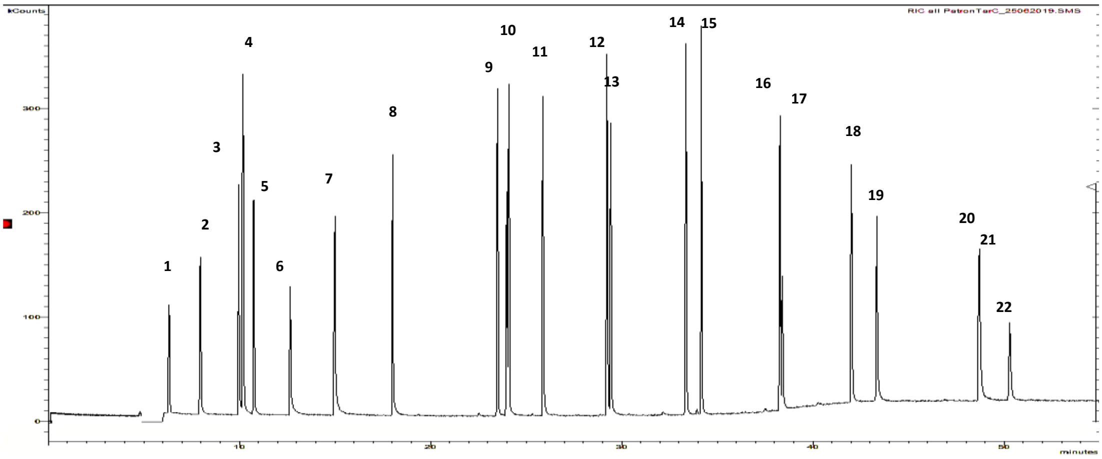

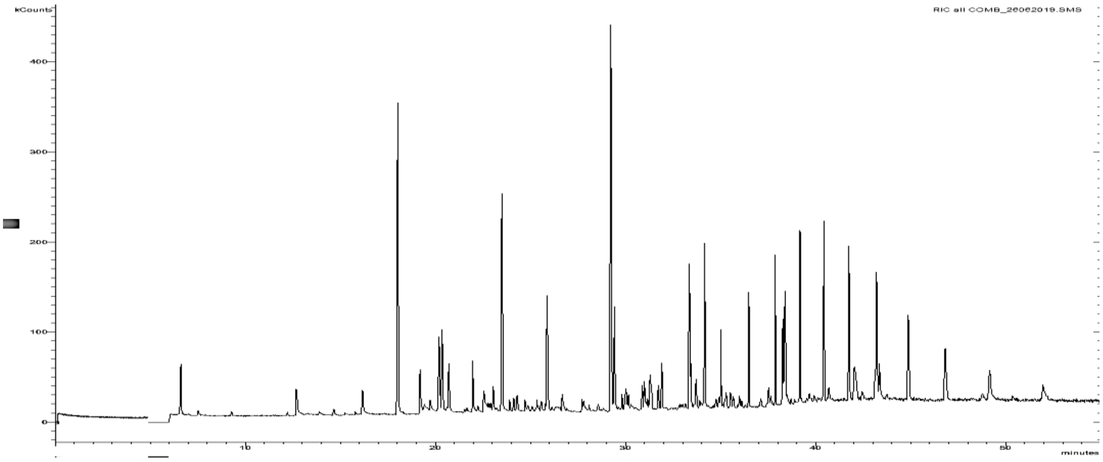

Figure 9 Chromatograms obtained for a standard solution containing a total of 22 compounds (up), and combustion/calcination experiment for grape seeds char (down) with 1=Benzene, 2=Toluene, 3=Ethylbenzene, 4=p+m Xylene, 5= o-Xylene, 6= Phenol, 7= 4-Methyl phenol, 8= Napthalene, 9= Acenaphtylene, 10=Acenapthene, 11=Fluorene, 12=Phenanthrene, 13=Anthracene, 14=Fluoranthene, 15=Pyrene, 16= Benzo(a)anthracene, 17= Chrysene, 18=Benzo(b)fluoranthene, 19=Benzo(a)pyrene, 20= Indeno(1,2,3-cd)pyrene, 21=Dibenzo(a,h)anthracene, 22=Benzo(g,h,i)perylene.

1.1.3 Experimental routines

1.1.3.1 Sorption enhanced gasification tests

At the beginning of each SEG experiment, solid bed in the reactor consisted of fully calcined CO_2 sorbent without any char particles obtained after complete combustion in air at the end of the previous SEG test. The experimental routine followed in each SEG test is represented in Figure 10. A first heating period in air (using a flow rate of 0.06-0.1 Nm^3/min) is performed using the electric resistances until a temperature of around 730-750 ºC. At this point biomass and CaO start to be fed to the reactor, using the desired flow rates according to the thermal input and CaO/C ratio established. N_2 flowing into the evaporator and into the CO_2 sorbent screw feeder are switched on and the air flowing into the reactor is stopped. At this point, the desired flow rate of steam is set. Bed temperature starts decreasing due to the endothermic nature of the gasification reactions as it is shown in Figure 10, and H_2, CH_4, CO_2 and CO start to be detected by the online gas analyser in the gas phase. Both gas composition and solid bed temperature stabilize sufficiently fast but the solid composition is still changing since CaO is being saturated in CO_2 and char is being accumulated and converted into syngas. Afterwards, steady state conditions are fulfilled and maintained during one hour in order to proceed with the gas and solid sampling. Gas sampling bags and solid samples are taken every 15 min from the beginning of the steady state. Commonly during SEG tests, tar sampling is switched on after 15 min once the first gas and solid samples were taken. Since gas starts to flow through the tar sampling line, the signal measured by the online analyser is slightly altered as shown in this figure.

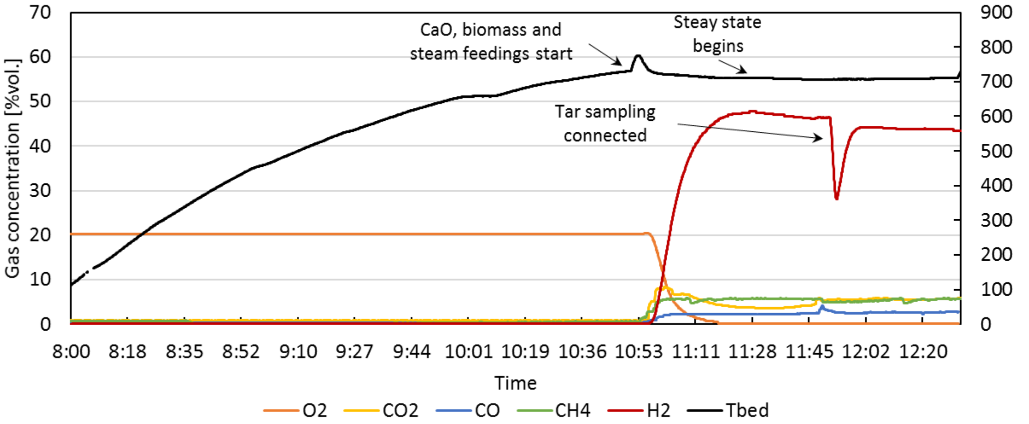

Figure 10 Solid bed temperature and flue gas composition evolution from start-up until the end of the steady-state period in a sorption enhanced gasification experiment

For shutting down after 1 h of steady-state period, biomass and CaO screw feeders are stopped and then steam is exchanged by a flow rate of air of 0.06 Nm^3/min. The electric resistances are then switched off to stop heating the reactor. Unconverted char in the solid bed is then burnt, making the temperature increase up to 920 ºC. $CaCO_3$ contained in the solid bed is also decomposed into CaO, and CO_2 is therefore released. When CO_2 is no longer present in the gas phase, complete char combustion and $CaCO_3$ calcination are fulfilled and then temperature of the reactor starts going down. Air flow rate is stopped when temperature is sufficiently low.

1.1.3.2 Combustion/calcination tests

At the beginning of each combustion/calcination experiment, solid bed in the reactor corresponded to completely calcined CO_2 sorbent without any char particles obtained after complete combustion in air at the end of the previous SEG or combustion/calcination test. The experimental routine followed in any combustion/calcination test is represented in Figure 11. Flue gas composition in these experiments (i.e. O_2, CO_2, NO_x (NO_2+NO) and SO_2) has been measured using a combustion gas on-line analyser Testo 350 XL.

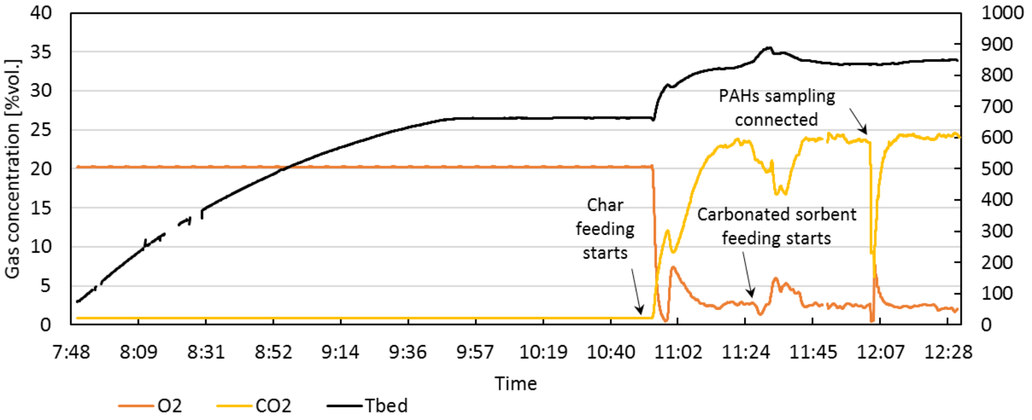

Figure 11 Solid bed temperature and flue gas composition evolution from start-up until the end of the steady-state period in a combustion/calcination experiment

At the beginning, the reactor is heated up using the electric heating up to around 700 ºC fluidizing with air (using a flow rate of 0.06 Nm^3/min). Once this temperature is reached, the air flow rate is increased up to the desired value (i.e. between 0.12 and 0.14 Nm^3/min for the tests explained below in section 1.3) and biomass char is then fed to the reactor to speed up the heating process. A char mass flow rate of around 1-1.1 kg/h is selected, which is the mass flow rate kept as constant during the whole combustion/calcination experiment. At this moment, temperature starts increasing faster, CO_2 concentration starts to become significant and the O_2 content in the flue gas decreases since the combustion of the char occurs (see Figure 11). Electric resistances are no longer needed from this point onwards in the experiment. When the O_2 and CO_2 contents in the flue gas remain more or less constant, the carbonated CO_2 sorbent starts to be introduced into the reactor using the mass flow rate corresponding to the char/sorbent mass ratio desired. Mass flow rates of carbonated CO_2 sorbent have been modified between 4 and 6 kg/h according to the char/sorbents ratios assessed in section 1.3. CO_2 and O_2 contents in the flue gas as well as temperature stabilized after a little bit of time, and then the steady-state period begins. During this period, solid samples are taken every 10 min from the overflow and cyclones of the plant, and the polycyclic aromatic hydrocarbons (PAHs) collecting system is connected, which corresponds with the fluctuation observed in the flue gas composition in Figure 11. This steady-state period is maintained for only 30 min, which is the sampling time for PAHS.

For shutting down after the steady-state period, char and sorbent screw feeders are stopped, leaving the reactor being fluidized exclusively with air. Once the char and the carbonated sorbent have been fully burnt and calcined, respectively, solid bed temperature starts to decrease, while CO_2 content in the flue gas goes quickly down to almost zero. Similarly to SEG experiments, air flow rate is stopped when solid bed temperature is sufficiently low.

1.2 Sorption enhanced gasification tests: Results and discussion

In this section, all the SEG tests performed in the 30 kW_{th} BFBR at ICB-CSIC are discussed. The operation parameters analyzed have been:

1. The steam-to-carbon (S/C) molar ratio, related to the amount of steam introduced into the gasifier, which is calculated as the ratio between the moles of steam introduced into the gasifier (i.e. without including the steam introduced with the moisture of the biomass) per mole of carbon in the biomass fed to this reactor;
2. The calcium-to-carbon (CaO/C or Ca/C) molar ratio, related to the amount of CO_2 sorbent introduced into the gasifier, which is calculated as the moles of CaO introduced with the CO_2 sorbent (which has a purity of about 90 to 98 %wt. of CaO as indicated in Table 3 depending on the lime used) into the gasifier per mole of carbon in the biomass, according to its ultimate analysis given in Table 1
3. The CO_2 sorption capacity of the sorbent. As explained in section 1.1.2.1, CO_2 carrying capacity of the CO_2 sorbents used decreases with the calcination/carbonation cycles. To assess the impact of the CO_2 carrying capacity of the CaO-based material, experiments using both lime #1 and #2 having experienced different number of calcination/carbonation cycles have been undertaken as explained below.
4. Type of CO_2 sorbent; two different sorbents have been used (i.e. lime #1 and #2) whose characteristics have been explained in section 1.1.2.1.

From the beginning of the project until June 20th of 2019, all the experiments explained in the coming sections were performed. In this period, the BFBR at ICB-CSIC has been operated for about 670 h, accounting for SEG tests, combustion/calcination tests and calcination of the limestones #1 and #2, as follows:

- SEG tests using lime #1 as CO_2 sorbent and grape seeds and wood pellets as biomass feedstocks: 175 h
- SEG tests using lime #2 as CO_2 sorbent for the 6 biomass feedstocks in Table 1: 266 h
- Combustion/calcination tests: 24 h
- Calcination of limestone #1: 112 h
- Calcination of limestone #2: 93 h

1.2.1 Wood pellets

SEG tests performed in the BFB gasifier with wood pellets as biomass correspond to those included in Table 5. Two different calcium-to-carbon (CaO/C) molar ratios (0.3 and 0.36) have been tested at S/C ratios between 1.4 and 1.6. As indicated in this table, both CO_2 sorbents (lime #1 and #2) have been tested with this biomass feedstock.

Table 5 Experimental matrix of the SEG tests performed with wood pellets as biomass in the BFBR at ICB-CSIC

CaO/C	Lime #1	Lime #2
	S/C=1.5	S/C=1.4-1.6
0.36		14.6 kW_{th} (667-670ºC)
0.30	19.5 kW_{th} (712-723ºC)	16.6 kW_{th} (718-720ºC)

1.2.1.1 Analysis of the gas yield and char conversion

Figure 12 shows the calculated gas yields and fixed carbon conversion (X_{FC}) for the SEG tests performed with wood pellets. As shown in this figure, X_{FC} obtained for the two SEG experiments at the same solid bed temperature of around 714-715 ºC was similar and close to 37-42 %. Main operating variables influencing char conversion are gasification temperature, residence time and steam-to-carbon ratio. For the two SEG tests compared in Figure 12, differences in the temperature, residence time and S/C ratio were not substantial, and therefore X_{FC} fulfilled was almost the same. However, when decreasing the gasification temperature by around 45 ºC, X_{FC} reduces dramatically to 16 % as shown in this figure. Concerning gas yield, it increases with the increasing temperature due to: (i) increased gas production during the primary pyrolysis stage, (ii) steam cracking and reforming of heavier hydrocarbons and tars, and (iii) enhanced char gasification reactions [7,8]. Calculated gas yield for the SEG experiments with lime #2 was 1.08 Nm^3 dry gas/kg_{BS} at 714 ºC, and decrease to 0.91 Nm^3 dry gas/kg_{BS} at 667 ºC. A slightly lower gas yield (i.e. 1.0 Nm^3 dry gas/kg_{BS}) was calculated for the experiment with lime #1 at 714 ºC than for the experiment at the same temperature with lime #2. As explained below, this lower gas yield is linked to the lower CO_2 carrying capacity of lime #1, which leads to a lower H_2 yield and larger C_3-C_4 hydrocarbons content.

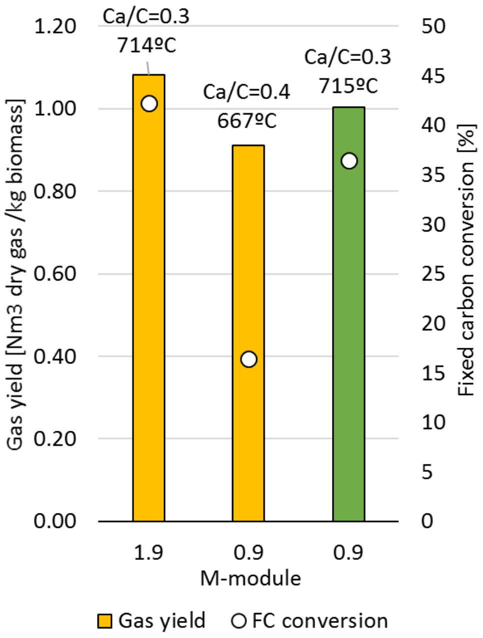

Figure 12 Gas yield, fixed carbon conversion and M-module obtained for the SEG tests with wood pellets (yellow bars correspond to tests performed with lime #2 as CO_2 sorbent and green bar with lime #1)

1.2.1.2 Analysis of gas quality

Figure 13 shows the syngas composition obtained for two SEG experiments with similar gasification temperature, S/C and CaO/C ratios but performed using a different CO_2 sorbent (i.e. lime #1 and #). As it can be noticed, the main influence of the type of CO_2 sorbent is on the H_2 content, being significantly higher for the experiment performed with lime #2 that has a greater CO_2 carrying capacity (as seen before in Figure 4). H_2 content in the syngas resulted 44 %vol. (H_2-N_2 free basis) for the SEG test with lime #1 and 55 %vol. (H_2-N_2 free basis) using lime #2. Considering the gas yield in each case, these differences result in a H_2 yield of 0.36 and 0.48 Nm^3 of H_2/kg_{BS} for lime #1 and #2, respectively. Given that solid inventory was constant (6-6.4 kg) for both experiments and that the CaO/C ratio was similar, the amount of CO_2 captured is exclusively linked to the CO_2 carrying capacity. From the characterization of the solids collected through the overflow pipe, it was calculated a $CaCO_3$ content of 0.18 mol_{CaCO3}/mol_{Ca} for the experiment with lime #1 and 0.35 mol_{CaCO3}/mol_{Ca} for the experiment with lime #2. Moreover, doing a C balance to the non-captured C leaving the BFBR with the overflow and cyclones solids as well as with the syngas in the form of CO, CH_4 and C_2-C_4 hydrocarbons, a CO_2 capture ratio of 20 % has been calculated for the SEG test with lime #1 and 35.5 % using lime #2.

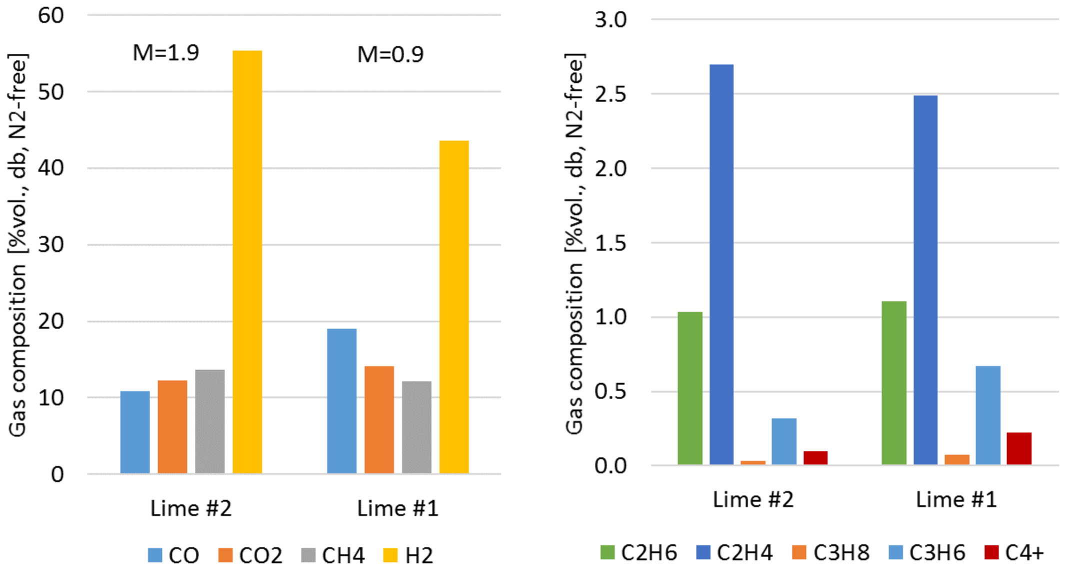

Figure 13 Gas concentration (dry and N_2 free basis) during steady state measured by GC for two experiments with wood pellets, similar CaO/C ratio (0.30), similar S/C ratio (1.5), similar gasification temperature (714-715 ºC) but different CO_2 sorbent

As for the rest of the permanent gases (Figure 13 left), CO_2 content resulted at equilibrium conditions for these two SEG experiments (i.e. around 5 %vol.), but the differences in the amount of CO_2 removed from the gas phase make the CO concentration to be higher for the test with lime #1. Overall, M-module resulted around 0.9 when using lime #1 and close to 2 using lime #2. There are also differences in the hydrocarbons present in the syngas when modifying the CO_2 sorbent used. As appreciated in Figure 13, C_3-C_4 content decrease when using lime #2, probably due to the enhancement of H_2 production that favors the cracking of these C_3-C_4 compounds into C_2H_4 and CH_4. Even if it is not appreciated in Figure 13, CH_4 content was around 5.5 %vol. (inc. H_2O and N_2) in the SEG test using lime #2 and around 4.7 %vol. using lime #1).

The effect of the gasification temperature can be also evaluated if comparing the two SEG experiments performed with lime #2 in Table 5. Figure 14 shows the syngas composition fulfilled during the steady state conditions for these two SEG tests. As it is noticed in this figure, the lower the temperature the lower the H_2 content in the syngas. In terms of gas yield, 0.29 Nm^3 of H_2/kg_{BS} are obtained operating at 667 ºC and 0.48 Nm^3 of H_2/kg_{BS} when moving to 714 ºC. This lower amount of H_2 produced is limited by the conversion of the char, which is greatly reduced as temperature goes down. In this way, even if carbonation reaction is favored at lower temperatures [9] (the CO_2 content is lower at 665 ºC including H_2O and N_2 in the syngas), the amount of H released as char is being converted is limited at low temperatures and therefore there is less C in the gas phase to react with the CaO particles. Corroborating this fact, CaO particles leaving the overflow pipe in the experiment at 667 ºC have 0.24 mol_{CaCO3}/mol_{Ca}, whereas this was 0.35 mol_{CaCO3}/mol_{Ca} at 714 ºC. As a result of these trends, the M-module resulted at a value of 0.9 for the experiment at 665 ºC. Concerning the light hydrocarbons, reducing the gasification temperature makes the C_3-C_4 content to be raised probably due to the fact that reforming and cracking reactions are less favored.

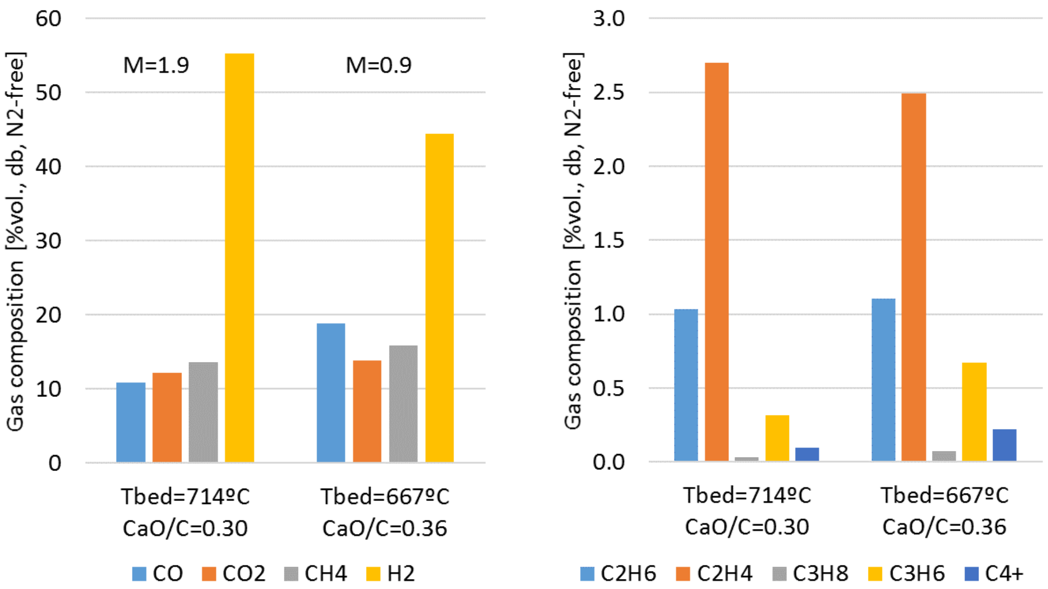

Figure 14 Gas concentration (dry and N_2 free basis) during steady state measured by GC for two experiments with wood pellets and lime #2 as CO_2 sorbent, similar S/C ratio (1.4-1.6), similar CaO/C ratio (0.30-0.36) but different gasification temperature

1.2.1.3 Analysis of tars

For the two SEG experiments performed with lime #2 indicated in Table 5, tar sampling was done according to the procedure explained in section 1.1.2.4, obtaining the samples shown in Figure 15. For these experiments, gasification temperature, CaO/C and S/C ratios changed as shown in Table 5.

Figure 15 Pictures of the tar sampling impingers for the SEG experiments with wood pellets at (left) S/C=1.4, CaO/C=0.30 and 717 ºC and (right) S/C=1.6, CaO/C=0.36 and 665 ºC

For each tar sampling, a total of three samples were obtained: the collected and the gravimetric tars determined by GC-MS and the gravimetric tar determined by weight (see section 1.1.2.4 for more information about these samples). For both experiments, it was observed that the collected tar as well as the gravimetric tar (GC-MS) decreased with the solid bed temperature (Figure 16) favoring the high temperature the cracking of tar compounds. Regarding the gravimetric tar (weight), it also decreased with the temperature, resulting in 21.9 and 31.4 g/Nm^3 dry gas at 717 ºC and 665 ºC of solid bed temperature, respectively.

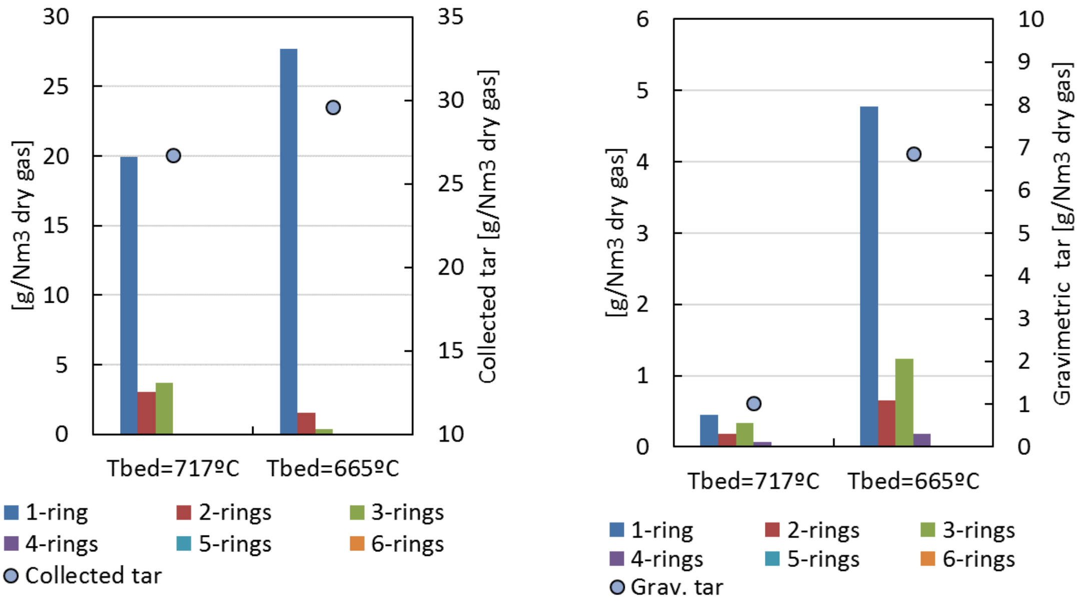

Figure 16 (left) Collected tar (calculated by GC-MS, in g/Nm^3 dry gas) and composition by number of rings compounds, and (right) gravimetric tar (GC-MS) and composition by number of rings, for the two SEG tests with wood pellets at different temperature (1-ring= Benzene, Toluene, Ethylbenzene, p+m-Xylene, o-Xylene, Phenol, Phenol, 4-methyl-, 2-rings= Naphthalene, 3-rings: Acenapthylene, Acenapthene, Fluorene, Phenanthrene, Anthracene, 4-rings= Fluoranthene, Pyrene, Benzo(a)anthracene, Chrysene, 5-rings= Benzo(b)fluoranthene, Benzo(a)pyrene, Dibenzo(a,h)anthracene and 6-rings= Indeno(1,2,3-cd)pyrene and Benzo(g,h,i)perylene)

The composition of the collected and gravimetric tars (GC-MS) was analyzed as a function of the number of rings (Figure 16). For the collected tar, at both temperatures, the one-ring compounds were the major compounds emitted whereas 4 to 6 rings compounds were not detected. As appreciated, when increasing the solid bed temperature the contribution of the 2 and 3-rings compounds decreased. With regard to the gravimetric tar (by GC-MS) in Figure 16 (right), the 1-ring compounds also were the major compounds emitted although it was at the lowest solid bed temperature when the 1-ring compounds reached 70 % wt. versus the 44 %wt. at 717 ºC. However, the contribution of 2 to 4 rings become more important at increasing solid bed temperatures. The main difference between the composition of the collected and gravimetric (GC-MS) tars was related to the presence of 4-rings compounds, which were not detected in the collected tar due to these compounds were present at very low concentrations.

Regarding the composition of the 1-ring compounds for the collected tar, it is remarkable to say that phenolic compounds such as phenol and phenol, 4-methyl- were major components in addition to benzene, toluene and xylenes (Figure 17 (up)). Benzene seemed not to be affected by the solid bed temperature as very similar concentrations were obtained for both cases. However, the rest of 1-ring compounds increased when the solid bed temperature was reduced. Ethylbenzene was not detected at any of the gasification temperatures. The presence of phenolic compounds was characteristic of the feeding material composition, in this case, wood pellets that contain lignin made of cross-linked phenolic polymers that could be released and/or formed during the gasification process. Concerning the composition of the major compounds emitted for the gravimetric tar (GC-MS) (Figure 17 (down)), only phenolic compounds were detected for the 1-ring compounds. As mentioned in the tar sampling description section (1.1.2.4), the most volatile 1-rings compounds like benzene, toluene, ethylbenzene and xylenes were not present or at very low concentrations due to the evaporation process that takes place in the rotary evaporator. Other compounds of higher molecular weight like naphthalene, acenapthylene, fluorene and phenanthrene are therefore the dominant compounds of the gravimetric tar associated to 2 and 3-rings compounds.

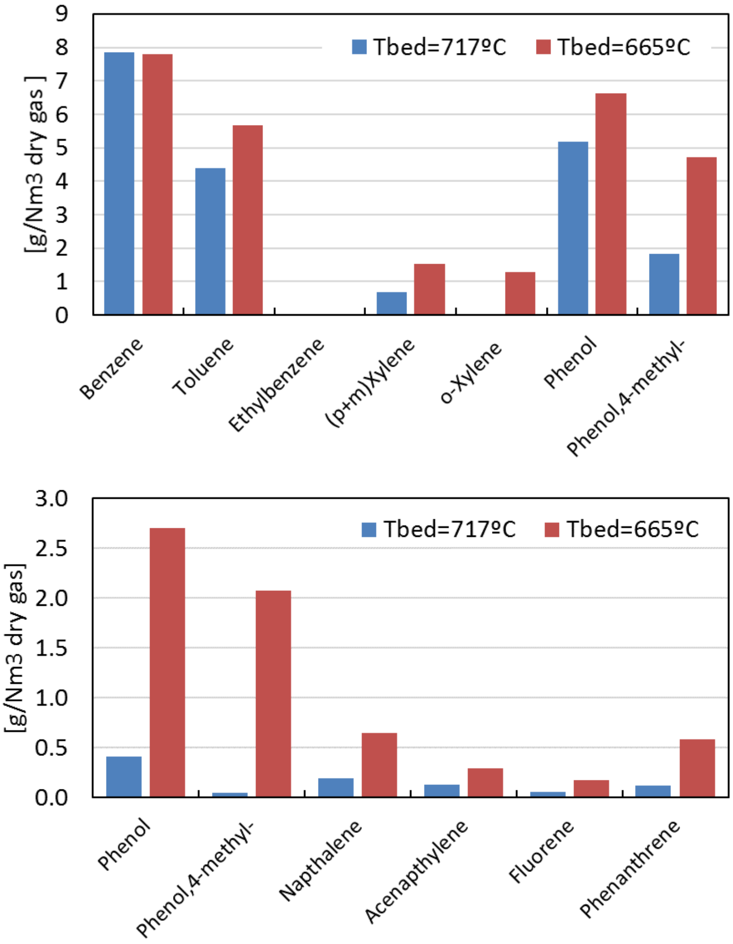

Figure 17 (up) Major 1-ring compounds emitted for the collected tar and (down) major compounds emitted for the gravimetric tar (GC-MS) (1, 2, 3- rings compounds) as a function of the average solid bed temperature for the SEG experiments with wood pellets

1.2.2 Grape seeds

Up to 15 SEG tests have been performed in the BFB gasifier using grape seeds and both limes (#1 and #2) as feedstocks as shown in Table 6. Within these tests, the steam-to-carbon (S/C) molar ratio has been modified between 0.85 and 24; the calcium-to-carbon (CaO/C) molar ratio between 0.25 and 0.65 and the effect of sorbent activity and sorbent type has been also assessed. Especial attention has been payed to gas yield, gas quality (linked to the M-module) and char conversion. Moreover, tar analysis has been performed on several tests performed with lime #2 for comparison with the results obtained with different biomass feedstock.

Table 6 Experimental matrix of the SEG tests performed with grape seeds as biomass in the BFBR at ICB-CSIC

	Lime #1			Lime #2		
CaO/C	S/C=0.85-1.2	S/C=1.5	S/C=1.8	S/C=1	S/C=1.8	S/C=2.4
0.65	13 kW_{th} (755 ºC)				13 kW_{th} (737-740 ºC)	
0.45-0.50	21 kW_{th} (717-722 ºC)	21 kW_{th} (705-716 ºC) 21 kW_{th} (686-696 ºC)	13 kW_{th} (740-745ºC)			13 kW_{th} (727-733 ºC)
0.35-0.40	21 kW_{th} (722-724 ºC) (S/C=1.1) 21 kW_{th} (729-735 ºC) (S/C=0.85)	21 kW_{th} (736-748 ºC)			13 KW_{th} (730-737 ºC) 13 kW_{th} (660-671 ºC)	
0.25-0.30		21 kW_{th} (733-745 ºC)		21 kW_{th} (630-638ºC)		

1.2.2.1 Effect of the S/C molar ratio

The effect of S/C molar ratio on SEG process has been analyzed between 0.85 and 1.8 for lime #1 and between 0.85 and 2.4 for lime #2. As an example, Figure 18 shows the syngas composition measured by gas chromatography (GC) during the steady-state period for two experiments performed at different S/C ratios (1 and 1.5) and similar CaO/C molar ratio (0.4) using lime #1. Solid bed stabilization temperature in both experiments is also indicated in the figure. Slightly lower temperature was reached for the test with the higher S/C ratio of 1.5 due to the larger sensible heat required to heat up the fluidizing gas and the endothermicity of the gasification reaction. As appreciated in the figure, the main effect of the S/C ratio relies on the C_2-C_4 concentration in the syngas as shown in Figure 18 (right). The amount of C_3-C_4 and unsaturated C_2 hydrocarbons in the syngas is noticeably reduced below 1 %vol. (dry and N_2 free basis) when increasing the S/C ratio up to 1.5. Raising the amount of steam introduced into the gasifier makes the higher C_3-C_4 hydrocarbons and unsaturated C_2 convert into C_2H_6 and CH_4, as shown in the figure. As a result, C_2H_6 concentration increases from 6.8 %vol. to 10.3 %vol. (dry and N_2 free basis) when moving from S/C=1 to S/C=1.5, and so does also CH_4 concentration that increases from 9.1%vol. to 12.9 %vol. The decomposition of each molecule of heavier hydrocarbon into lighter ones translates into a larger gas yield that resulted in 0.92 Nm^3(dry basis)/kg BS for the test with S/C=1.5 and 0.82 Nm^3(dry basis)/kg BS for S/C=1.

Regarding to the concentration of H_2, CO and CO_2 in the syngas obtained in the gasifier, small differences can be noticed in Figure 18 (left). Similar amount of CaO was fed to the gasifier in both experiments (≈ 3.7 kg/h) with respect to the C fed with the biomass (i.e. same CaO/C ratio), which makes the amount of CO_2 separated in both cases to practically match, resulting in this way into similar H_2 content as shown in the figure. Concerning the CO_2 concentration in the gas phase, this will be exclusively affected by the operating temperature of the gasifier through the carbonation reaction equilibrium, i.e. larger CO_2 concentration as temperature increases [9]. Therefore, the small differences observed in the CO_2 content (11.6 %vol. vs. 10.8 %vol. both in H_2O-N_2 free basis) are linked to this temperature difference of 15 ºC. Finally, the larger amount of H_2O and the smaller CO_2 content in the syngas for the experiment with S/C=1.5 turn into a slightly lower CO content in the syngas. On the whole, and due to the smaller differences in the H_2, CO and CO2 contents in the syngas when modifying the S/C ratio, almost the same module $M=(H_2-CO_2)/(CO+CO_2)$ of around 2.4-2.5 was fulfilled in both tests. Considering the information calculated from the solids characterization, X_{OM} and X_{CF} calculated resulted around 80 and 32 %, respectively, for both tests since the differences in temperature and solid residence time were negligible.

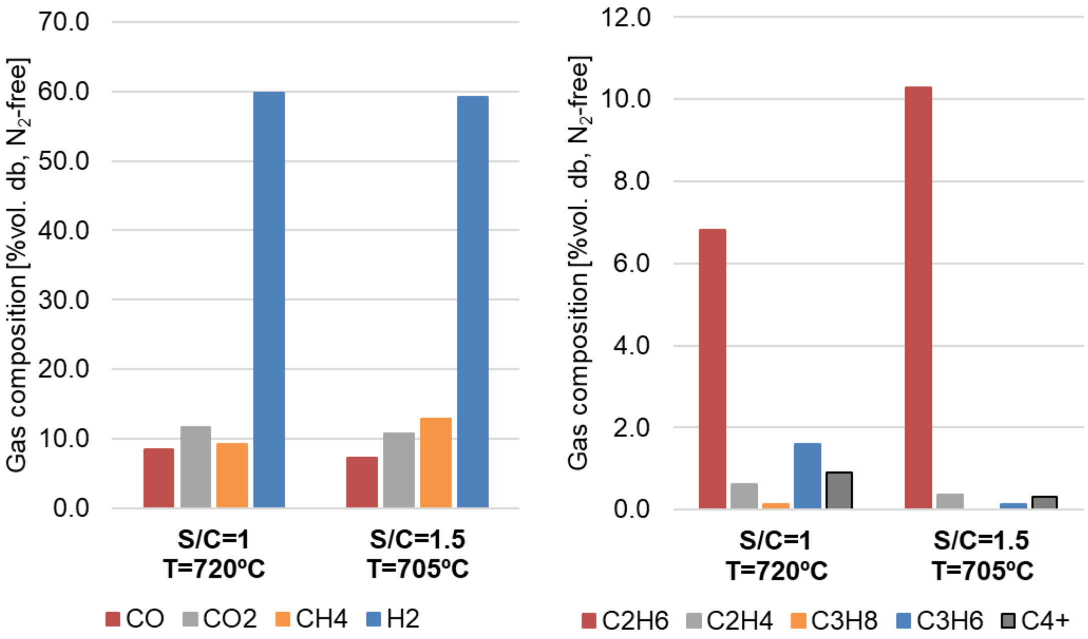

Figure 18 Gas concentration (dry and N_2 free basis) during steady state measured by GC for two different S/C ratios of 1 and 1.5, keeping a constant CaO/C ratio of 0.40 using lime #1 and a biomass thermal input of 21 kW_{th}. Stabilization temperature of the solid bed during the experiments is shown in the X-axis legend

A similar analysis has been performed to the experiments performed with lime #2 as sorbent and varying the S/C molar ratio. Figure 19 (left) shows the syngas composition for two different tests performed with an S/C of 2.4 and 1.8 respectively for a CaO/C molar ratio of around 0.4. In both tests, the bed stabilized at a very similar temperature of approximately 730 ºC. Figure 19 (right) shows the syngas yield (in dry basis) produced during the steady-state period for these operating conditions. The figures also include a third test performed with a similar S/C and CaO/C ratios of 1.8 and 0.4, respectively, but with a lower stabilization bed temperature (i.e. 660 ºC). It can be observed that increasing the S/C ratio over 1.8 (for a fixed CaO/C molar ratio and similar gasification temperature) has a low impact on product gas composition and gas yield. Slightly higher H_2 concentration was obtained for the experiment performed at the highest S/C molar ratio (70.5 %vol. at S/C 2.4 versus 68.6 %vol. at S/C 1.8), the CO_2 concentration in both cases was determined by the equilibrium CO_2 partial pressure at gasifier conditions, while very similar CH_4 and CO was obtained for both tests. As it happened for the tests performed with lime #1 at lower S/C ratios, the presence of C_{2+} diminishes with increasing S/C ratio in the gasifier, but increasing the S/C from 1.8 to 2.4 has a rather low impact in gas quality and on gas yield (see Figure 19 (right)). The M module obtained in these tests was 3.0 for the test at the highest S/C and 2.6 for the test performed with an S/C of 1.8.

As appreciated in Figure 19, the gasification temperature has an important impact on gas quality and gas yield. The presence of C_{2+} becomes relevant when decreasing the gasification temperature from around 735 ºC to 660 ºC, being around 10 % vol. of the syngas obtained (dry and N_2 free) even at this relatively high S/C molar ratio. The total gas yield produced is reduced (0.82 Nm^3(dry basis)/kg BS) with respect to the experiments at higher temperature (see Figure 19 (right)), and this must be related with char (or fixed carbon) conversion at gasifier conditions. These two factors (higher C_{2+} and lower gas yield) result in a lower H_2 concentration in the syngas produced (55 % vol.) and therefore an M module of 1.71 was obtained for this test.

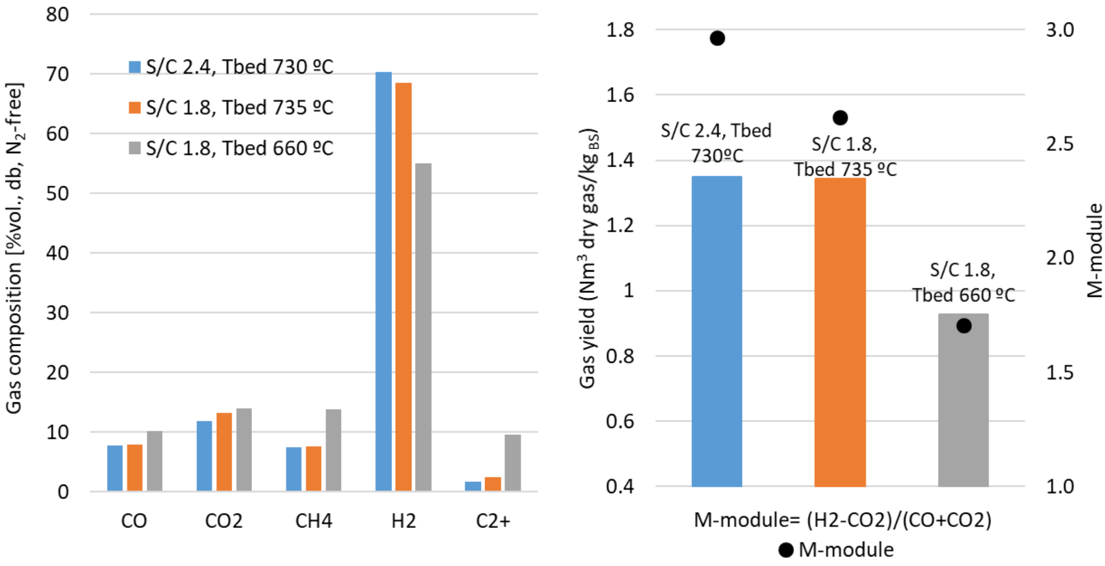

Figure 19 Gas concentration (dry and N_2 free basis) during steady state measured by GC for two different S/C ratios of 1.8 and 2.4, keeping a CaO/C ratio around 0.40 using lime #2 and a biomass thermal input of 13 kW_{th}. The stabilization temperature of the solid bed during the experiments is shown in the legend

From the information obtained through the characterization of the samples of solids taken along the stationary period, it has been determined a X_{CF} of 65.7 % and 68 % for the experiments performed at around 730 ºC and S/C molar ratio of 1.8 and 2.4 respectively. This results in X_{OM} over 80 % for both experiments. In contrast, X_{CF} below 20% and X_{OM} of about 70 % was determined for the experiment performed with an S/C of 1.8 and bed temperature of 660 ºC.

1.2.2.2 Effect of the CaO/C molar ratio and sorbent activity

Figure 20 shows the syngas composition measured by GC during the steady-state period for two different CaO/C ratios (0.35 and 0.45), which correspond to 3.1 and 4.0 kg/h flow rates of CO_2 sorbent (i.e. lime #1), respectively, and an S/C ratio of 1.5. As shown in this figure, solid bed temperature stabilized at a lower value of 705 ºC for the test with higher CaO/C ratio since the amount of CaO fed to the BFB gasifier from the hopper was larger, and so the amount of sensible heat absorbed by this stream of solids for heating up. Concerning the permanent gas composition in the syngas obtained that is shown in Figure 20 (left), H_2 concentration resulted close to 60 %vol. (H_2O and N_2 free basis) for the experiment with larger CaO/C ratio, which was around 5 percentage points higher than the H_2 content fulfilled with CaO/C of 0.35. This behavior is linked to the higher amount of CO_2 separated in the test with larger CaO/C ratio that pushes gasification reactions towards H_2 formation. Considering the solid inventory of solids in the BFB reactor and the flow rate of CO_2 sorbent used, solid residence time for the CO_2 sorbent particles was sufficiently high for fulfilling their maximum CO_2 carrying capacity in every test (it was observed in the TGA tests that the maximum CO_2 carrying capacity was attained in just 2-3 min). Therefore, varying the sorbent-to-biomass ratio the amount of CO_2 separated is being modified, increasing as the CaO/C ratio increases. Estimating a Carbon Capture Ratio (CCR) as the fraction of the C fed with the biomass that is separated as $CaCO_3$ with the sorbent, a CCR of around 22 % resulted for the test with a CaO/C=0.34 and around 44 % for the test with a CaO/C=0.45, corroborating the trend observed for the H_2 content.

Concerning the CO_2, as shown in Figure 20 (left), CO_2 concentration for the test with the lowest solid bed temperature turns out into a lower value (≈ 10.8 %vol.(db) vs. 14.1 %vol.(db), which corresponds to around 4 %vol. vs. 6 %vol. when considering real syngas composition (i.e. including H_2O and N_2) at the BFB reactor outlet). At the same time, CO concentration is linked to that of CO_2 through the Water Gas Shift (WGS) reaction (i.e., $CO+H_2O \rightarrow CO_2+H_2$), which is pushed towards H_2 as the separation of the CO_2 formed proceeds. Therefore, CO concentration would be reduced when the CO_2 concentration diminishes, as appreciated in Figure 20 (left). Based on these effects, the module M became around 2.5 for the test with CaO/C=0.45. For the experiment with CaO/C=0.35 the M module resulted in 1.7 since the amount of carbon in the form of CO and CO_2 in the syngas was higher, being more appropriate for situations with no additional H_2 available downstream the gasification unit.

The concentration of higher hydrocarbons for these tests with different CaO/C ratio is depicted in Figure 20 (right). As shown, the concentration of C_3-C_4 and unsaturated C_2 hydrocarbons remained below 0.8 %vol. in both experiments since the S/C ratio used was high. However, the concentration of C_2H_6 and CH_4 resulted in 10.3 and 12.9 %vol. (H_2O and N_2 free), respectively, for the test with larger CaO/C ratio, around 2 percentage points higher than the corresponding values found for the experiment with lower CaO excess. This effect is linked to the lower stabilization temperature of the solid bed for this test with larger Ca/C ratio, which hampers the decomposition of C_2H_4 and CH_4 into lighter compounds. This higher CH_4 and C_2H_4 yields for the experiment at lower stabilization temperature would be accompanied by a higher yield of tars, as expected according to thermodynamics [8], which would increase the demand for downstream gas cleaning section.

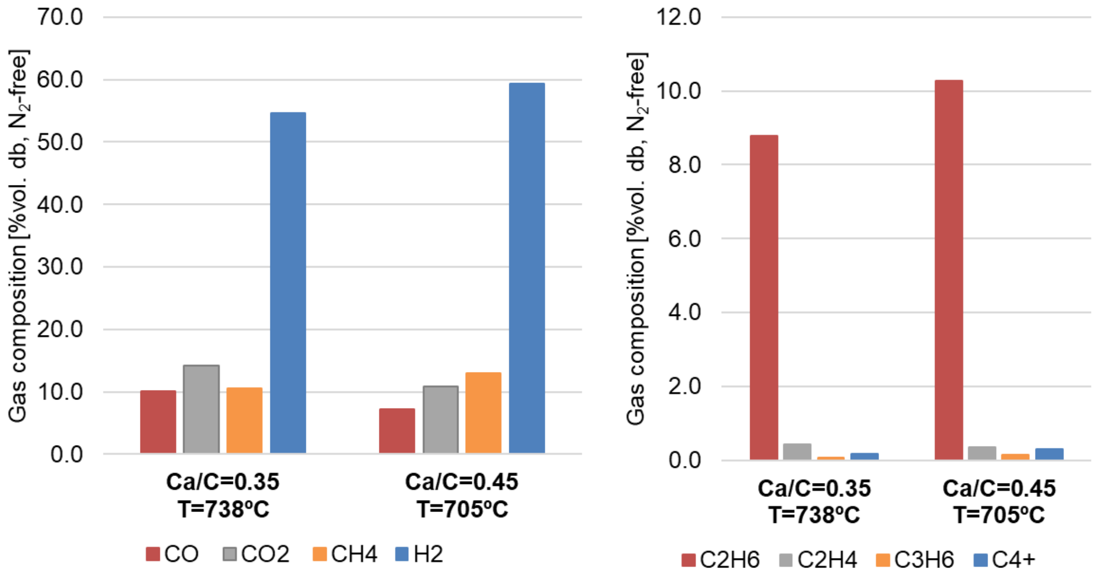

Figure 20 Gas concentration (dry and N_2 free basis) during steady state measured by GC for two different CaO/C ratios of 0.34 and 0.49 (using lime #1) for a thermal input of biomass of 21 kW_{th} and a constant S/C ratio of 1.5. Stabilization temperature of the solid bed during the experiments is shown in the X-axis

Similarly to the analysis of S/C molar ratio explained in previous section 1.2.2.1, some experiments were also performed with lime #2 to assess the effect that the CaO/C molar ratio has on gas quality, gas yield and the fixed carbon and biomass conversions. Figure 21 shows the gas composition measured by GC and gas yield (figure on the right) for two experiments performed with lime #2 for CaO/C ratios of 0.4 and 0.6, at an S/C of 1.8 and a gasification bed temperature of 740 ºC. As it can be observed, there are only slight differences between the gas composition for the experiments performed with lime #2 presenting higher H_2 concentration and slightly lower CO_2 the test performed with the highest CaO/C molar ratio. As a result, a very similar M module close to 2.7 is obtained for both tests. Considering the total gas yield the presence of a higher CaO flow in the reactor increases the CO_2 captured from the gas phase, and therefore the gas yield is decreased. Figure 21 also includes a test performed with lime #1 at similar conditions of CaO/C, S/C and bed temperature. As it was described in the sorbent characterization section, lime #1 presented a lower activity in terms of CO_2 carrying capacity. In this way although total CaO in bed was similar to the test used as comparison with lime #2, the active CaO content in bed was lower. As a consequence, the H_2 concentration in the producer gas was noticeable lower, the CO_2 concentration (dry basis and free of N_2) was slightly higher and also the presence of light hydrocarbons was significant (close to 10 %vol.). In this case the M module was approximately 2.1. From the point of view of solids characterization, the sorbent abandons the reactor with a CaO conversion of 0.195 mol $CaCO_3$/mol CaO and 0.189 mol $CaCO_3$/mol CaO for the tests using lime #2 and CaO/C of 0.4 and 0.65 respectively. Based on these results, and as described above, a larger amount of CO_2 is separated in the test performed at CaO/C of 0.65 that will affect the total gas yield and char conversion as the displacement of the reactions will help the gasification reaction of the char. According to the characterization of the solid samples recovered during the stationary period, X_{CF} of 66 % was achieved with the test performed at CaO/C 0.65 while 58 % of the FC reacted for the test performed at CaO/C of 0.4. Within the experiment performed with lime #1, an X_{CF} of 53.8 % was achieved, and the sorbent conversion was 0.097 mol $CaCO_3$/mol CaO.

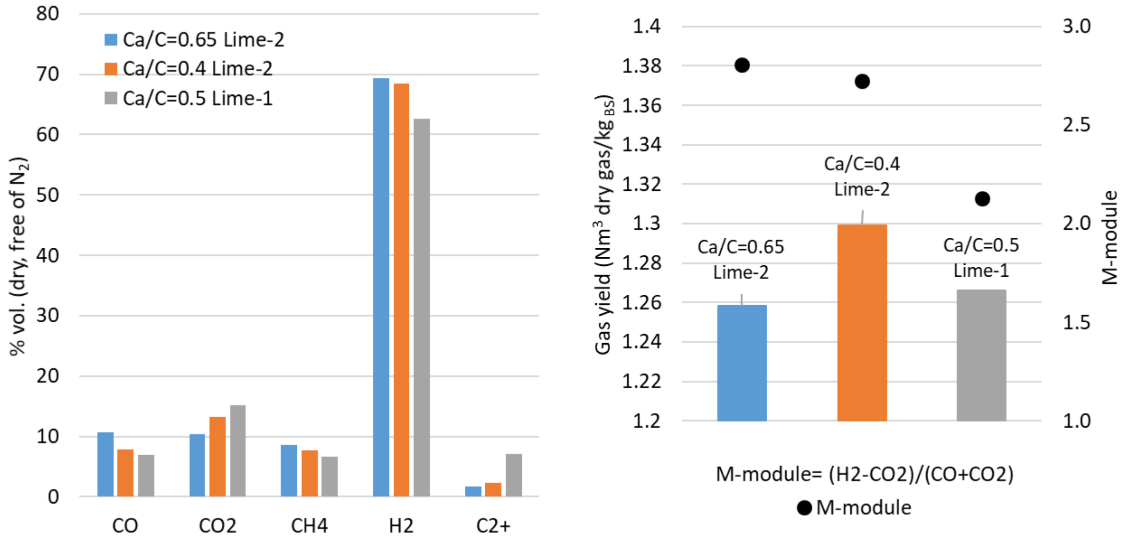

Figure 21 Gas concentration (dry and N_2 free basis) during steady state measured by GC for two different CaO/C ratios of 0.4 and 0.65 for a thermal input of grape seeds of 13 kW_{th} a constant S/C ratio of 1.8, and the two limes tested. Bed temperature was stabilized around 740 ºC

1.2.2.3 Effect of char conversion

Finally, although the data on fixed carbon conversion have been commented when analyzing the effect of the different operational variables, the following paragraphs are dedicated to resume how these variables affect to X_{FC} as the amount of unconverted char that leaves the gasifier in a dual fluidized bed SEG system influences noticeably the overall efficiency of the SEG process. The higher the conversion of the char particles in the gasifier, the higher the efficiency of the biomass-to-syngas conversion process. However, certain amount of unconverted char flowing into the combustor is needed to provide the energy for $CaCO_3$ calcination, hence avoiding the supply of additional biomass into this reactor, which would otherwise turn down the efficiency of the process. For these reasons, it is important to know which variables influence most the conversion of the char particles, as well as the influence of char conversion in the gas yield.

Figure 22 shows the gas yield and fixed carbon conversion calculated for different operating conditions (gasification bed temperature and CaO/C and S/C ratios). As noticed when comparing results obtained at different temperatures (shown in Figure 22 left), fixed carbon conversion (X_{FC}) is favored with gasifier temperature (being 18 % at 660 ºC, and 57 % at 738 ºC) and contributes to the increase in the gas yield production. The gas yield calculated for the test at 738 ºC was 1.33 Nm^3 (dry basis)/kgBS, whereas it was 0.82 Nm^3(dry basis)/kgBS for the experiment at 660 ºC. Such variation in the gas yield is also influenced by the different CCR fulfilled in these tests, since the CO_2 separated from the gas phase as $CaCO_3$(s) does not contribute to the gas production. Variation in the biomass conversion (X_{OM}) with the temperature was not as significant as the variation of X_{FC} in these two tests as the relatively high amount of volatile matter with respect to the fixed carbon content of the biomass (see analysis in Table 1) lessen the impact of such variation for fixed carbon conversion.

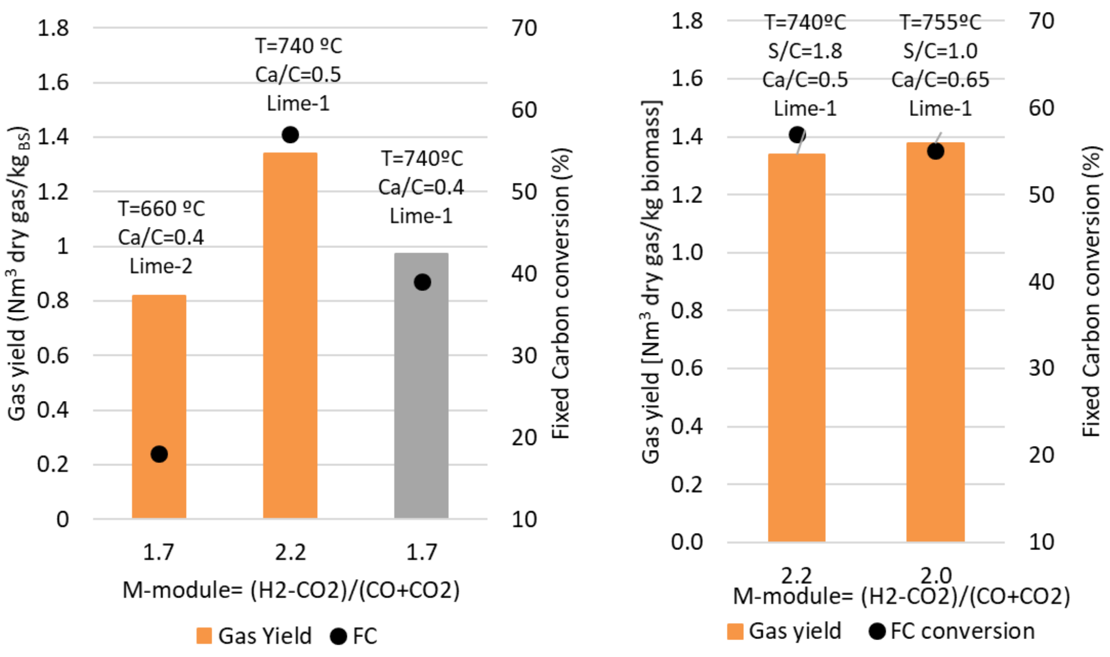

Figure 22 (left) Gas yield (Nm^3 dry/kg BS), FC conversion and M-module obtained during the steady state for two tests (grey bars) with a thermal input of 13 kW_{th} and different gasification temperature for a similar S/C of 1.8 and a 21 kW_{th} input test (white dotted bar) with similar S/C and CaO/C. (Right) Gas yield (Nm^3 dry/kg BS), FC conversion and M-module for the two tests with 13 kW_{th} thermal input performed with Lime-1, different S/C and CaO/C ratios.

In addition to the gasifier operating temperature, residence time of char particles in the gasifier can significantly affect their conversion. With the aim of assessing the impact of the char particles residence time, results obtained for a thermal input of biomass of 21 kW_{th} and a CaO/C ratio of 0.4 have been included in Figure 22 (left) (grey bar in the right hand side). As appreciated, this experiment resulted in the same solid bed temperature of 740 ºC as the left hand side experiment with lower thermal input. As noticed, reducing the solid residence time in the reactor by increasing proportionally the feeding rates of biomass and CO_2 sorbent into the gasifier influences noticeably X_{FC} and, ultimately, the gas yield. A reduction of about 60 % in the solid residence time in the gasifier makes X_{FC} to reduce from around 57 % down to 38 % while the temperature and the S/C ratio remained constant and equal to 738ºC and 1.8, respectively. Such decrease in the fixed carbon conversion translates into a lower syngas yield of 0.97 Nm^3(dry basis)/kgBS as shown in Figure 22 (left).

In Figure 22 (right) it is shown the gas yield and X_{FC} when modifying the S/C ratio at BFB gasifier inlet from 1.8 to 1.0. As appreciated, the excess of steam used for the gasification barely affects the

X_{FC} reached for the tests shown in this figure (i.e. X_{FC}= 57 % for S/C=1.8 and X_{FC}=55.1 % for S/C=1.0), being slightly reduced as the S/C ratio diminishes. The main reason of such behavior is the differences in the gasifier temperature fulfilled in each experiment, which stabilized at a higher value for the test with lower S/C ratio (i.e. 755 ºC at S/C=1.0 and 740 ºC at S/C=1.8). As a result, the higher gasification temperature reached for the experiment with a lower S/C ratio makes the X_{FC} to be increased and so gets closer to the X_{FC} fulfilled for the test with a higher S/C ratio and lower temperature.

1.2.2.4 Analysis of tars

Finally tar measurements have been performed to the tests carried out at lower gasification temperature and S/C molar ratios of 1 and 1.8 with lime #2 as bed material. Reactor bed temperature stabilized at 625-630 ºC and 660-670 ºC for these experiments with S/C ratio of 1 and 1.8, respectively. Results obtained for the analysis of the tars are shown in Table 7. The analysis revealed that the tar yields (gravimetric tar) were 47.4 g/Nm^3 and 21.1 g/Nm^3 respectively, indicating that the presence of a higher S/C in the gasifier and the difference of 30 ºC in the reactor temperature help to reduce the tar content of the produced gas.

Table 7 Pictures of the tar sampling impingers and information of the GC-MS tar characterization for the tests performed with (left) an S/C of 1 and a CaO/C of 0.25 and (right) an S/C of 1.8 and a CaO/C of 0.4

		
	TAR N	**TAR O**
Gravimetric tar (g/Nm^3 dry gas)	47.4	21.1
Gravimetric tar by GC-MS (g/Nm^3 dry gas)	18.8	7.8
Collected tar (g/Nm^3 dry gas)	57.01	28.47

The same results that for the gravimetric tar were obtained for the collected and the gravimetric tar determined by GC-MS where the increase of the solid bed temperature and the higher S/C avoided higher tar contents. The collected tar decreased with the increase of the solid bed temperature being the one-ring aromatic compounds the dominant ones independently of the solid bed temperature (Figure 23 left). Benzene, toluene and phenol were the major compounds formed during the gasification process (Figure 23 right). It is remarkable to say that ethylbenzene and 4-methyl phenol were only detected at lower temperatures. The nature of the feeding material, grape seeds containing lignin was also reflected on the formation of specific compounds like phenol and substituted phenols, which were promoted at low temperatures.

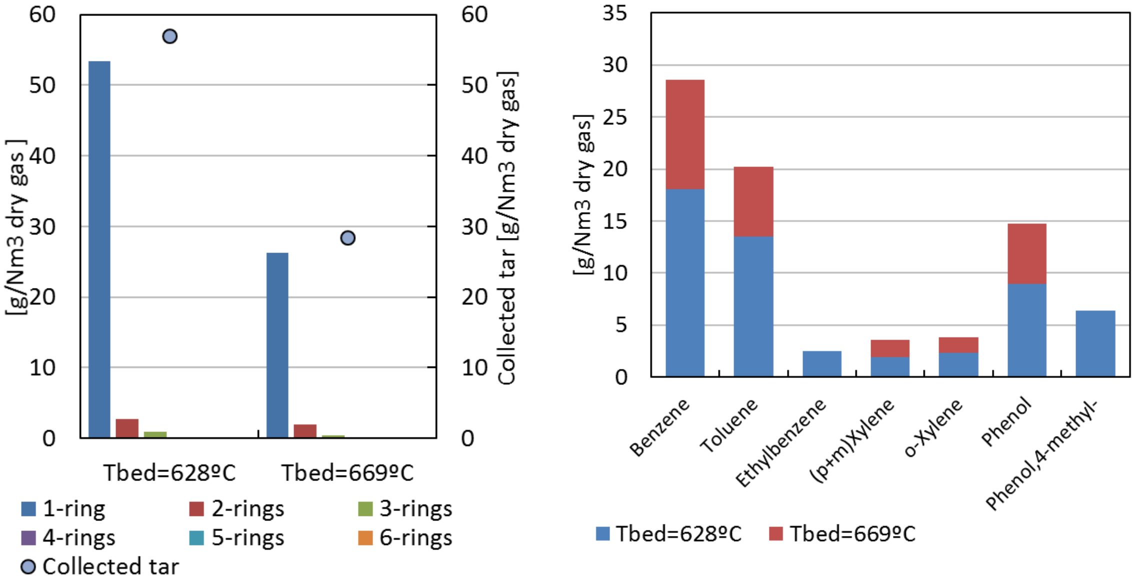

Figure 23 (left) Collected tar (calculated by GC-MS, in g/Nm^3 dry gas) and composition by number of rings compounds and (right) 1-ring compounds in the collected tar (GC-MS) for the two experiments with grape seeds collected in Table 7 that resulted in different solid bed temperature (628ºC for S/C=1 and 669ºC for S/C=1.8)

For the gravimetric tar, it was also analyzed the nature of the emitted compounds by GC-MS and it was also obtained that the lower the solid bed temperature and the lower S/C, the higher the emitted compounds (Figure 24). The one-ring compounds also prevailed on the rest of compounds and the 3-ring compounds constituted the 17-16% of the total gravimetric tar (GC-MS). In this case, the less volatile one-ring compounds were detected for the gravimetric tar with dominance of phenol and phenol, 4-methyl-. Napthalene, acenaphtylene, phenanthrene and compounds like benzo(a)anthracene and chrysene of 4-rings were also present. The influence of the solid bed temperature was reflected on the concentrations of these compounds increasing at the lowest temperature.

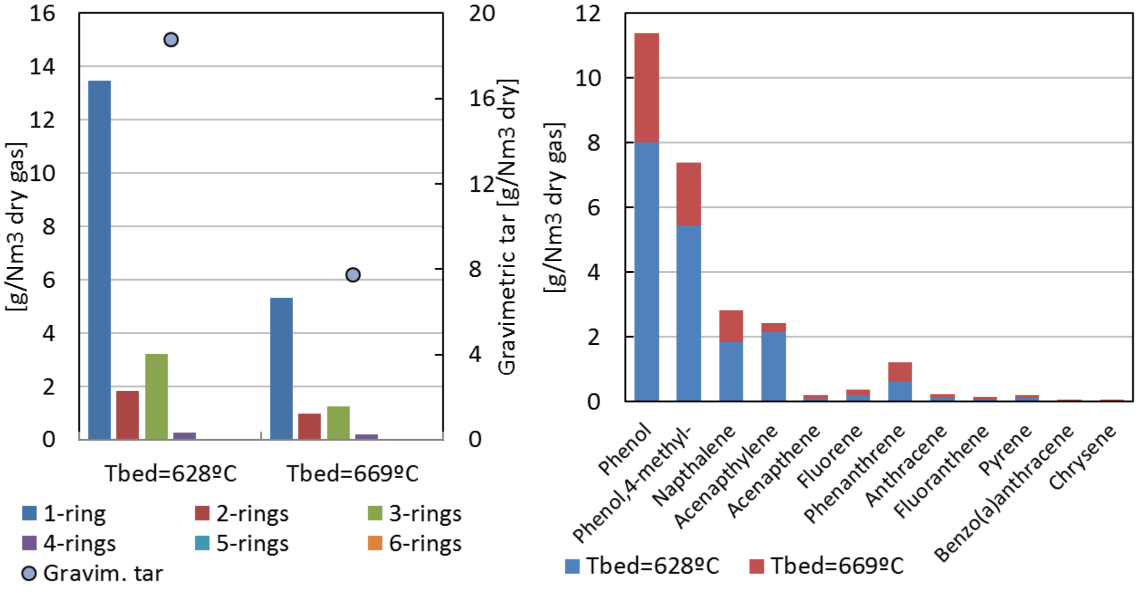

Figure 24 (left) Gravimetric tar (calculated by GC-MS, in g/Nm^3 dry gas) and composition by number of rings compounds and (right) major compounds emitted for the gravimetric tar (g/Nm3 dry) for the two experiments with grape seeds collected in Table 7

1.2.3 ECOH pellets

A total number of 11 SEG tests have been performed with ECOH pellets as biomass using the CaO/C and S/C ratios indicated in Table 8. All these tests have been carried out using calcined lime #2 as CO_2 sorbent. As appreciated in this table, the thermal input of biomass has been modified from 8.4 kW_{th} (LHV-based) until 18.4 kW_{th} to evaluate the effect of the char residence time in the BFB gasifier. Most of the experiments have been performed at an S/C ratio of around 1.4 but modifying the CaO/C molar ratio from 0.28 and 1.22 for analyzing the effect of such variable. As noticed, the values of the CaO/C molar ratio reached the maximum value of 1.22, which is noticeably larger than the maximum value of 0.65 reached for the SEG tests using grape seeds (Table 6). While performing the experimental campaign with ECOH pellets, the screw feeder of the CO_2 sorbent was heated with tracers at 400 ºC and insulated with glass wool, which allowed increasing the proportion between CaO and biomass significantly with respect to grape seeds. Using ECOH pellets as biomass, a maximum CaO flow rate of 5 kg/h was fed to the BFB gasifier, which corresponds to the test with a CaO/C ratio of 1.22 in Table 8.

Table 8 Experimental matrix of the SEG tests performed with ECOH pellets as biomass in the BFBR at ICB-CSIC. Lime #2 was used as CO_2 sorbent for all the experiments

CaO/C	S/C=1.0	S/C=1.3-1.4
1.22		9.0 kW_{th} (707-710ºC)
1.11	9.0 kW_{th} (708-710ºC)	
0.55		11.7 kW_{th} (631ºC) CaOx2*
0.50		11.3 kW_{th} (676-687ºC)
0.43		11.4 kW_{th} (682-690ºC)
0.38		11.3 kW_{th} (697-705ºC)
0.35		16.6 kW_{th} (682ºC)
0.30		8.4 kW_{th} (665-670ºC)
0.28		18.4 kW_{th} (625-635ºC) 9.2 kW_{th} (734ºC) transient
0.20	8.4 kW_{th} (616-628ºC)	

**This experiment has been performed with CaO-based CO_2 sorbent being calcined 2 times in the BFBR*

1.2.3.1 Analysis of the gas yield and char conversion

Figure 25 shows the gas yield obtained in the SEG experiments with ECOH pellets as a function of the solid bed temperature for different biomass thermal inputs. As appreciated in this figure, gas yield varied from around 0.8 Nm^3 (dry gas)/kg_{BSwaf} at temperatures around 630 ºC for a thermal input of 18.4 kW_{th} (i.e. 5.2 kg/h of biomass) to 1.6 Nm^3 (dry gas)/kg_{BSwaf} obtained at around 710 ºC, S/C=1 and 8.7 kW_{th}. For a given biomass thermal input, it is appreciated that syngas yield increases with increasing temperature, which is due to: (i) increased gas production during the primary pyrolysis stage, (ii) steam cracking and reforming of heavier hydrocarbons and tars, and (iii) enhanced char gasification reactions [7,8]. Temperature, particle size and type of biomass influence the product yields (i.e. gas or volatiles, tars and solid products) obtained in the primary pyrolysis reactions. Once this primary pyrolysis has occurred, cracking and reforming reactions as well as char gasification reactions take place. Char gasification (generally represented as $C_{(s)} \rightarrow$ CO, CO_2, H_2, CH_4) is influenced by operating parameters such as temperature, solid residence time or the steam-to-carbon ratio. In Figure 25, the effects of the solid residence time and the S/C ratio in the solid conversion into gas could be elucidated. For a given temperature the syngas yield increases with the solid residence time of the particles in the BFB gasifier through the biomass thermal input. Reducing the biomass flow rate in the gasifier the solid residence time of char particles in the BFBR gets larger (see equation (3)).

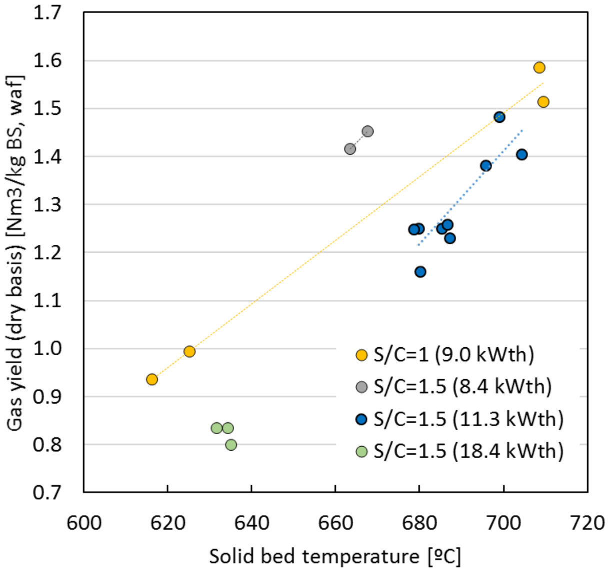

Figure 25 Gas yield (in Nm^3 of dry gas/kg of biomass, water-ash-free (waf) basis) as a function of solid bed temperature for different ECOH pellets thermal inputs

Figure 26 (left) represents the variation of the char residence time of the particles (calculated according to equation (3)) for the different experiments represented in Figure 25. In addition to the biomass thermal input, the gasifier temperature influences the char residence time in the BFBR through the expansion of the solid bed, making the residence time to diminish as temperature gets higher, as shown in Figure 26 (left). Biomass conversion X_{OM} calculated according to equation (1) for each experiment is indicated in this figure. There is no a clear influence of the temperature and the residence time on X_{OM}, and all the X_{OM} values calculated using equation (1) fall in the range between 82 and 90 %. Volatile matter constitute the major contribution to X_{OM} according to the proximate analysis of ECOH pellets (55.4 %wt. of volatile matter and 6.6 %wt. of fixed carbon as given in Table 1), being almost fully released in the gasifier since the proximate analysis of char particles collected from the overflow revealed a volatile content of 11-15 %wt. However, if representing the fixed carbon conversion X_{FC} (equation (2)) with the temperature for the different experiments with ECOH pellets such influence of temperature and residence time is elucidated (Figure 26 (right)). In this figure, the largest X_{FC} of around 70 % was reached working S/C=1.5 and relatively high residence times in the gasifier (i.e. around 48-55 min according to Figure 26 (left) for a thermal input of 8.4 kW$_{th}$) at around 670 ºC. However, X_{FC} calculated for the experiments at S/C=1.5 and smaller residence times in the BFBR (i.e. between 32 and 48 min in most of the tests with 11.3 kW$_{th}$) were markedly smaller (X_{FC} between 25 and 60 %).

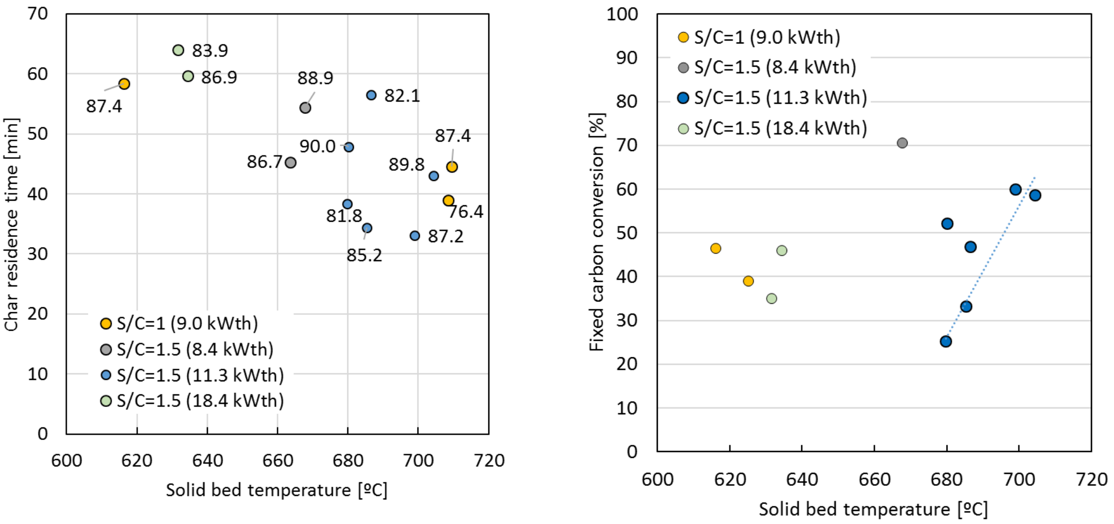

Figure 26 (left) Char residence time and biomass conversion (indicated as labels) as a function of bed temperature, and (right) fixed carbon conversion as a function of temperature for different ECOH pellets thermal inputs

1.2.3.2 Analysis of gas quality

Figure 27 compares the gas concentration measured by GC during the steady-state period for two different experiments performed at different S/C ratios (1 and 1.3) but similar CaO/C ratios (1.1-1.2) and similar solid bed temperature (707-710 ºC). Biomass thermal input was around 9 kW$_{th}$ (i.e. 2.45 kg/h) in both experiments. As it is noticed in the figure, no influence can be found in the permanent gas composition when modifying exclusively the steam-to-carbon ratio. H_2 and CO contents result in 64 %vol. and 5.4 %vol., respectively, in both experiments, whereas CO_2 concentration slightly changes (i.e. 10.6 and 11.4 %vol. for S/C=1.3 and 1.0, respectively) due to the small differences in the CaO/C molar ratio reached in each case. As a result, the M-module reached barely changed and resulted around 3 in both experiments. Based on Figure 27 (right), the steam-to-carbon ratio influences the content of light hydrocarbons (C_2-C_4) in the syngas. When increasing the steam-to-carbon ratio, the content of C_4 hydrocarbons diminishes, increasing the content of C_3H_6, C_3H_8, C_2H_4 and C_2H_6. For the experiment at S/C=1.0, C_4 compounds corresponded to trans-2-butene, 1-butene, isobutene and cis-2 butene, and it was mainly isobutene at S/C=1.3. The cracking of the C_4 hydrocarbons into C_2 and C_3 compounds, metathesis of (trans/cis)-2-butene and 1-butene into propene or self-metathesis of 1-butene into ethane could be favored when increasing the S/C ratio aided by the presence of K, Al, Si, Mg in biomass ashes, which would explain the increase of C_3 and C_2 olefins as well as C_2H_6 when increasing the S/C ratio at a constant gasification temperature.

In terms of fixed carbon conversion, X_{FC} resulted about 24% for the experiment at S/C=1.0 and around 22 % for the experiment at S/C=1.3 (both experiments at the same temperature). The influence of the S/C ratio in the X_{FC} reached is not significant since the variation in the S/C value is not so important, and the differences in the CaO/C ratio make the solid residence time of the char particles to be also affected (larger residence time for the experiment with lower CaO/C ratio, i.e. with S/C=1.0). As a result of this similar X_{FC}, gas yield obtained in both cases is similar (around 0.9-0.94 Nm^3 (dry gas)/kg$_{BSwaf}$). Concerning the conversion of the CaO particles collected from the overflow, the $CaCO_3$ content calculated was around 0.17-0.18 mol$_{CaCO3}$/mol$_{Ca}$ for the experiment at S/C=1.3 (CaO/C=1.2) and around 0.17-0.19 mol$_{CaCO3}$/mol$_{Ca}$ for the experiment at S/C=1.0 (CaO/C=1.1). This small difference between both values is linked to the small difference in the sorbent-to-biomass proportion in each case (i.e. the CaO/C ratio), which makes that for the same amount of CO_2 released the carbonation degree of CaO particles gets slightly higher for the test with smaller CaO/C ratio. The Carbon Capture Ratio has been estimated with the Carbon balance to the solids (i.e. CO_2 separated= CO_2 as $CaCO_3$ with the overflow solids and cyclone solids; CCR=CO_2 separated/C fed with the biomass), and it resulted around 22 % for both experiments.

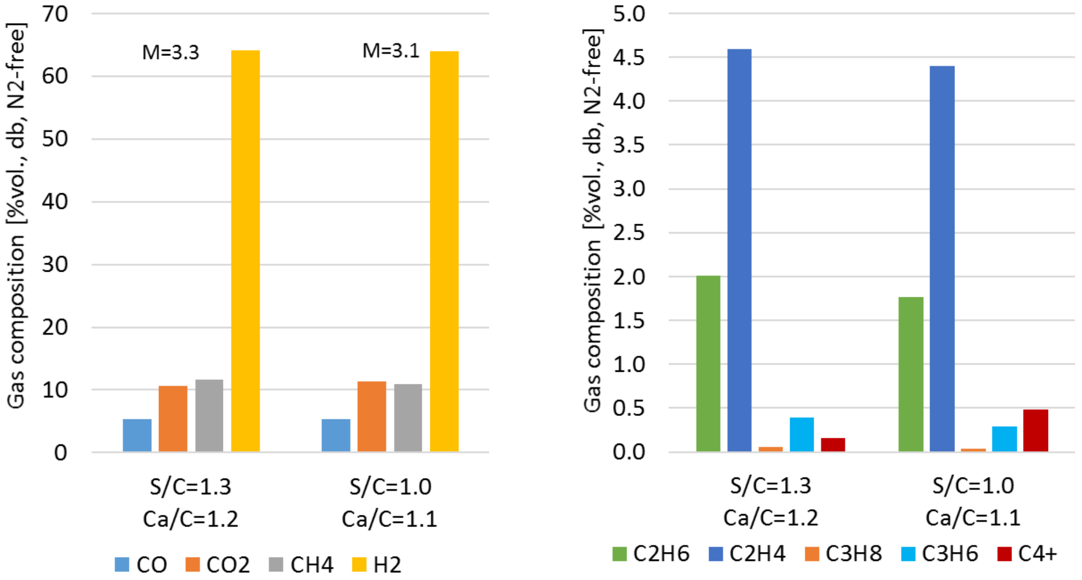

Figure 27 Gas concentration (dry and N_2 free basis) during steady state measured by GC for two different S/C ratios of 1.3 and 1.0 for a thermal input of ECOH pellets of 9 kW_{th}. Stabilization temperature of the solid bed during the experiments was around 707-710 ºC in both experiments

The influence of the S/C ratio on the tar formation can be also evaluated for the two experiments represented in Figure 27. Values of collected tar calculated by GC-MS and the amount of each group of compounds with different number of rings for these two experiments have been depicted in Figure 28 (left). As it is observed, the increase of the S/C ratio seemed to promote tar formation, not only the collected tar but also the gravimetric tar, which corresponded to values of 7.82 and 6.26 g/Nm^3 dry respectively for the S/C=1.3 and S/C=1.0. When the composition of the collected tar by rings number was compared, it was observed that one-ring followed by 2 and 3-rings compounds were the major compounds independently of the S/C ratio.

In Figure 28 (right) the amount of the major compounds in the collected tar by GC-MS are represented. When increasing the S/C ratio, the formation of naphthalene (the only 2-ring compound determined) was favored with percentages of 9% versus 7% at the lowest S/C ratio. Moreover, regarding the 1-ring compounds, the formation of high molecular weight 1-ring compounds such as toluene and phenol was also promoted at the higher S/C ratio compared to benzene, which decreased with an increasing S/C ratio (i.e. from 69 % at S/C=1.0 to 58 % at S/C=1.3). As appreciated in Figure 28 (right), phenol disappeared at the lower S/C ratio of 1.0 at the temperature of 707-710 ºC chosen for this comparison. As noticed in Figure 27 (right), at high S/C ratios, the presence of C_2H_4 in the syngas was favored, which is known to be a precursor of aromatic rings formation. Therefore, the larger content of C_2H_4 at S/C=1.3 would explain the increase of aromatic compound tars.

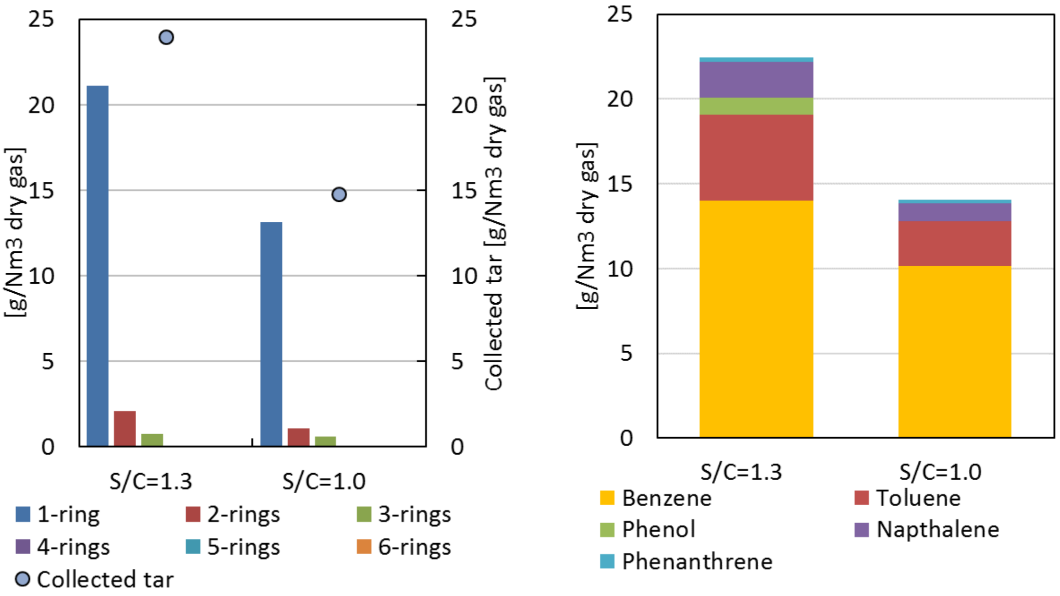

Figure 28 (left) Collected tar (calculated by GC-MS, in g/Nm^3 dry gas) and composition by number of rings compounds and (right) major compounds in the collected tar (GC-MS) for two experiments with ECOH pellets at different S/C ratios of 1.3 and 1.0, but similar solid bed temperature (707-710ºC) and thermal input (9 kW$_{th}$)

Figure 29 allows evaluating the effect of the gasification temperature on the syngas composition. The molar CaO/C ratio used in the experiments compared in this figure was 0.28, whereas the S/C ratio was similar but not the same (i.e. S/C=1.24 for the experiment with 9 kW$_{th}$ of biomass input and S/C=1.4 for the experiment with 18.4 kW$_{th}$ of biomass input). As noticed in Figure 29 (left), gasification temperature influences the content of permanent gases, especially CH_4, CO and CO_2 concentrations. An increase in the temperature favors the endothermic water gas reactions of $C_{(s)}$ into CO, CO_2 and H_2 (4-5), as well as the Boudouard (6), water gas shift (7) and methane reforming (8) reactions [7]. Consequently, considering these reactions, the content of H_2, CO, CO_2 should increase with the temperature whereas the CH_4 content should diminish. However, the presence of the CaO carbonation reaction (9) influences such trend since CaO reacts with the CO_2 from the gas phase. As temperature increases, the CaO/$CaCO_3$ equilibrium limits the carbonation kinetics towards $CaCO_3$ formation and the carbonation degree, which makes the CO_2 content in the gas phase to increase [9]. Based on this behavior, CO_2 content in the syngas increases from 7.6 %vol. (H_2O-N_2 free basis) at 635 ºC to 15.5 %vol. at 734 ºC as appreciated in Figure 29 (left). Water gas shift reaction (7) links CO and CO_2 behavior in the gas phase, favoring CO conversion into CO_2 as CO_2 is removed from the gas phase through the carbonation reaction (9). For this reason, CO content in the syngas is raised when CO_2 content gets larger, and vice versa. H_2 content increases up to 53 %vol. (H_2O-N_2 free basis) when decreasing the gasifier temperature down to 635 ºC since the carbonation and water gas shift reactions are favored when moving down in temperature, which enhances H_2 formation. The combination of the behavior explained for CO, CO_2 and H_2 contents in the syngas makes the M-module reached at 635 ºC to be 3.8 whereas it is 1.2 at 734 ºC under the operating conditions represented in Figure 29.

$$C + H_2O \rightarrow CO + H_2 \qquad (4)$$
$$C + 2H_2O \rightarrow CO_2 + 2H_2 \qquad (5)$$
$$C + CO_2 \rightarrow 2CO \qquad (6)$$
$$CO + H_2O \leftrightarrow CO_2 + H_2 \qquad (7)$$
$$CH_4 + H_2O \leftrightarrow CO + 3H_2 \qquad (8)$$
$$CaO + CO_2 \leftrightarrow CaCO_3 \qquad (9)$$

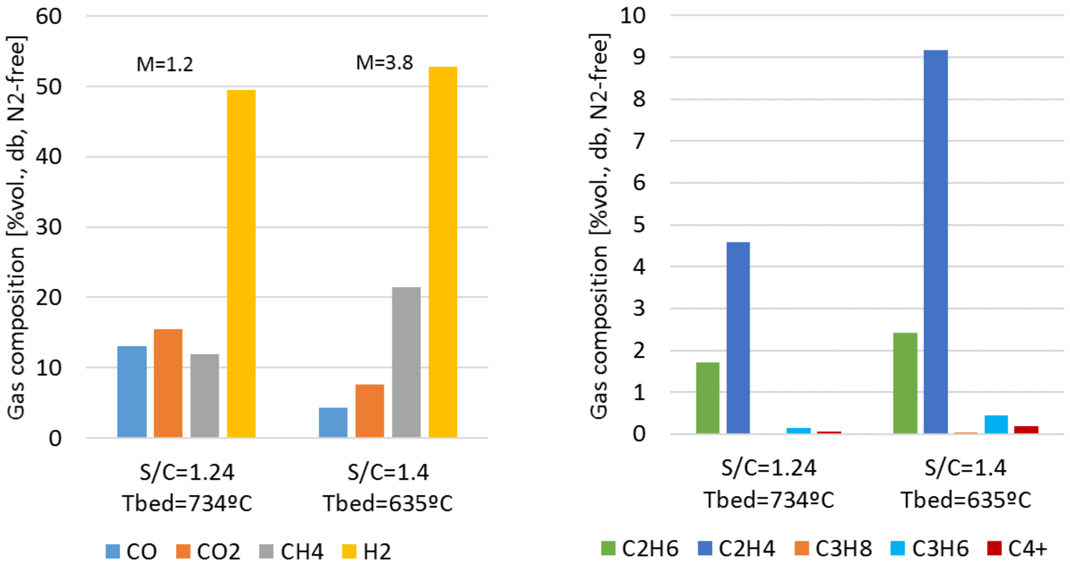

Figure 29 Gas concentration (dry and N_2 free basis) during steady state measured by GC for two experiments with similar CaO/C ratio (0.28) and different ECOH pellets thermal inputs of 9 and 18.4 kW_{th} (S/C=1.24 and 1.4, respectively)

Cracking and reforming reactions of light and heavy hydrocarbons are favored with the temperature, making the light hydrocarbons content (i.e. C_2-C_4) to be greatly reduced with this variable as shown in Figure 30. As appreciated in this figure, CH_4 content is the compound being influenced the most by the temperature, accounting for around 21 %vol. (dry basis and N_2-free syngas) at the lowest temperature (635 ºC) and decreasing to 12 %vol. when increasing the gasification temperature to 734 ºC. C_2H_4 content is also noticeably reduced with the gasification temperature although not as deeply as CH_4, being reduced to less than 5 %vol. at 734 ºC. Information shown in Figure 30 corresponds to experiments performed at an S/C of 1.3-1.4, therefore larger hydrocarbon contents may be expected when decreasing the S/C ratio below such values.

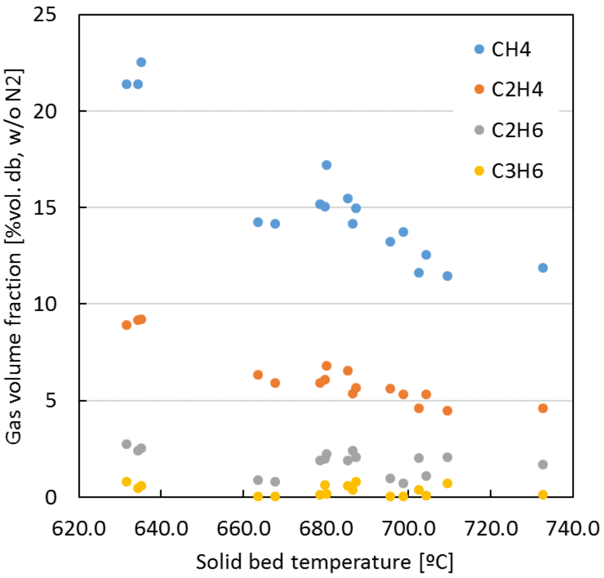

Figure 30 Variation of the CH_4, C_2H_4, C_2H_6 and C_3H_6 contents in the syngas (H_2O and N_2-free basis) as a function of the solid bed temperature at an S/C ratio of 1.3-1.4 for ECOH pellets

Figure 31 allows evaluating the influence of the gasification temperature on tar formation for the two SEG experiments compared before for evaluating such influence on syngas composition (i.e. CaO/C ratio of 0.28, S/C ratio similar but not the same and different solid bed temperature, 635 and 734 ºC). As it is noticed in Figure 31 (left), lower solid bed temperatures favored the formation of high contents of collected tar (62.2 g/Nm^3 dry gas) when compared to the higher solid bed temperature (23.9 g/Nm^3 dry gas). The same behavior was observed for the gravimetric tar values, which resulted in 7.4 and 43.2 g/Nm^3 dry gas at 732 ºC and 635 ºC, respectively. Moreover, 4-ring compounds were detected in the collected tar by GC-MS at 635 ºC that were not detected in the experiment at 732 ºC. If the individual composition of the major compounds detected in the collected tar is analyzed (Figure 31 (right)), it can be observed that benzene was the major compound emitted in both cases, followed in quantity by toluene and naphthalene. When the gasification temperature decreases from 734 ºC to 635 ºC, the major compounds (i.e. benzene, toluene, phenol, naphthalene and phenanthrene) increase but those with higher ring number (naphthalene and phenanthrene) increase in a larger proportion (i.e. by a factor of 4 compared to a factor of 2 for 1-ring compounds). In this way, low solid bed temperatures promoted the formation not only of tars content but also of higher rings compounds, which are undesirable from an experimental point of view in a gasification process.

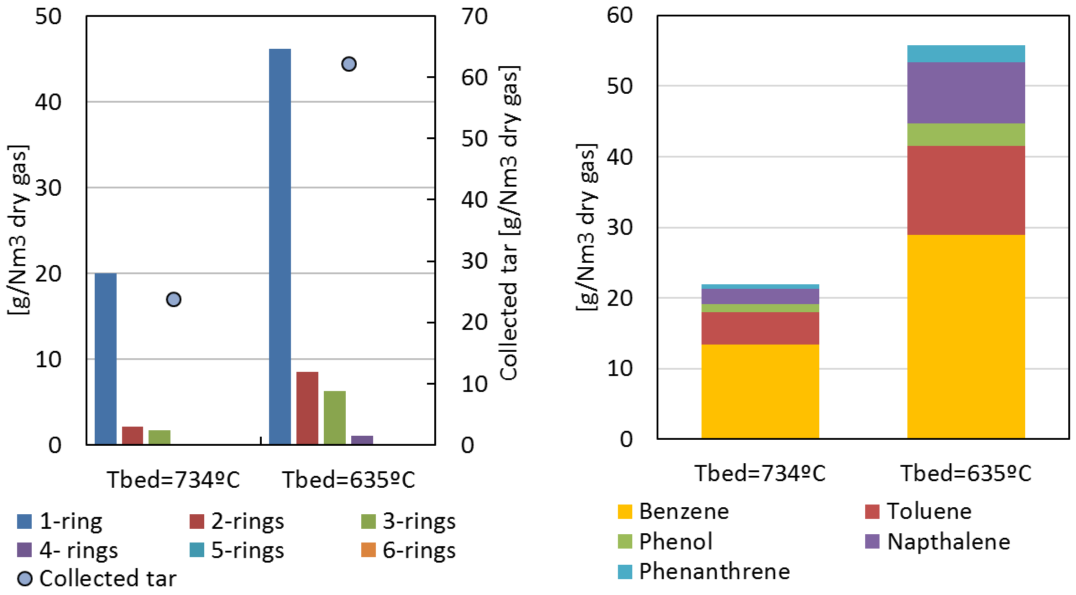

Figure 31 (left) Collected tar (calculated by GC-MS, in g/Nm^3 dry gas) and composition by number of rings compounds and (right) major compounds in the collected tar (GC-MS) for two experiments with ECOH pellets at different solid bed temperatures (734 and 635 ºC). Similar CaO/C molar ratio (0.28) and S/C ratio (i.e. S/C=1.24 and 1.4) were used in both experiments

Finally, the influence of the sorbent-to-biomass ratio on the syngas composition is evaluated. Figure 32 compares the syngas composition measured by GC for two different SEG experiments performed with similar S/C ratio (1.3-1.4) and similar solid bed temperature but with substantially different CaO/C molar ratios (i.e. 0.4 and 1.2). Main influence of the CaO/C ratio is found in the C_3-C_4 hydrocarbons content (Figure 32 (right)), which represented 0.15 %vol. (H_2O-N_2 free basis) at CaO/C=0.38 and 0.61 %vol. (H_2O-N_2 free basis) at CaO/C=1.22. Such increase at a higher sorbent-to-biomass ratio is linked to the catalytic tar cracking effect of the CaO, which is confirmed when increasing the CaO/C ratio (as explained below) and so makes the aromatic tar compounds to be cracked into linear olefins and non-saturated C_2-C_4 hydrocarbons. Concerning the concentration of CO_2 in the syngas, even if it is not appreciated in Figure 32 due to the H_2O-N_2 free basis, CO_2 content in the syngas remained constant around 3.5-3.9 %vol. (including N_2 and H_2O) for both experiments shown in Figure 32 since temperature remained stable at 705-707 ºC in both tests. Similarly, the CO content that is linked to the CO_2 content through the water gas shift equilibrium (as explained before) remained constant at 1.8-2.0 %vol. (including N_2 and H_2O) for both tests. However, the H_2 content remained around 24-28 %vol. (inc. H_2O and N_2) for the test at CaO/C=0.38 and around 19-24 %vol. (inc. H_2O and N_2) when working at CaO/C=1.22. This behavior is linked to the fixed carbon conversion of the biomass into H_2 (reactions 4-5), which is larger for the experiment at smaller CaO/C ratio (X_{FC} around 22 % at CaO/C=1.22 and around 60 % at CaO/C=0.38) since the solid residence time was significantly increased by 2-3 times when decreasing the CaO/C ratio. As a result of the combination of large solid residence times and larger conversion of $C_{(s)}$ into CO and CO_2, $CaCO_3$ content of the sorbent particles resulted in 0.45-0.56 mol_{CaCO3}/mol_{Ca} for the experiment at CaO/C=0.38.

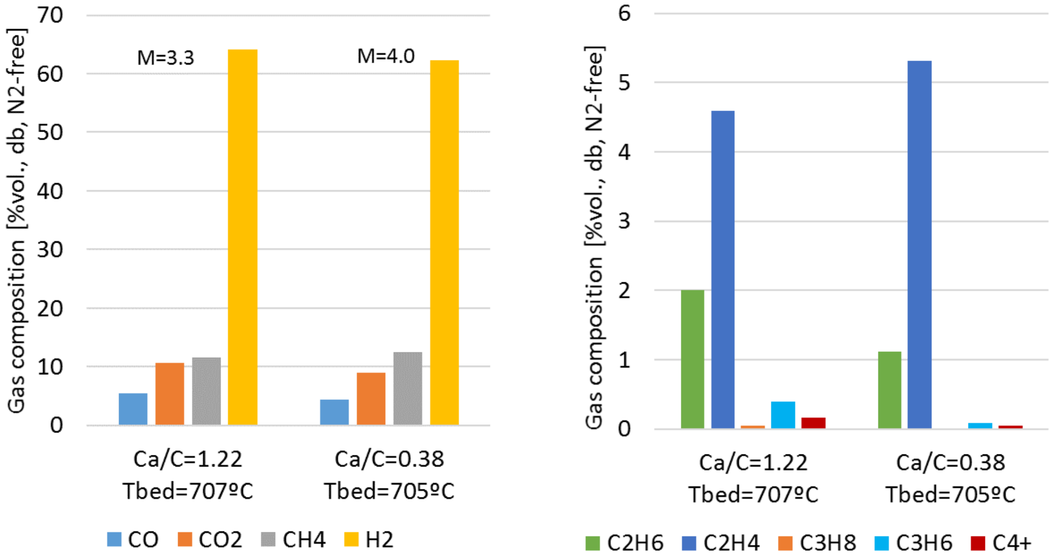

Figure 32 Gas concentration (dry and N_2 free basis) during steady state measured by GC for two experiments with similar S/C ratio (1.3-1.4) and similar solid bed temperature (705-707 ºC) but different CaO/C molar ratio using ECOH pellets as biomass

Figure 33 allows evaluating the influence of the sorbent-to-biomass ratio on tar formation for the two SEG experiments compared before for evaluating such influence on syngas composition. Solid bed temperature and S/C ratio were similar in these two experiments (i.e. 705-707ºC and 1.3-1.4, respectively). It can be observed that the higher CaO/C ratio improves the effectiveness of the catalytic role of the CaO in tar cracking by decreasing the collected tar (Figure 33 (left)) from 33.2 g/Nm^3 dry gas at CaO/C=0.38 to 24.0 g/Nm^3 dry gas at CaO/C=1.22. The gravimetric tar, not depicted in Figure 33, also showed a remarkable increase with the decrease in the CaO/C ratio, corresponding to values of 7.8 and 24.8 g/Nm^3 dry gas for CaO/C =1.22 and 0.38, respectively, corroborating the beneficial role of CaO on the tar formation. This catalytic activity of CaO was also observed in the composition of the major emitted compounds in the collected tar (Figure 33 right) by avoiding at high Ca/C ratios the formation of 4-6 ring compounds, the heaviest compounds, which are the most dangerous polycyclic aromatic hydrocarbons (PAH) for human health. Although in Figure 33 (left) it cannot be appreciated, for the Ca/C=0.38 the 4-rings compounds were 0.05 g/Nm^3 dry disappearing at Ca/C=1.22. With regard to the individual compounds, benzene was the major emitted compound and lower ratios of Ca/C increased the proportion of 2-rings compounds like naphthalene and heavier compounds like phenanthrene. One exception was phenol, which was only emitted at the highest Ca/C ratio as noticed in Figure 33 (left).

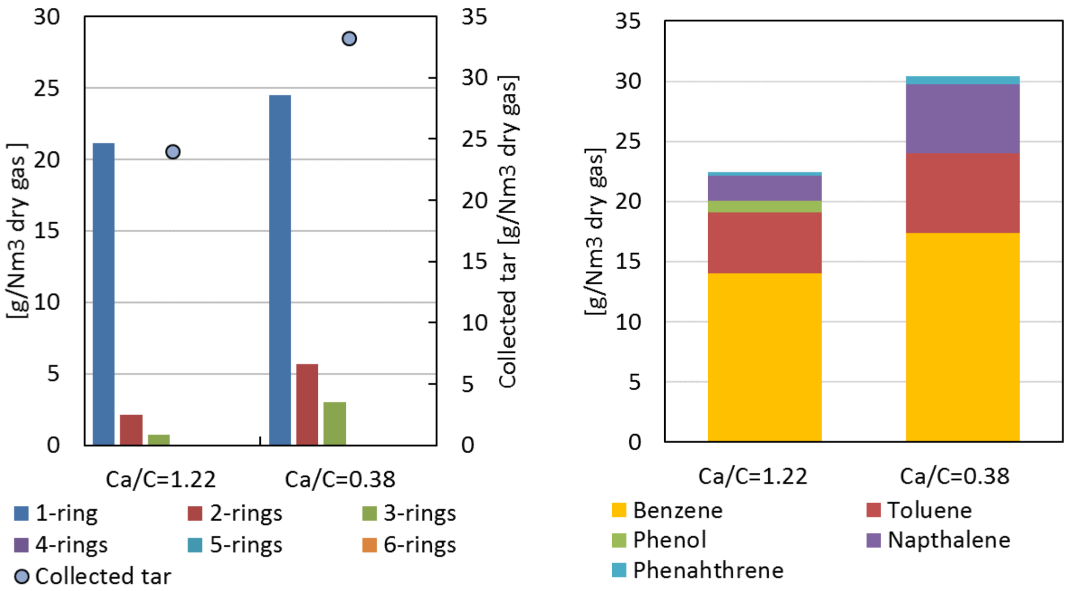

Figure 33 (left) Collected tar (calculated by GC-MS, in g/Nm^3 dry gas) and composition by number of rings compounds and (right) major compounds in the collected tar (GC-MS) for two experiments with ECOH pellets at different CaO/C ratios (1.22 and 0.38). Similar solid bed temperature (705-707 ºC) and S/C ratios (1.3-1.4) were used in both experiments

1.2.3.3 Analysis of the sulfur compounds

Figure 34 shows the distribution of the Sulphur introduced with the biomass among the solid (i.e. unconverted char and partially converted sorbent collected from the overflow) and gas products. As indicated, as the solid bed temperature increases and the conversion of the organic fraction of the biomass is enhanced, S remaining in the char becomes smaller since part of the S should be linked to the organic fraction of the biomass and so it is released to the gas phase as biomass conversion proceeds. Once in the gas phase, it could be detected as H_2S, COS and CH_4S in the gas (S_{gas} in Figure 34) or be retained as CaS by the CaO in the sorbent. In all the SEG tests performed with ECOH pellets, CaS content in the sorbent particles remained below 1 %wt. Similarly, S in the char particles collected was always below 1 %wt.

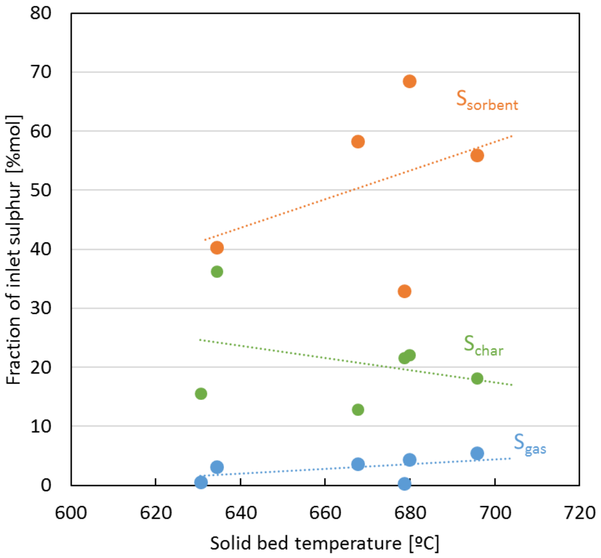

Figure 34 Sulfur fate as a function of solid bed temperature for SEG experiments with ECOH pellets

1.2.3.4 Analysis of tars

For the 11 experiments performed with ECOH pellets the sampling of tars was undergone. As explained throughout the previous sections, the gravimetric tar (weight) and the collected and gravimetric tars by GC-MS were determined, although the analysis by GC-MS of the gravimetric tar was only carried out for a set of experiments. In Figure 35 it is shown the collected tar and the gravimetric tar (weight) as a function of the solid bed temperature. Results indicated a negative trend, decreasing both, the collected and gravimetric (weight) tars, with an increase of solid bed temperature. Overall, this trend was more remarkable for the collected tar than for the gravimetric tar, although as appreciated there are a couple of points where this trend was less accurate due to the highest temperature difference between the freeboard and the bed reactor temperature, increasing in this way the gravimetric tar content.

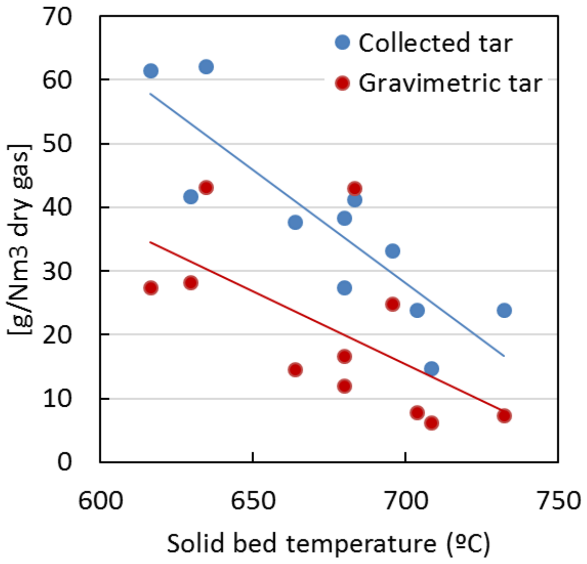

Figure 35 Collected tar and gravimetric tar (weight) as a function of the solid bed temperature for the SEG tests with ECOH pellets

Figure 36 shows the differences in collected tar composition as a function of the gasification conditions for these SEG tests with ECOH pellets. As observed, 1-, 2- and 3-ring compounds decrease with the solid bed temperature. Moreover, independently of temperature, the 1-ing compounds were the major compounds found in the collected tar and the ones being affected the most by the temperature.

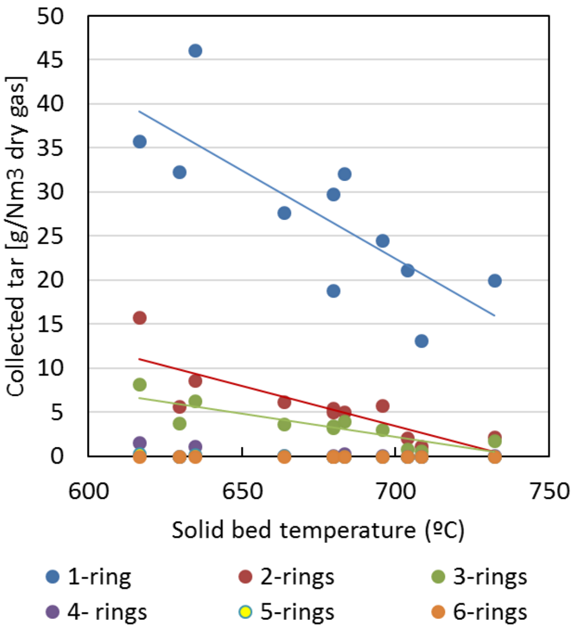

Figure 36 Composition of the collected tar (g/Nm^3 dry gas) by rings number as a function of the solid bed temperature for the SEG tests with ECOH pellets

Analyzing the composition of the individual compounds for the collected tar (Figure 37), the hydrocarbons with 1-ring were the major compounds emitted in the gasification process independently of the solid bed temperature, being benzene the major compound formed with contributions between 43-79 % to the collected tar. Toluene was the second compound detected at high concentrations among the 1-ring compounds and phenol was only present at specific conditions (629, 635, 680, 683, 704 and 732 ºC). Naphthalene, the only 2-ring compound determined, also contributed remarkably to the collected tar with percentages that ranged between 7 and 26 %. Phenanthrene was the most contributing compound in the group of 3-rings compounds. The results for the individual compounds of the collected tar revealed not a clear trend with the temperature contrary to what happened with the 1, 2 and 3-rings compounds that decreased with increasing temperatures.

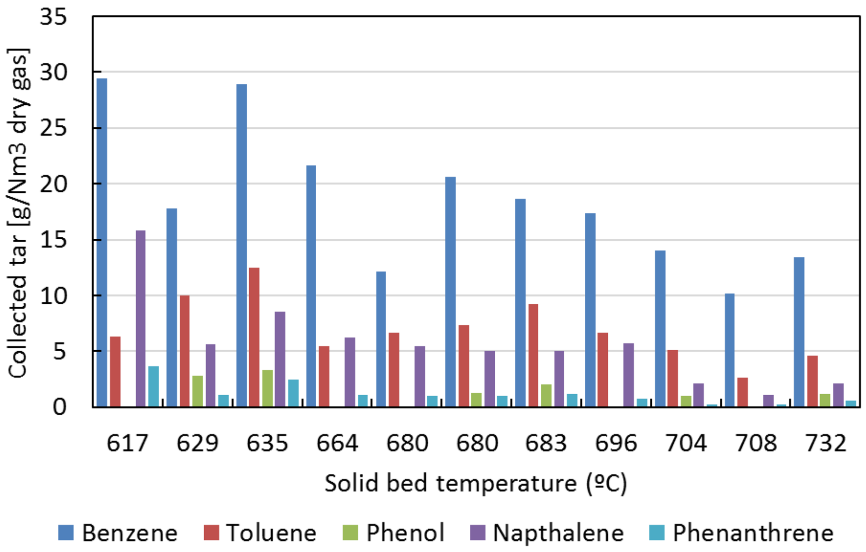

Figure 37 Major compounds emitted for the collected tar (g/Nm^3 dry gas) as a function of the solid bed temperature for the SEG tests with ECOH pellets

For the gravimetric tar (GC-MS), hydrocarbons with 2-rings followed by 3-rings were the dominant compounds (Figure 38). This could be expected due to the nature of the gravimetric tar, which has been evaporated in a rotary evaporator decreasing the concentration of the most volatile compounds such as benzene, toluene and xylenes (see tar characterization procedure in section 1.1.2.4). The influence of the solid bed temperature was not as remarkable as for the collected tar, with the exception of 2 and 3-rings compounds at the lowest solid bed temperature.

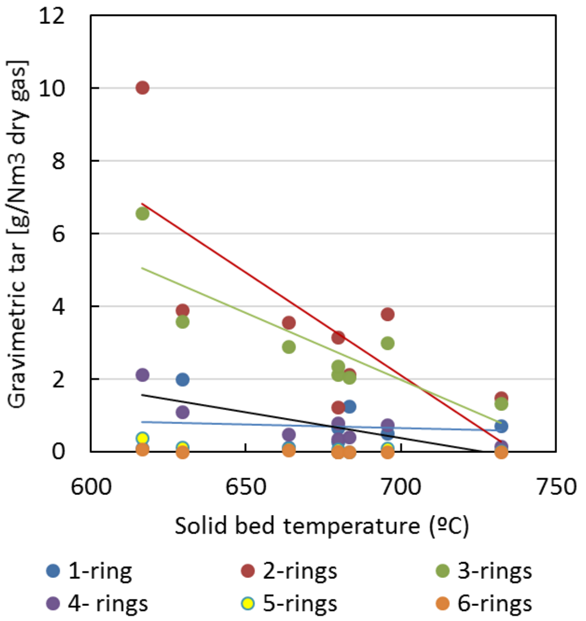

Figure 38 Composition of the gravimetric tar (g/Nm3 dry) by rings number as a function of the solid bed temperature for the SEG tests with ECOH pellets

In this case, naphthalene was the compound formed at higher concentrations following a slight negative trend with the solid bed temperature and with percentages varying between 27-52% of the gravimetric tar (GC-MS) (Figure 39). Other compounds with remarkable contribution were phenanthrene, fluorene and anthracene in the group of 3-ring compounds. Regarding the 1-ring compounds, only phenol contributed in some cases to the gravimetric tar followed by phenol, 4-methyl-.

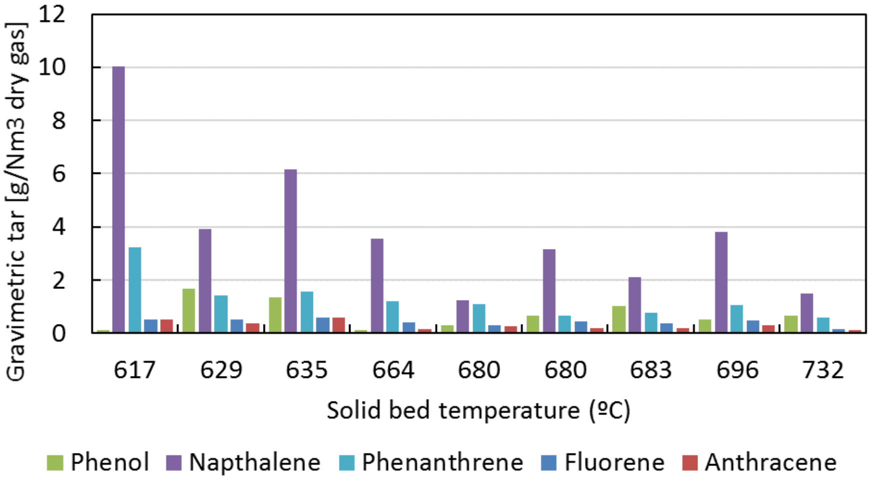

Figure 39 Major compounds emitted for the gravimetric tar (GC-MS) (g/Nm^3 dry gas) as a function of the solid bed temperature for the SEG tests with ECOH pellets

1.2.3.5 Transient test

A transient SEG test was performed with ECOH pellets in order to follow the evolution of the syngas composition and solids conversion with the time. Moreover, two samples of tar were taken during this transient experiment: one at the beginning when the solid bed consisted mainly of CaO (referred to as "tar P1") and the second one at the end when the solid bed reached an almost constant content of $CaCO_3$ (referred to as "tar P2"). This last sample corresponded to the steady-state period in the experiments shown before (as explained in section 1.1.3.1). A reduced flow rate of 2.6 kg/h of ECOH pellets was used for this test to ensure that the solid bed was converted at a sufficiently low rate as for following the fulfillment of the steady state through solid sampling. Moreover, a minimum CaO flow rate of 1.1 kg/h was set in order to push the solids out from the BFBR through the overflow and so allow taking solid samples. Both solid flows resulted in a CaO/C ratio of 0.28 as indicated in Table 8. The steam-to-carbon ratio used for this experiment was 1.3 as indicated in such table.

Figure 40 shows the temperatures, syngas composition and solid composition profiles as a function of time from the beginning of the experiment (when biomass started to be fed into the BFBR). Grey zones indicate the tar sampling periods performed during this experiment. H_2 content in the gas reached its maximum value of 57 %vol. (H_2O and N_2 free basis) at the beginning of the experiment when the sorbent particles were practically CaO with very low $CaCO_3$ content (0.06-0.08 mol_{CaCO3}/mol_{Ca}) and so the carbonation of CaO proceeded at its maximum allowable rate. CH_4, C_2H_4 and C_2H_6 contents in the syngas were practically constant since the solid bed temperature remained constant at an average value of 734 ºC (average between thermocouples placed in the solid bed reactor according to the scheme shown in Figure 2). CO_2 concentration in the syngas increased with the time as the sorbent present in the solid bed was progressively converted and less CaO was then available for reacting with the CO_2 formed. In this transient test, the CaO fed to the reactor was not enough for reacting with the CO_2 generated from gasification reactions (4-5).

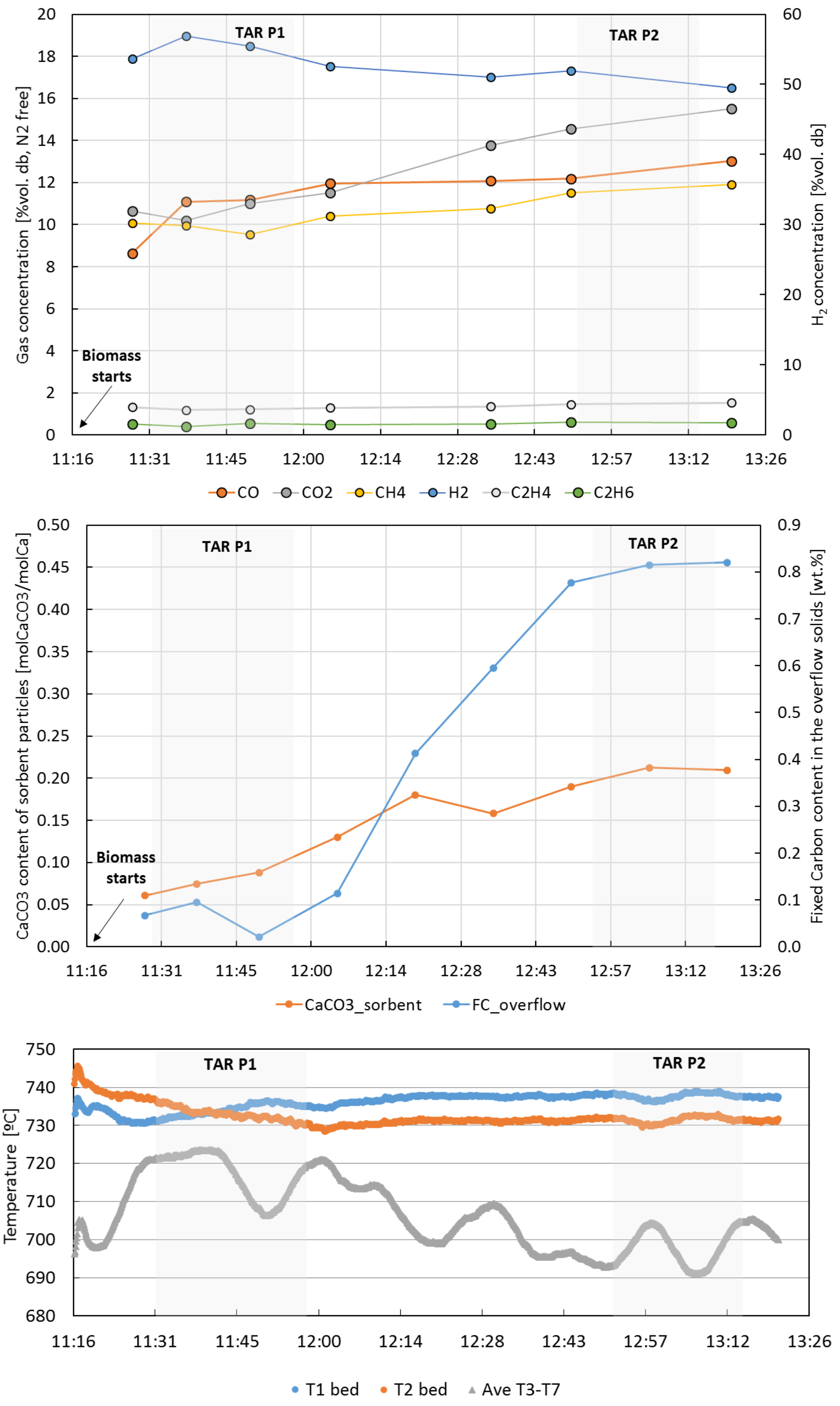

Figure 40 Syngas composition profile (H_2O and N_2 free basis) measured by GC (up), solid composition ($CaCO_3$ and fixed carbon content) in the solids collected in the overflow (middle) and temperature profile along the BFBR (down) during the transient SEG experiment performed with ECOH pellets

Table 9 collects the characterization of the two tar samples taken during this transient experiment. As explained, two tar sampling measurements were done during this experiment to check the influence of the catalytic role of CaO on the tar composition. Tar P1 corresponded to a tar sample taken when the CaO was fresh, it means, with full catalytic activity whereas tar P2 was taken after the gasification plant was already working after some time and the CaO was partially carbonated. The obtained results proved that independently of the determined tar (gravimetric, collected and gravimetric tar (GC-MS), the presence of more active CaO decreased the tar formation. Regarding the nature of the tar composition, it was observed that the presence of more active CaO avoided the formation of heavier compounds, in particular those with 3- or more rings, with more than 90% of the tar composition associated with compounds with one aromatic ring for the collected tar. In both cases, benzene was the major compound emitted, followed by toluene and naphthalene (Figure 41).

Table 9 Pictures of the impingers and tar characterization for the tar samples P1 and P2 taken during the transient SEG experiment with ECOH pellets as biomass

	 **TAR P1**	 **TAR P2**
Gravimetric tar (g/Nm^3 dry gas)	4.61	7.42
Gravimetric tar by GC-MS (g/Nm^3 dry gas)	2.04	3.67
Collected tar (g/Nm^3 dry gas)	19.60	23.90
Composition of the collected tar		
1-ring comp. (g/Nm^3 dry gas)	17.84	20.00
2-ring comp. (g/Nm^3 dry gas)	1.42	2.14
3-ring comp. (g/Nm^3 dry gas)	0.35	1.75
4-5-6-ring comp. (g/Nm^3 dry gas)	0	0.02

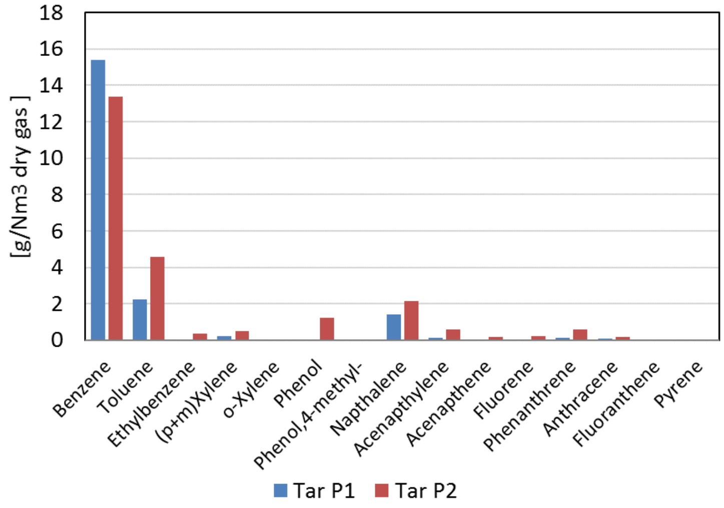

Figure 41 Major compounds emitted for the collected tar (g/Nm^3 dry gas) at the beginning (P1) and at the end (P2) of the transient test with ECOH pellets

1.2.4 ECOH biomass

For the ECOH biomass shown in Figure 3 it has been carried out one SEG experiment, corresponding to a biomass thermal input of 9.6 kW_{th} (i.e. 2.70 kg/h of biomass), a CaO/C ratio of 1 and using an S/C ratio of 1.8. The handling of this feedstock was not easy since it formed cavities in the hopper, being difficult to have a continuous flow of biomass into the reactor. Solid bed temperature stabilized at around 670-672 ºC in this SEG test. Composition of the syngas obtained is shown in Figure 42. As appreciated, H_2 content in the syngas reached 65 %vol. (H_2O-N_2 free basis), which is close to the value of 64 % reached for ECOH pellets SEG testing with S/C=1.0 and 1.3 and a CaO/C ratio of 1.1-1.22 at around 705 ºC (tests chosen for S/C analysis in section 1.2.3.2). Biomass composition for ECOH pellets and ECOH biomass is rather similar (see Table 1) and therefore results obtained should not be so different. As already observed when analysis gas quality for ECOH pellets, the influence of the S/C ratio on permanent gas composition was not significant when gasification temperature was kept constant. However, for this SEG test with ECOH biomass, solid bed temperature remained constant at around 670 ºC, which is around 35 ºC less than for the mentioned SEG tests with ECOH pellets. As a result of this lower temperature, CO_2 content in the syngas becomes smaller since it is determined by the $CaO/CaCO_3$ equilibrium [9]. Consequently, due to the influence in the water gas shift reaction (7), CO content reduces also and M-module reached becomes higher than at 705 ºC (i.e. M=4.1 compared to M=3.1-3.3 in the SEG tests compared in section 1.2.3.2). Regarding CH_4 content, it was around 14 %vol. (H_2O-N_2 free basis), slightly higher than the CH4 content measured in the SEG tests with ECOH pellets at 705 ºC, as expected according to Figure 30. Another important difference can be observed in the C_2-C_4 hydrocarbons content, which accounts for 12 %vol. (H_2O-N_2 free basis) in the SEG test with ECOH biomass. This light hydrocarbons content is between 3.5 and 5 percentage points higher than the C_2-C_4 content measured during SEG tests with ECOH pellets and similar solid bed temperature. The larger S/C ratio fulfilled in this case (1.8 vs. 1.3-1.4) could explain this result since it favors the cracking of heavier compounds into lighter ones (as observed also in the tar analysis explained below).

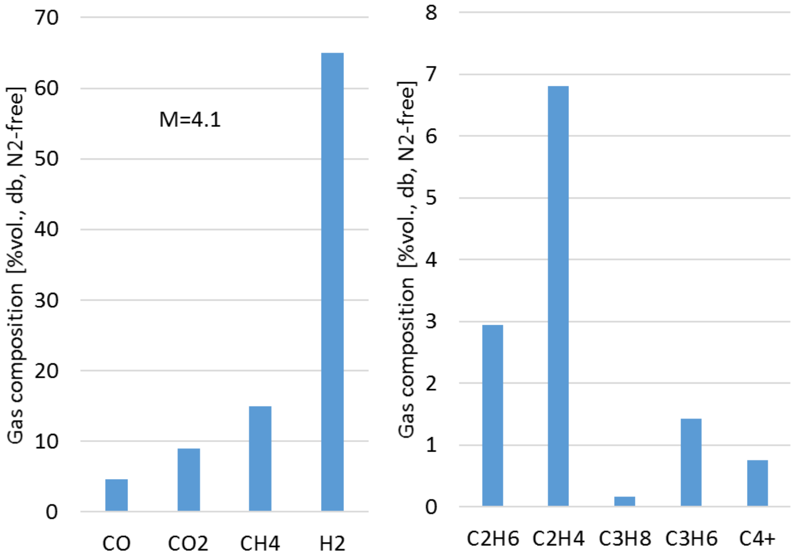

Figure 42 Syngas composition (H_2O and N_2 free basis) during steady state measured by GC a SEG experiment with ECOH biomass as feedstock at S/C=1.8, CaO/C=1.0 and 9.6 kW_{th} of thermal input. Solid bed temperature stabilized at 670-672 ºC

Table 10 shows the results for the collected tar, its composition with regard to the ring number compounds and gravimetric tar (weight) for the SEG test with ECOH biomass. As expected, the gravimetric tar (weight) was lower than the collected tar and similar results were obtained to the ones with ECOH pellets regarding the dominance of one-ring compounds in the collected tar. Benzene, toluene, phenol, ethylbenzene and p+m-Xylene following a decreasing order (Figure 43) were the major compounds in this group. Napthalene, as 2-rings compound, contributed 13 % to the tar content. Among the 3-rings compounds, phenanthrene and acenapthylene were the most emitted compounds. There were not aromatic compounds with more than 3-rings. Comparing this SEG test to results for the ECOH pellets (shown in section 1.2.3.4) at similar solid bed temperature, it is observed that a higher percentage of 1-ring compounds is obtained for the ECOH biomass (81% versus 68% and 77% for two experiments of ECOH pellets with solid bed temperature of 679.7 and 679.8 ºC, respectively). This should be linked to the higher S/C ratio fulfilled in the SEG experiment with ECOH biomass (1.8 vs 1.3-1.4) that favors the cracking of heavier aromatic compounds into lighter ones.

Table 10 Pictures of the impingers and tar characterization for the tar sample taken during the SEG experiment with ECOH biomass

	TAR V
Gravimetric tar (g/Nm^3 dry gas)	11.93
Collected tar (g/Nm^3 dry gas)	30.03
Composition of the collected tar	
1-ring comp. (g/Nm^3 dry gas)	24.22
2-ring comp. (g/Nm^3 dry gas)	3.83
3-ring comp. (g/Nm^3 dry gas)	1.98
4-5-6-ring comp. (g/Nm^3 dry gas)	0.00

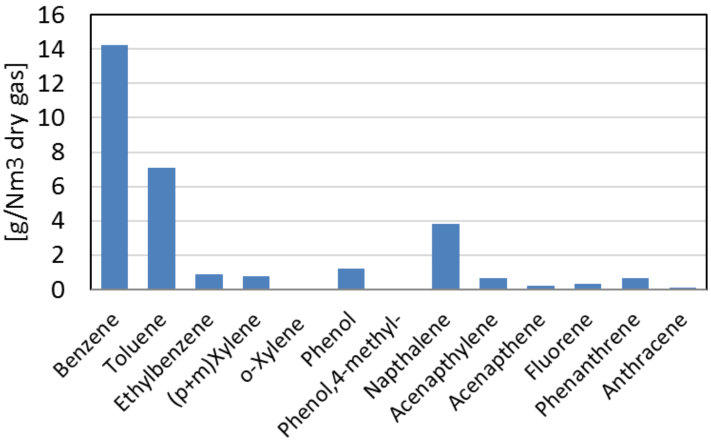

Figure 43 Major compounds emitted for the collected tar (g/Nm^3 dry gas) for the ECOH biomass

1.2.5 STRAW pellets

A total number of 6 SEG tests have been performed with straw pellets as biomass using the CaO/C and S/C ratios indicated in Table 11. All these gasification tests have been carried out using lime #2 as CO_2 sorbent. Most of the experiments performed with straw pellets were performed with a reduced biomass thermal input, i.e. between 8.3 and 10.5 kW$_{th}$. The experiment performed at CaO/C=0.80 was done with the screw feeder of the CO_2 sorbent heated with tracers at 400 ºC, which allowed increasing the proportion between CaO and biomass up to such value. As explained below in this section, a transient experiment was also performed with straw pellets as biomass, similarly to what was done with ECOH pellets. Regarding the testing, it is worth mentioning that straw pellets were fragile and most of them broke along the BFBR. As a result, the smaller fraction of the collected solids from the overflow (<1-2mm) contained (generally) larger char amount than the smaller fraction collected with ECOH pellets. In this way, the ash content in this solid fraction was higher and larger amounts of KCl were detected by XRD analysis (with ECOH pellets were only detected in the collected solids in the cyclones, where the ash content was substantial). For those experiments with ECOH pellets with similar amounts of char contents in this solid fraction <1-2 mm no KCl was detected by XRD, which could mean that ash content remained in the coarse particles for these SEG tests with ECOH.

Table 11 Experimental matrix of the SEG tests performed with straw pellets as biomass in the BFBR at ICB-CSIC. Lime #2 was used as CO_2 sorbent for all the experiments

CaO/C	S/C=1.9	S/C=1.3-1.5
0.8		10.5 kW$_{th}$ (697ºC)
0.5		9.6 kW$_{th}$ (650ºC)
0.4	8.3 kW$_{th}$ (640-646ºC)	
0.3		10.5 kW$_{th}$ (665-670ºC) X2 (640ºC)
0.2		Transient 10.8 kW$_{th}$ (735-738ºC)

1.2.5.1 Analysis of the gas yield and char conversion

Figure 44 shows the gas yield (in Nm^3 dry gas/kg of biomass, water-ash-free basis) and the fixed carbon conversion calculated for the different SEG experiments performed with straw pellets as biomass. As it is appreciated, the variation of the gas yield goes between 0.9 Nm^3 (dry gas)/kg$_{BSwaf}$ at temperatures around 645 ºC and 1.1 Nm^3 (dry gas)/kg$_{BSwaf}$ at temperatures around 700 ºC. Fixed carbon conversion of the straw pellets was around 27-45 % (with the exception of the value of 65 % calculated at 735 ºC, which corresponds to the transient test) that is lower than for the ECOH pellets char for a given temperature, which indicates that the reactivity of the straw pellets char could be lower than for ECOH.

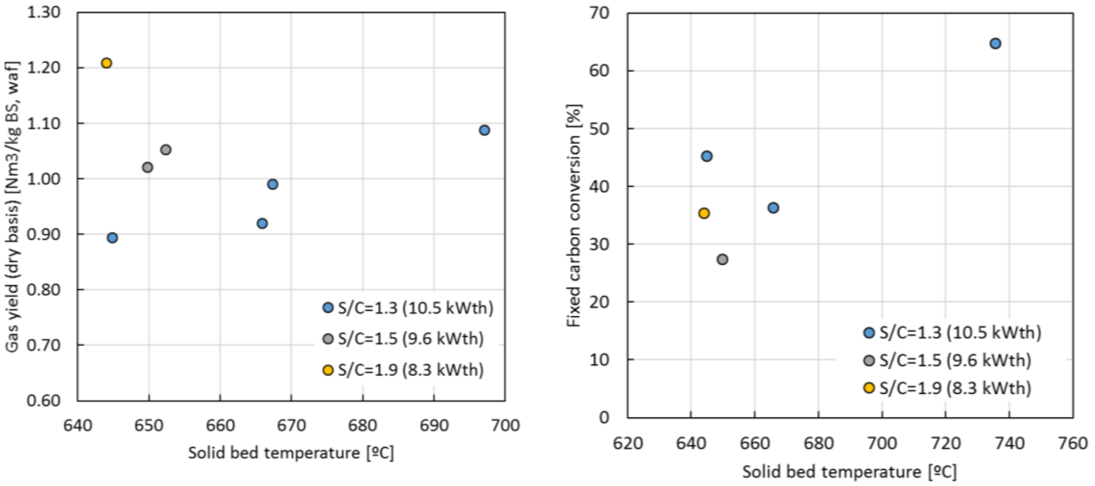

Figure 44 (left) Gas yield (in Nm^3 of dry gas/kg of biomass, water-ash-free (waf) basis) and (right) fixed carbon conversion as a function of solid bed temperature for different S/C ratios and straw pellets thermal inputs

1.2.5.2 Analysis of the gas quality

Figure 45 compares the syngas composition obtained for two experiments at different solid bed temperature. The CaO/C molar ratio in these two experiment was similar (0.28 and 0.20) as well as the S/C ratio (1.3) and the biomass thermal input (10.5-10.8 kW_{th}). As already observed for ECOH pellets, gasification temperature influences noticeably the hydrocarbons C_2-C_4 content due to the cracking and reforming reactions being favored with the increasing temperature. As observed in this figure, C_3-C_4 content was greatly reduced from 1.35 %vol. (H_2O-N_2 free basis) to 0.16 %vol. when rising the gasification temperature from 671 ºC to 737 ºC. Such cracking of C_3-C_4 compounds make content of the lighter C_2H_4 to be slightly improved (Figure 45 (right)) as well as CO and CO_2 contents, which could indicate that such cracking leads to these compounds as final products. Regarding the permanent compounds, differences among them are not as significant as for the cases compared with ECOH pellets (Figure 29). CO and CO_2 contents correspond to 14 and 17 %vol. at 665 ºC and 21 and 18.5 %vol. (H_2O-N_2 free basis) at 737 ºC, respectively, as shown in Figure 45. Expressed in humid basis (i.e. including H_2O and N_2), 3.7 and 4.5 %vol. at 665ºC and 6.7 and 6.0 %vol. at 737ºC, respectively, result. These numbers indicate that at 665 ºC, CO_2 content is further from $CaCO_3$/CaO equilibrium [9] than at 737 ºC, where CO_2 concentration of 6.0 %vol. practically matches the concentration at equilibrium conditions. This behavior could be linked to segregation issues, which could be more pronounced at 665 ºC and so make unconverted char particles to be accumulated in the upper part of the solid bed (close to the overflow) where there is no CaO available to react with the CO and CO_2 generated from gasification reactions (4-6). Concerning fixed carbon conversion, it resulted around 50-65 % for the experiment at 665 ºC and around 65-68 % at 737 ºC, which would contribute to the higher gas yield calculated at the highest temperature (1.2 Nm^3 dry gas/kg $_{BS,waf}$ vs 1.0 Nm^3 dry gas/kg $_{BS,waf}$). In addition, CaO particles left the reactor with a larger $CaCO_3$ content for the experiment at 665 ºC, X_{carb}=0.47-0.48 mol_{CaCO3}/mol_{Ca} at 665 ºC and X_{carb}=0.19-0.20 mol_{CaCO3}/mol_{Ca} at 737 ºC, which is linked to a higher CO_2 capture ratio (25 % vs 15 %, since the CaO/C proportion was similar) that contributes to a lower gas yield.

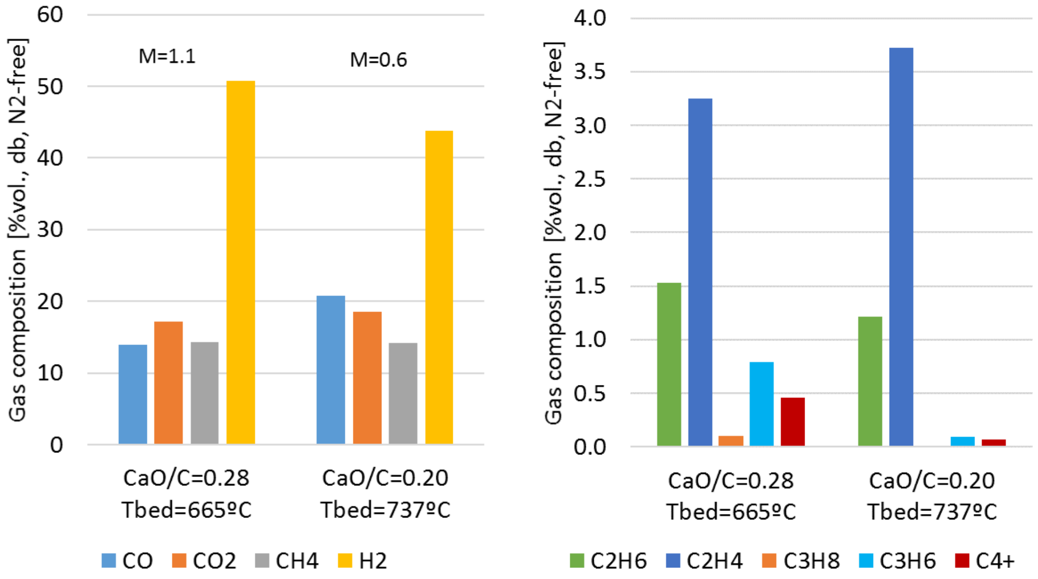

Figure 45 Gas concentration (dry and N_2 free basis) during steady state measured by GC for two experiments at same S/C ratio (1.3), similar thermal input (10.5 and 10.8 kW_{th}) and similar CaO/C ratios but different solid bed temperatures using straw pellets as biomass

Figure 46 allows evaluating the influence of the gasification temperature on tar formation for these two SEG experiments with straw pellets. As mentioned previously, the increase of the solid bed temperature decreased the content of the collected tar. Tar-cracking reactions are endothermic [5,10–15], and the increase of the temperature was expected to promote the cracking reactions decreasing the tar content in the produced gas. This decreasing trend of the tars content with the increase of the temperature has been reflected for the different biomasses along this deliverable. By analyzing the composition by ring number (Figure 46 (left)), it was observed that 1-ring compounds were the major compounds produced independently of the temperature. However, the 1-ring compounds decreased whereas the 2, 3 and 4-rings compounds were promoted with the increase of temperature, indicating that more stable compounds with high molecular weight were formed.

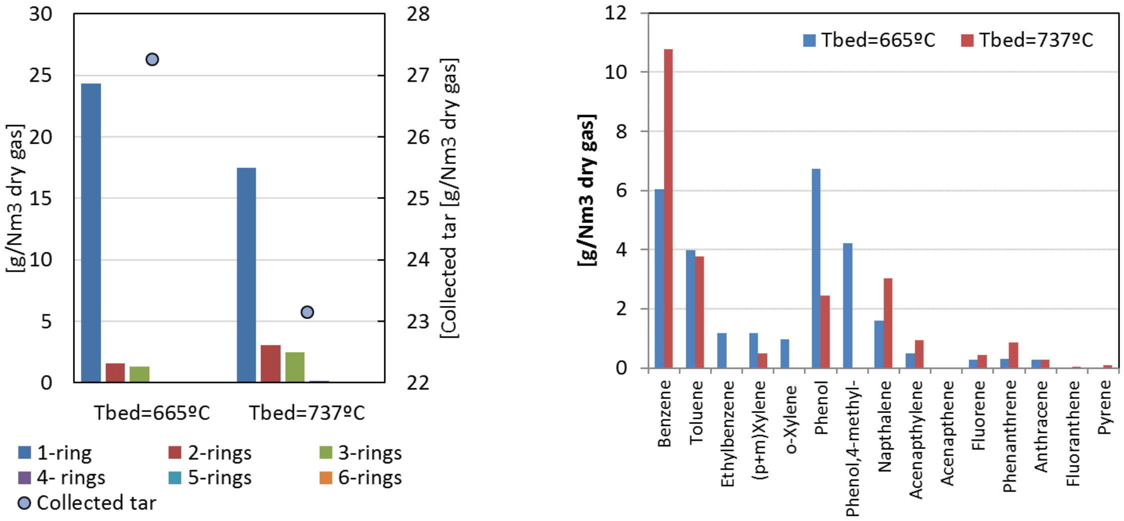

Figure 46 (left) Collected tar and composition by ring number and (right) major compounds emitted for the collected tar for two experiments with straw pellets at two different solid bed temperatures

When the individual composition of the collected tar was analyzed (Figure 46 (right)), it was observed a different trend between the most volatile compounds and the heaviest ones. On the one hand, benzene increased with the temperature but, overall, the 1-ring compounds decreased with the temperature. This was mainly due to other one-ring compounds like ethylbenzene, the different xylenes, phenol and phenol, 4-methyl- that increased at low temperatures. On the other hand, less volatile compounds like naphthalene, fluorine and phenanthrene were favored at high temperatures. This could be related to the different mechanisms involved in the tar formation during the gasification process. High temperatures would favor the decomposition of the aromatic fraction of the straw (lignin) which would release more stable aromatic compounds. In addition, it would be promoted the dealkylation and decarboxylation reactions of the aromatic compounds originating benzene and other volatile compounds, which would stabilize producing more heavy aromatic compounds with 2,3,4-rings.

Finally, the influence of the sorbent-to-biomass ratio on the syngas composition is also evaluated for straw pellets. Figure 47 compares the syngas composition measured by GC for two different SEG experiments performed with similar S/C ratio (1.3-1.35) and but with different CaO/C molar ratios (i.e. 0.28 and 0.81). For doing this comparison, solid bed temperature was not the same since for the experiments performed for straw pellets (Table 11) it was not possible to keep constant this variable when modifying the CaO/C ratio. The experiment at CaO/C=0.28 was already commented when analyzing the effect of the gasification temperature in Figure 45. CO and CO_2 contents correspond to 14 and 12.5 %vol. for the experiment with CaO/C=0.81 (Figure 47) those expressed in humid basis (i.e. including H_2O and N_2) result in 4.1 and 3.7 %vol. Compared with the CO_2 equilibrium content for the CaO/$CaCO_3$ reaction, it is corroborated that CO_2 content corresponds to equilibrium and so it is influenced by the gasification temperature. The H_2 content remained around 11-13 %vol. (inc. H_2O and N_2) for the test at CaO/C=0.28 and around 16-17 %vol. (inc. H_2O and N_2) when working at CaO/C=0.81. This behavior is linked to the differences in the CO_2 separated, which is larger for the experiment at CaO/C=0.81. CaO particles leave the BFBR with a higher $CaCO_3$ content when operating with the smaller CaO/C ratio of 0.28 (i.e. X_{carb}=0.47-0.48 mol_{CaCO3}/mol_{Ca} with CaO/C=0.28 and X_{carb}=0.20-0.21 mol_{CaCO3}/mol_{Ca} with CaO/C=0.81), due to the larger residence time of CaO particles in the BFBR (which is inversely proportional to the CaO/C ratio) and the lower temperature that improves the carbonation kinetics. Calculating the global CO_2 capture ratio through the C balance to the solids, it results in 21 % for the experiment at CaO/C=0.81 that is around 6 points higher than in the experiment with lower CaO/C ratio. The fixed carbon conversion calculated for the test at CaO/C=0.81 and 697 ºC resulted around 10-11 %, which is significantly lower than the X_{FC} values calculated for the SEG experiment at CaO/C=0.28 (50-65 %). Segregation issues during the SEG test at CaO/C=0.28 and the reduced solid residence time for the experiment at larger CaO/C ratio should be the reasons for such values.

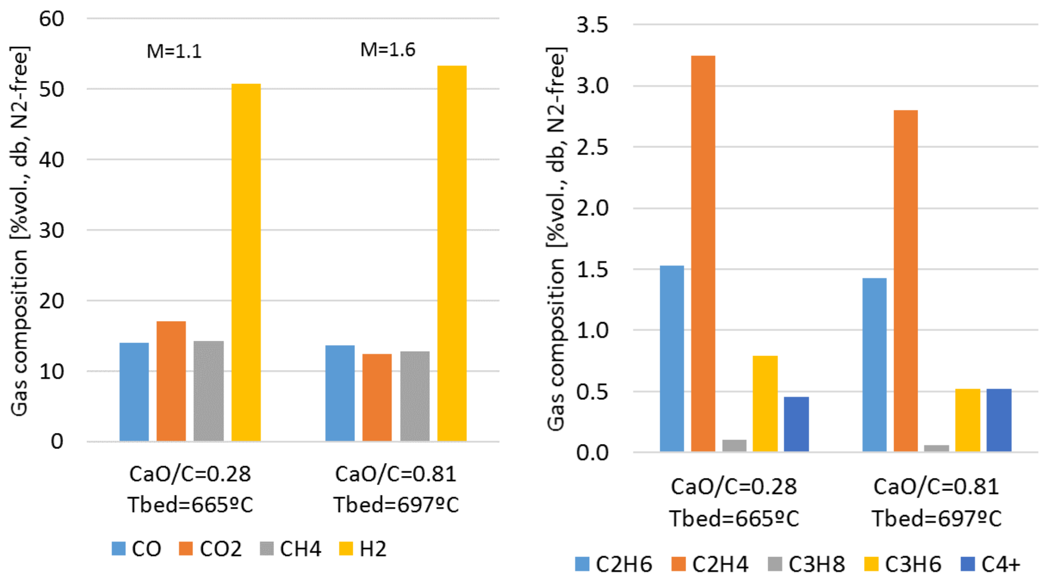

Figure 47 Gas concentration (dry and N_2 free basis) during steady state measured by GC for two experiments at similar S/C ratio (1.3-1.35) and same thermal input (10.5 kW_{th}) but different CaO/C ratios (0.28 and 0.81). Solid bed temperature in each case is indicated in the X-axis label

1.2.5.3 Analysis of tars

For the 6 SEG experiments performed with straw pellets, tar sampling was performed for 5 of them (i.e. except test at S/C=1.9), as indicated in Table 12. For each experiment, the gravimetric tar (weight), the collected tar and the gravimetric tar (GC-MS) were determined. Figure 48 shows the variations of the gravimetric (weight) and the collected tar (GC-MS) as a function of the solid bed temperature. As it is observed, both gravimetric and collected tars follow a decreasing trend with the solid bed temperature (as already explained before), but for the collected tar this trend is less steep than for the gravimetric tar. These trends were also observed for the ECOH pellets indicating that the higher the solid bed temperature, the lower the tar formation.

Table 12 Picture of the tar sampling impingers for each SEG test performed with straw pellets

CaO/C	S/C=1.9	S/C=1.3-1.5
0.8		 (697ºC)
0.5		 (650ºC)
0.4	No tar sampling	

0.3		 (670ºC)  (640ºC)
0.2		 S1  S2

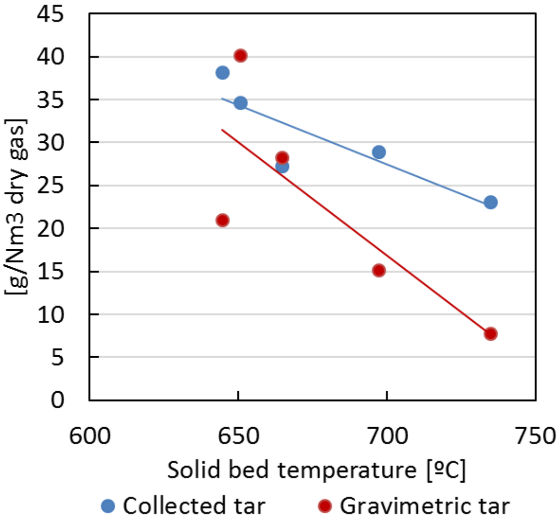

Figure 48 Collected tar and gravimetric tar (weight) as a function of the solid bed temperature for the SEG tests with straw pellets

Regarding the composition of the collected tar according to the ring number (Figure 49), it can be observed that 1-ring compounds are the major aromatic compounds with higher emissions at the lower solid bed temperatures. For these compounds, it is observed a slight decreasing trend with the increase of the temperature. In fact, when the 1-ring compounds are plotted against the solid bed temperature, it is obtained a good correlation with R^2=0.89 (Figure 49 right). 2 and 3-ring compounds were also present increasing their contribution at higher temperatures. It is also worth to remark the presence of 4-rings compounds at the highest temperatures of 697 and 735 ºC although at very low concentrations. According to the bibliography, more stable aromatic hydrocarbons are formed with the increase in temperature and the temperature constitutes a key factor for tar distribution [15].

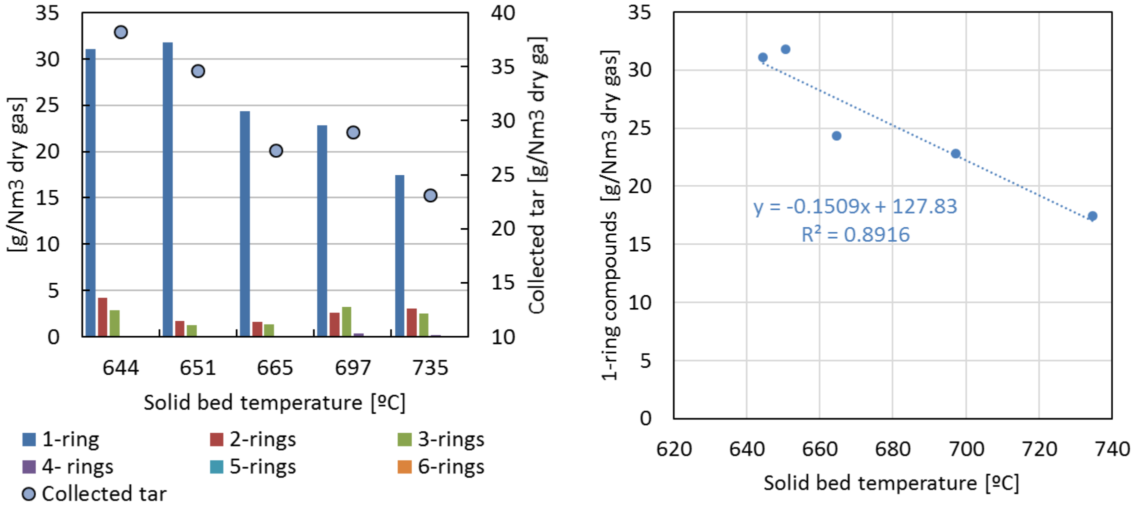

Figure 49 (left) Collected tar and composition by ring number as a function of the solid bed temperature and (right) correlation between 1-ring compounds and solid bed temperature for the collected tar for SEG tests with straw pellets as biomass

When the composition of the individual compounds is studied in more detail (Figure 50), it can be noticed that benzene is the dominant aromatic compound (i.e. 22-46 % of collected tar corresponds to benzene) at most of the temperatures analyzed. It is also remarkable the presence of phenol at similar concentrations to toluene at all temperatures with percentages ranging between 11-25 %. In fact, at the temperature of 665ºC, phenol was the dominant compound followed by benzene. The presence of phenol can be related to the nature of the feeding material, straw, where lignin with phenolic polymers is one of the main components. Lignin is formed by a large group of aromatic polymers including guaiacyl, syringyl units and p-hydroxyphenyl. Therefore, lignin represents a potential precursor for polyaromatic hydrocarbon formation [16]. Other aromatic compounds like naphthalene also had an important contribution, mainly at the lowest and the highest solid bed temperature, with contributions of 11 and 13% to the collected tar respectively.

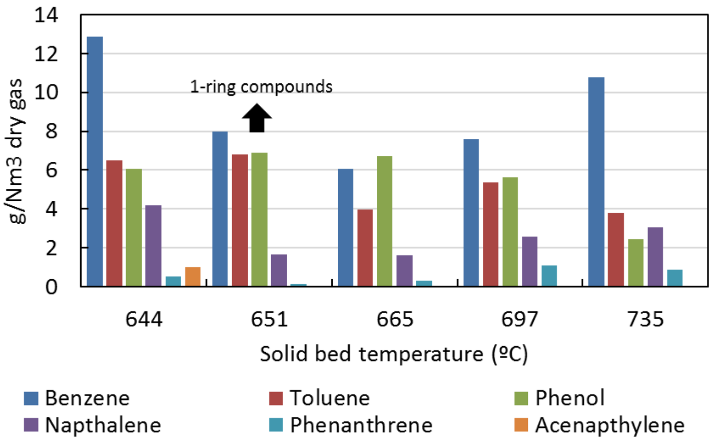

Figure 50 Major compounds emitted for the collected tar (g/Nm^3 dry gas) as a function of the solid bed temperature for SEG tests with straw pellets as biomass

1.2.5.4 Transient test

Similarly to ECOH pellets, a transient SEG test was performed with straw in order to follow the evolution of the syngas composition and solids conversion with the time. Two tar samples were taken during this transient experiment (i.e. one at the beginning, referred to as “tar S1”, and the second one at the end, referred to as “tar S2”). A reduced flow rate of 2.4 kg/h of straw pellets was used in this test to ensure that the solid bed was converted at a sufficiently low rate as for following the fulfillment of the steady state through solid sampling. Moreover, a minimum CaO flow rate of 1 kg/h was used to push the solids out from the BFBR through the overflow and so allow taking solid samples. Both solid flows resulted in a CaO/C ratio of 0.20 as indicated in Table 11. The steam-to-carbon ratio used for this experiment was 1.3 as indicated in such table. Figure 51 shows the temperatures, syngas composition and solid composition profiles as a function of time from the beginning of the experiment (when biomass started to be fed into the BFBR). Grey zones indicate the tar sampling periods performed during this experiment. As already happened in the transient test with ECOH pellets (1.2.3.5), H_2 content reached its maximum value of 60 %vol. (H_2O-N_2 free basis) at the beginning of the experiment when the sorbent particles had very low $CaCO_3$ content (≈ 0.08 mol_{CaCO_3}/mol_{Ca}) and the carbonation of CaO proceeded at its maximum allowable rate. C_2H_4 and C_2H_6 contents in the syngas were practically along the experiment, but CH_4 content experienced a steep increase from around 9 to 13-14 %vol. (H_2O-N_2 free basis) when the H_2 content reduced to around 40 %vol. (same basis). CO_2 concentration in the syngas increased also with the time as the sorbent present in the solid bed was progressively converted and less CaO was then available for reacting with the CO_2 formed. Also in this transient test, the CaO fed to the reactor was not enough for reacting with the CO_2 generated from gasification reactions (4-5).

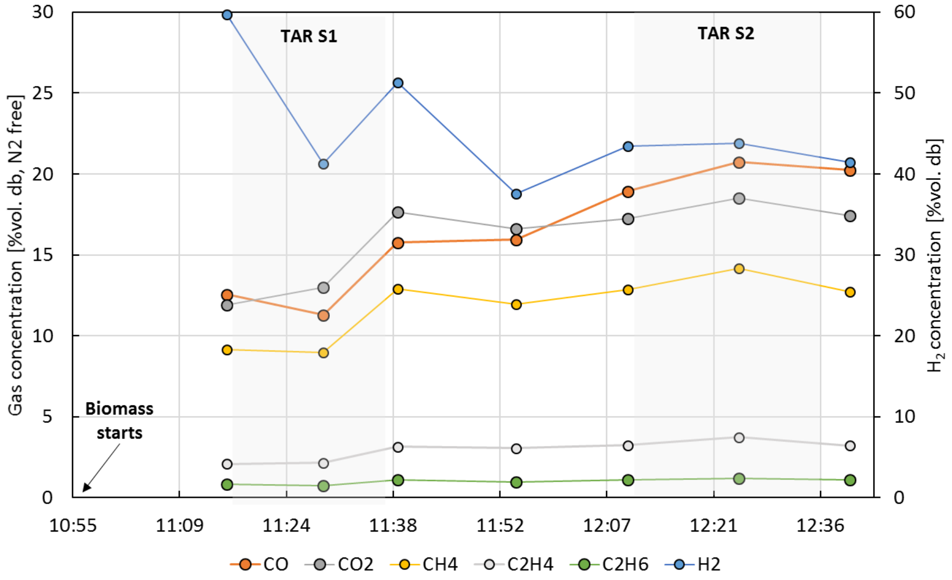

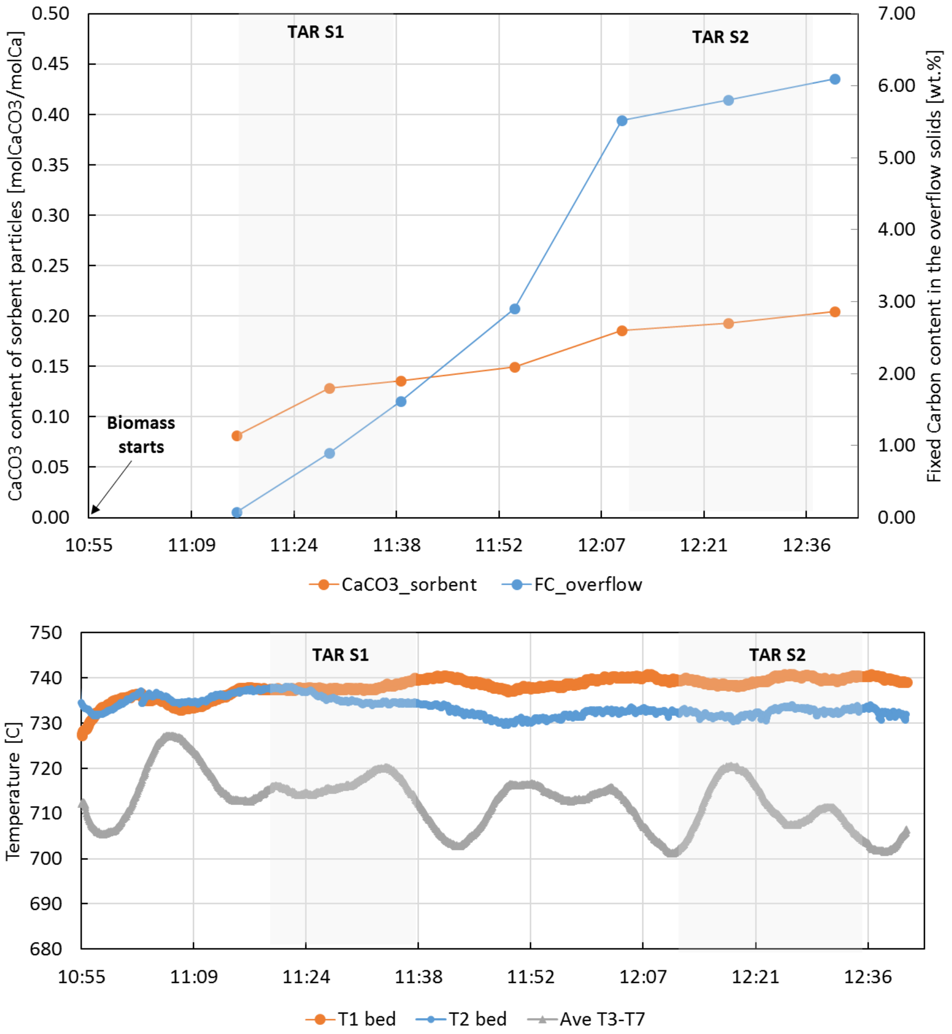

Figure 51 Syngas composition profile (H_2O and N_2 free basis) measured by GC (up), solid composition ($CaCO_3$ and fixed carbon content) in the solids collected in the overflow (middle) and temperature profile along the BFBR (down) during the transient SEG experiment performed with straw pellets

As for the tar formation, the same results regarding the transient test carried out with ECOH pellets can be observed (Table 13). Firstly, the amount of tar formed was lower with more active CaO, independently of the determined tar (gravimetric and collected tar). When CaO was more active (Tar S1), most of the compounds emitted consisted of one aromatic ring and no compounds with higher than 3 –rings were determined. On the contrary, when the CaO was less active, compounds of higher molecular weight were emitted (4-rings compounds). Concerning the composition of the formed tars (Figure 52), benzene, toluene and naphthalene, phenanthrene and acenapthylene were the dominant compounds. Phenol was also present in the tar composition and it was mainly related to the nature of the feeding, straw pellets with phenolic polymers present in lignin.

Table 13 Pictures of the impingers and tar characterization for the tar samples S1 and S2 taken during the transient SEG experiment with straw pellets as biomass

	 **TAR S1**	 **TAR S2**
Gravimetric tar (g/Nm³ dry gas)	3.77	7.79
Gravimetric tar by GC-MS (g/Nm³ dry gas)	13.82	23.16
Collected tar (g/Nm³ dry gas)	2.04	3.67
Composition of the collected tar		
1-ring comp. (g/Nm³ dry gas)	17.84	20.00
2-ring comp. (g/Nm³ dry gas)	1.42	2.14
3-ring comp. (g/Nm³ dry gas)	0.35	1.75
4-5-6-ring comp. (g/Nm³ dry gas)	0.00	0.02

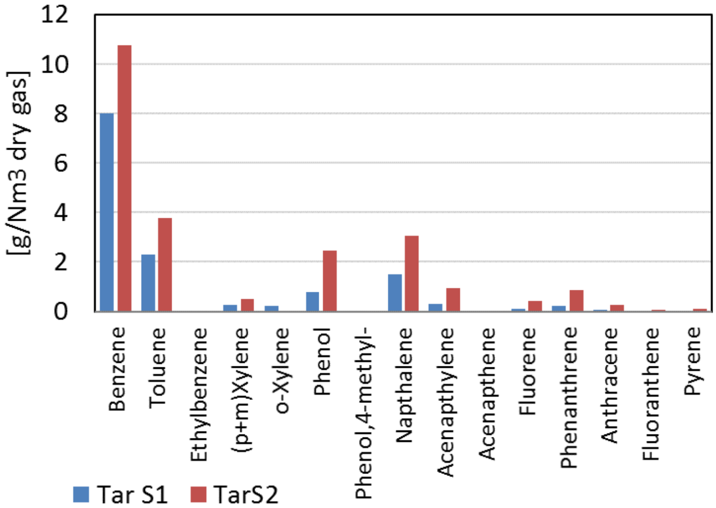

Figure 52 Major compounds emitted for the collected tar (g/Nm³ dry gas) at the beginning (S1) and at the end (S2) of the transient test with straw pellets

1.2.6 Wood chips

SEG performance using wood chips as a feedstock has been tested for a biomass thermal input of 5.3 kW_{th} (i.e. 1.13 kg/h) using lime #2 as CO_2 sorbent. A CaO flow rate of 4.70 kg/h has been introduced into the gasifier, which corresponds to a molar CaO/C ratio of 1.81 at gasifier inlet, for an S/C ratio of 3.0 (i.e. 2.5 kg/h of steam). Despite of the low density of this biomass, its handling was not difficult and its feeding into the BFBR was not problematic. Solid bed temperature was kept constant at around 707 ºC throughout the steady state in this experiment.

Composition of the syngas obtained is shown in Figure 53. As appreciated, H_2 content in the syngas was significantly high and remained around 72-74 %vol. (H_2O-N_2 free basis) along the experiment. Moreover, content of light hydrocarbons (C_2-C_4) was quite low (Figure 53 right), accounting for 2.2-2.8 %vol. (H_2O-N_2 free basis) in total. The high S/C and CaO/C ratios that resulted for this SEG test should be the reasons for the H_2 and C_2-C_4 contents observed in the syngas due to their effect on the cracking and reforming reactions as well as on the carbonation reaction, which have been extensively explained for the rest of the biomass tested before. The gas yield calculated was 1.96 Nm^3 dry gas/kg $_{BS,waf}$. $CaCO_3$ of the sorbent particles leaving the gasifier was around 0.16-0.17 mol_{CaCO3}/mol_{Ca} along the experiment. The high CaO/C ratio used in this gasification test made the carbonation degree of the CaO particles to be lower than those observed for the experiments performed with low CaO/C ratios. Fixed carbon conversion calculated from solid samples was between 45 and 40 %.

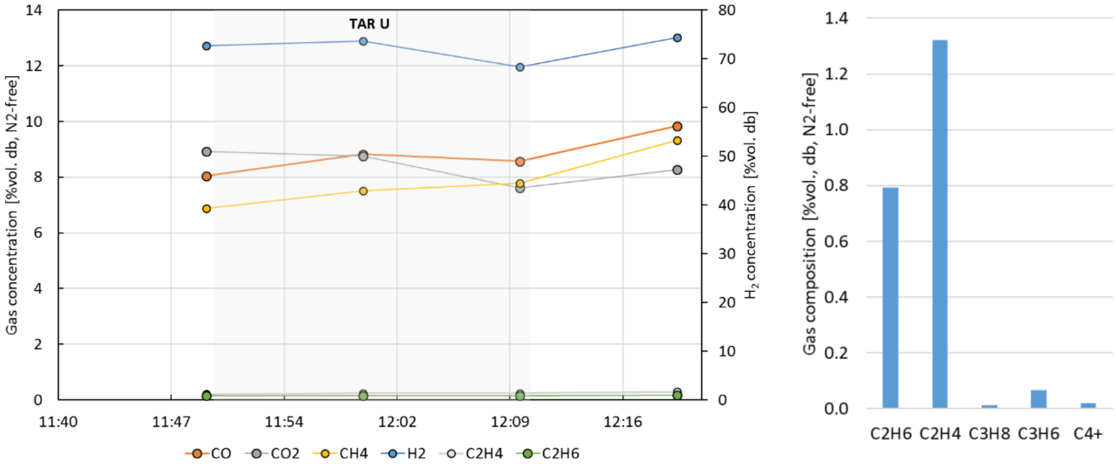

Figure 53 (left) Permanent gas concentration and (right) light hydrocarbons (C_2-C_4) content in the syngas (both in H_2O and N_2 free basis) measured by GC in the SEG experiment performed with wood chips

For this experiment, the gravimetric tar (weight) and the collected tar were determined. The composition of the collected tar according to the ring number compounds is shown in Table 14. Regarding the amount of tar, gravimetric and collected tar, low concentrations were obtained. As already seen before, the high S/C ratio used in this case that favors the cracking of the aromatic compounds into lighter compounds, as well as the catalytic effect of the excess of CaO used in this SEG test, are the reasons for the low tar yields obtained for wood chips SEG testing. In general, these values were lower than the ones obtained for the wood pellets (described in section 1.2.1.3), but the S/C and CaO/C ratios used were not the same (i.e. significantly higher for wood chips than for wood pellets) and that could be the reason of such difference. As happened also for wood pellets, 1-ring compounds were the major components of the collected tar. Analyzing the contribution of each individual compounds (Figure 54), benzene, toluene and xylenes were the ones contributing the most contributing to the 1-ring compounds. Phenol and phenol, 4-methyl- were not found at these conditions. Naphthalene as 2-rings compound had an important contribution to the collected tar whereas in the 3-rings compounds, phenanthrene, acenapthylene, fluorene and anthracene contributed in decreasing order to the collected tar.

Table 14 Picture of the impingers and tar characterization for the tar sample taken during the SEG experiment with wood chips as biomass

	TAR U
Gravimetric tar (g/Nm^3 dry gas)	3.0
Collected tar (g/Nm^3 dry gas)	6.7
Composition of the collected tar	
1-ring comp. (g/Nm^3 dry gas)	5.18
2-ring comp. (g/Nm^3 dry gas)	0.85
3-ring comp. (g/Nm^3 dry gas)	0.67
4-5-6-ring comp. (g/Nm^3 dry gas)	0.00

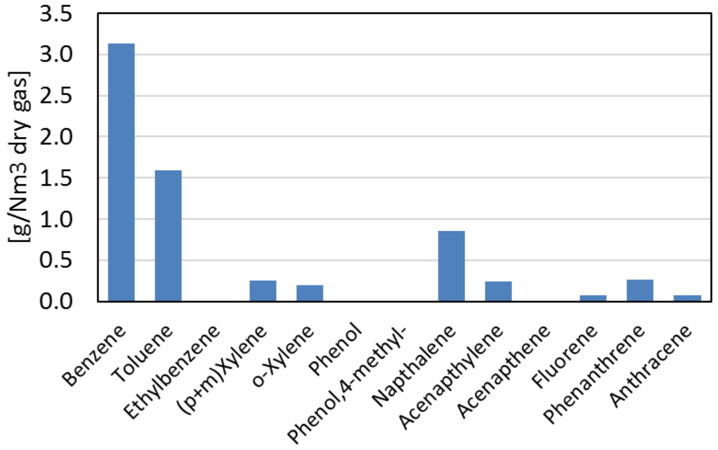

Figure 54 Major compounds emitted for the collected tar (g/Nm^3 dry gas) for the SEG test with wood chips

1.2.7 Performance comparison of the different biomasses tested

As already seen in the previous sections of this document, the performance of 6 different biomass feedstocks (Table 1) in a SEG process has been carefully studied. It is difficult to compare all the biomasses under the same operating conditions of temperature, CaO/C and S/C ratios since the experimental matrix in each case has been different. However, since the temperature has been one of the operating parameters influencing most the gas and tar yields, as well as the char conversion and M-modules fulfilled, it has been chosen for this analysis those experiments for each biomass that had a very similar gasification temperature of around 700-715 ºC.

1.2.7.1 Char reactivity comparison

As widely discussed in the previous sections, fixed carbon conversion (X_{FC}) is mainly influenced by gasification temperature and solid residence time. Figure 55 (left) shows the fixed carbon conversion calculated for each biomass under SEG conditions for similar solid bed temperatures and the closest as possible CaO/C ratio. When temperature and CaO/C ratio are very close (i.e. straw and ECOH pellets), differences in X_{FC} are due to the difference in char reactivity in the gasification reaction. As appreciated, X_{FC} reached for the straw pellets at around 700 ºC and CaO/C of 0.8 was 10 % whereas it was almost 34 % for ECOH pellets at 707 ºC and CaO/C=1.2, which is indicative of a higher reactivity of ECOH char compared to straw char. To corroborate these differences, char samples taken from the overflow pipe during SEG tests were gasified in a thermogravimetric equipment (TGA) at 750 ºC and 20 %vol. H_2O in N_2. These char samples were grinded (dp <200 μm), and approximately 5 mg sample was introduced in the TGA sample basket. Figure 55 (right) shows evolution of X_{FC} with time for the different chars tested. The X_{FC} has been calculated from the weight changes with time of the char samples according to the following expression:

$$X_{FC} = \frac{(w(t) - w_{final})}{(w_{initial} - w_{final})} \qquad (10)$$

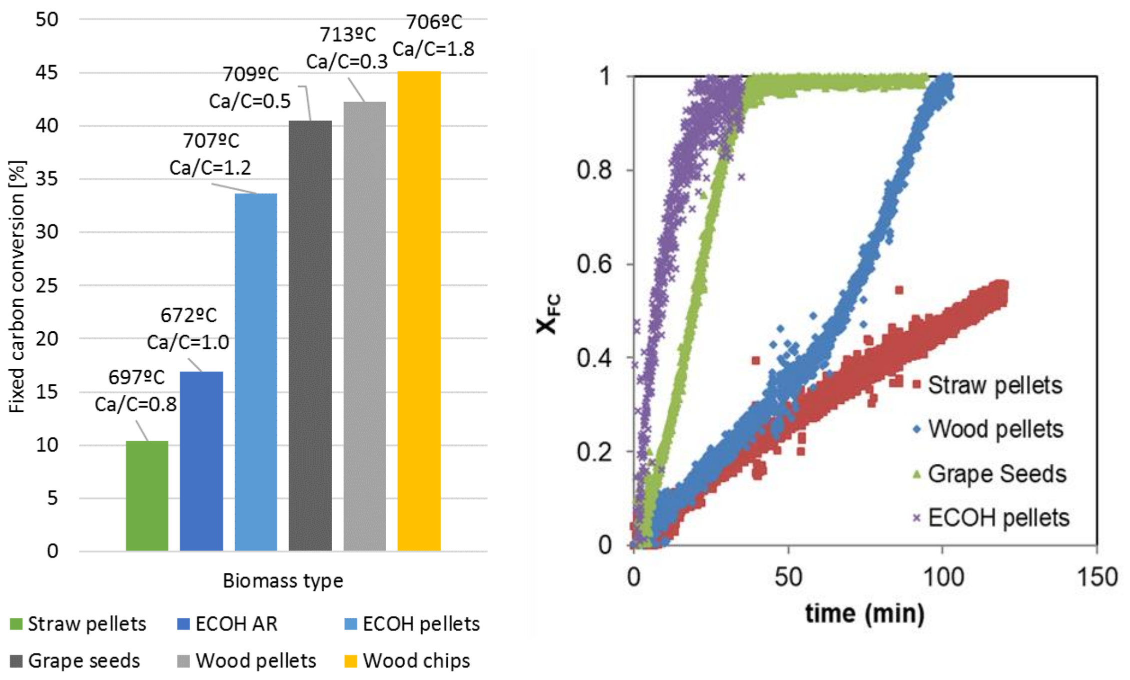

Figure 55 (left) Fixed carbon conversion calculated for each biomass under SEG conditions for different CaO/C ratios and similar solid bed temperatures (mostly between 700 and 713 ºC)

According to the reactivity measured in TGA (Figure 55 (right)), it is confirmed the lower reactivity for straw char compared to ECOH pellet char. Comparing wood pellets and grape seeds, similar X_{FC} has been calculated (i.e. X_{FC}=40.5 % for grape seeds at 709 ºC and CaO/C=0.5 and X_{FC}=42 % for wood pellets at 713 ºC and CaO/C=0.3), which is due to the similar char reactivity of both biomass feedstock under same conditions. Concerning ECOH biomass, its X_{FC} resulted around 17 % (significantly lower than the X_{FC} reached for the similar biomass but in pellet form), but this is due to the gasification temperature for this SEG test, which resulted at 672 ºC significantly lower than for the other biomass feedstocks.

1.2.7.2 Gas yield and M-module

As explained before, gas yield is mainly influenced by the temperature due to (i) increased gas production during the primary pyrolysis stage, (ii) steam cracking and reforming of heavier hydrocarbons and tars, and (iii) enhanced char gasification reactions [7,8]. Moreover, as for the char gasification reactions these are also influenced by the type of biomass. With the objective of evaluating the effect of the type of biomass used on the gas yield obtained, SEG experiments for each biomass with a similar gasification temperature have been chosen. Figure 56 (left) shows the gas yield obtained expressed per kg of biomass without ashes and moisture (i.e. waf basis), that gives an idea of gas yield from the conversion of the organic fraction of the biomass. Gas yields calculated for wood chips, straw pellets and ECOH pellets can be directly compared between them since these tests were performed at similar conditions of temperature and CaO/C ratio and also because these biomasses have the same proportion between volatile matter and fixed carbon (see Table 1). As a result of these issues, X_{FC} determines gas yield for these biomasses. Therefore, since X_{FC} was larger for wood chips than for ECOH pellets and for straw pellets, gas yield reached for wood pellets was the largest among these three. Considering the composition of the biomass in Table 1, grape seeds is the one with the largest proportion between fixed carbon and volatile matter. Therefore, even if X_{FC} reached for the grape seeds was among the highest ones (Figure 55), the gas yield calculated was not among the largest ones since the amount of fixed carbon to be converted with respect to the organic fraction of the biomass needs to be larger than for ECOH, straw or wood chips to have an impact on the gas yield.

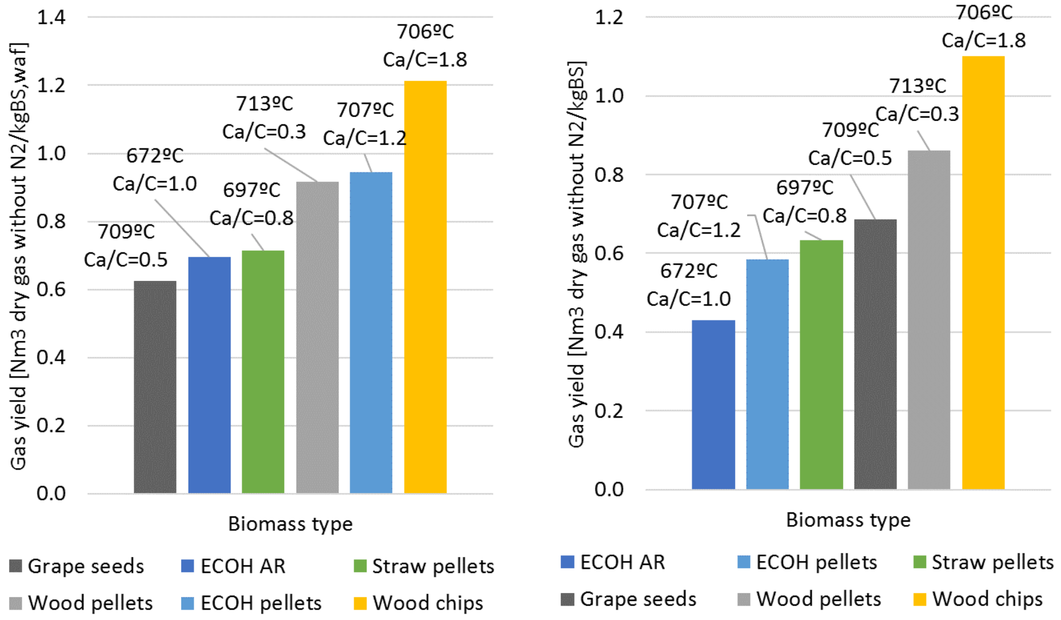

Figure 56 Gas yield in (left) Nm^3 dry gas without N$_2$/kg biomass water-ash-free and in (right) Nm^3 dry gas without N$_2$/kg biomass, for each biomass under SEG conditions for different CaO/C ratios and similar solid bed temperatures

From a process performance standpoint, the gas yield expressed per unit of biomass (i.e. including ashes and moisture) could be more indicative of the efficiency of the process. For this reason, Figure 56 (right) has been plotted. In this figure, it is appreciated that gas yield for ECOH pellets (0.59 Nm^3 dry gas w/o N$_2$/kg$_{BS,waf}$) results to be among the lowest gas yield values since this biomass is the one with the largest content of ashes. In ascending order of gas yield, ECOH pellets are followed by straw pellet (0.63 Nm^3 dry gas w/o N$_2$/kg$_{BS,waf}$) that is the least reactive char, and then by grape seeds that, despite of their reactivity, their fixed carbon content is significantly higher than the rest of the biomass feedstocks and so the contribution of X_{FC} to the gas yield becomes more important. Finally, the highest gas yields have been found for wood pellets and wood chips (0.9 and 1.1 Nm^3 dry gas w/o N$_2$/kg$_{BS,waf}$), which are the biomasses with the largest X_{FC} calculated at these conditions.

Concerning the M-module reached in the syngas, it has been observed the following:

- For ECOH and wood pellets/wood chips, char conversion is sufficiently high as for not being the limiting factor. Therefore, for these biomasses, CO$_2$ capture will determine the M-module reached. For reducing the M-module, CO$_2$ capture should be limited by raising the gasification temperature. Among these feedstocks, lignocellulosic biomasses are the most reactive and so need a higher temperature to get the desired M-module around 2 through a limited CO$_2$ capture ratio by the equilibrium. Alternatively, CO$_2$ capture can be limited using a CO$_2$ sorbent with a lower CO$_2$ carrying capacity (as lime #1), which will allow reaching M-modules around 2 at a lower temperatures than using more reactive sorbents

- Straw resulted in the lowest M-modules. For this biomass, reactivity of the char was the limiting factor. Therefore, the M-module of 2 is a compromise between having sufficient char reactivity and a limited CaO conversion. As seen during SEG testing with straw (section 1.2.5.2), temperature needed for reaching an M-module around 700 ºC, slightly lower than for the rest of the biomasses.

1.2.7.3 Tar analysis

Tar yield and composition for each biomass tested is also compared. In addition to the nature of the feeding material (content of cellulose, hemicellulose and lignin), which is an important variable to take into account in the gasification process, also the operating variables in the gasification process can be relevant in the tar content. Figure 57 compares the gravimetric tar and collected tar (by GC-MS) obtained for the six biomass feedstocks tested at the ICB-CSIC BFBR (these results have been already detailed for each specific feedstock in sections 1.2.1.3, 1.2.2.4, 1.2.3.4,1.2.4, 1.2.5.3, and 1.2.6). Operating conditions chosen correspond to similar temperature (when possible) in the range of 700-713ºC and the closest as possible CaO/C ratio. The S/C ratio was around 1.3-1.4 for ECOH, straw and wood pellets, 1.8 for grape seeds and ECOH biomass and 3 for wood chips.

Concerning the collected tar, it can be observed in Figure 57 that all biomasses were in the range between 24-30.0 g/Nm^3 dry gas with the exception of wood chips, which produced the lowest tar content. The reason for such low tar yield for the wood chips is that the CaO/C ratio for the selected experiment was the highest value (1.8), enhancing the tar cracking effect of the CaO introduced into the BFB reactor. Comparing ECOH pellets and ECOH biomass (ar, non pelletized), the ECOH pellets showed the lowest collected tar. Temperature was different in both SEG tests (higher for ECOH pellets), whereas the CaO/C ratio was not so different. Due to this difference in temperature, the collected tar resulted in a lower value for the SEG test with ECOH pellets. As for the gravimetric tar (Figure 57), higher variations than for the collected tar were found for the different biomasses. The lowest gravimetric tar was obtained for the wood chips (3.0 g/Nm^3 dry gas) and the highest for the wood pellets (21.9 g/Nm^3 dry gas) with similar content to the grape seeds (21.1 g/Nm^3 dry gas). The other biomasses, ECOH pellets, ECOH ar and straw showed values ranging between 7.8-15.2 g/Nm^3 dry gas.

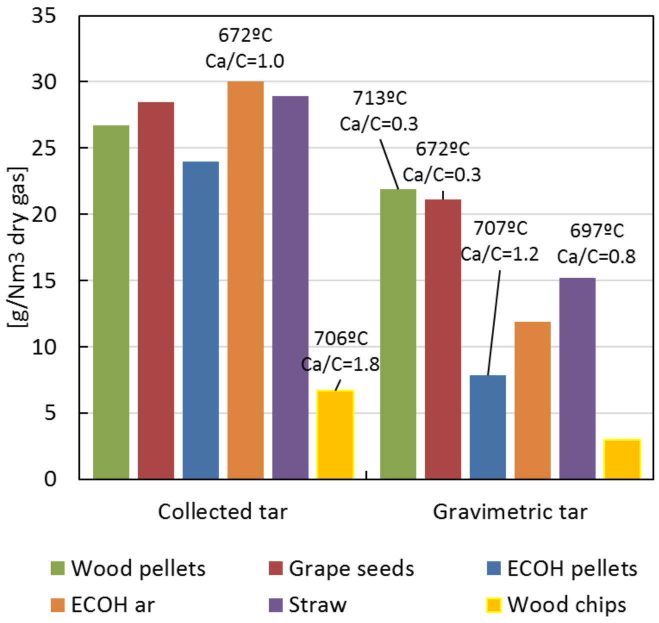

Figure 57 Collected tar and gravimetric tar [g/Nm^3 dry gas] for the different biomasses tested at similar conditions of temperature and the closest as possible CaO/C ratio

When these samples were analyzed according to the ring number distribution (Figure 58), the 1-ring compounds were the dominant compounds for all biomasses. For the 2 and 3-rings compounds, a different trend was observed depending on the biomass fed. For instance, for the straw and wood pellets, the 3-rings compounds were the second most emitted compounds whereas for the other biomasses (ECOH pellets, grape seeds, wood chips and ECOH ar), the 2-rings compounds, i.e. naphthalene, were the second most emitted compounds.

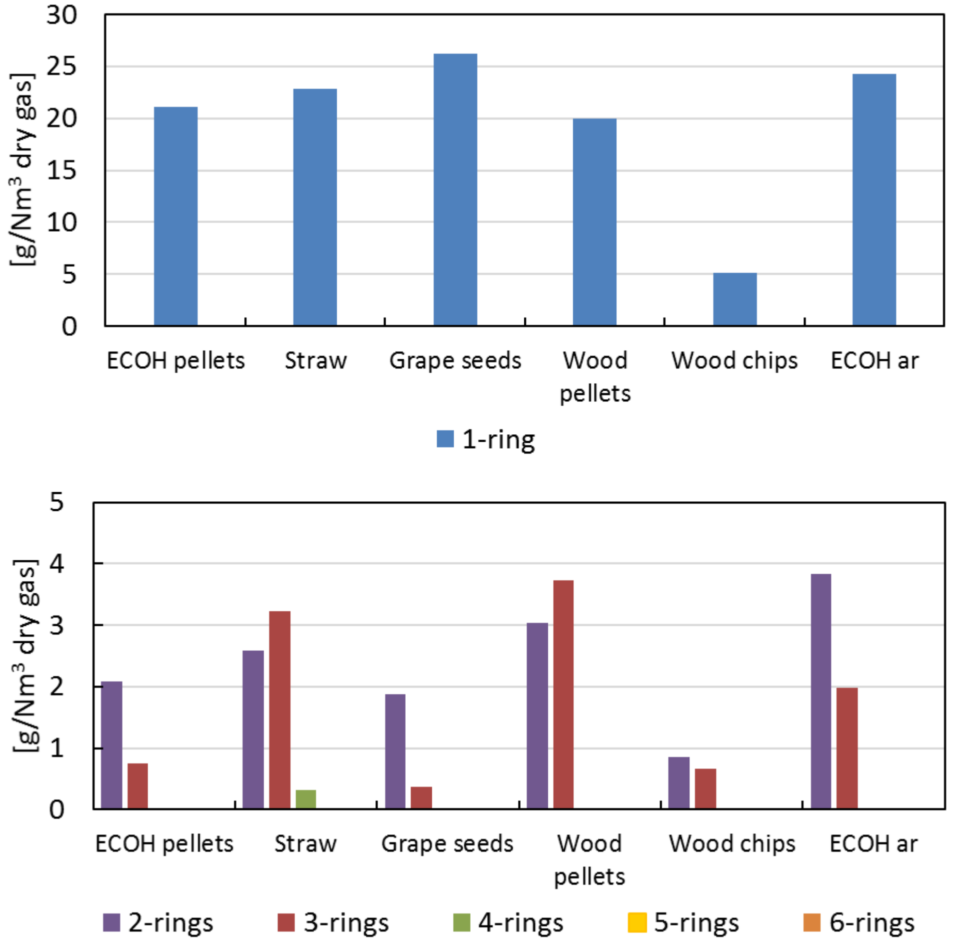

Figure 58 Ring number distribution of the collected tar [g/Nm3 dry gas] for the different biomasses tested (up) 1-ring compounds and (bottom) 2-6 rings compounds

When the individual compounds were studied for the different biomasses (Figure 59), in all cases, benzene was the compounds contributing the most to the collected tar. For both ECOH feedstocks, wood chips and grape seeds, toluene was the second contributing compound in the collected tar, whereas for straw and wood pellets phenol reached a higher percentage than toluene. In the case of the grape seeds, its concentration was similar to the toluene but a little lower. Taking into account the nature of the biomasses, the thermal degradation of cellulose and hemicellulose mainly form esters, ketones and other oxygenated compounds through decarbonylation and decarboxylation [17,18]. The main source of phenols would come from the degradation of lignin after volatilization. In straw, grape seeds and wood pellets the presence of phenols was quite remarkable and it could be related to lignin devolatilization [17–20]. Therefore, not only the gasification conditions seem to affect and play an important role on the tars formation but also the nature and the processing that undergo the feeding material.

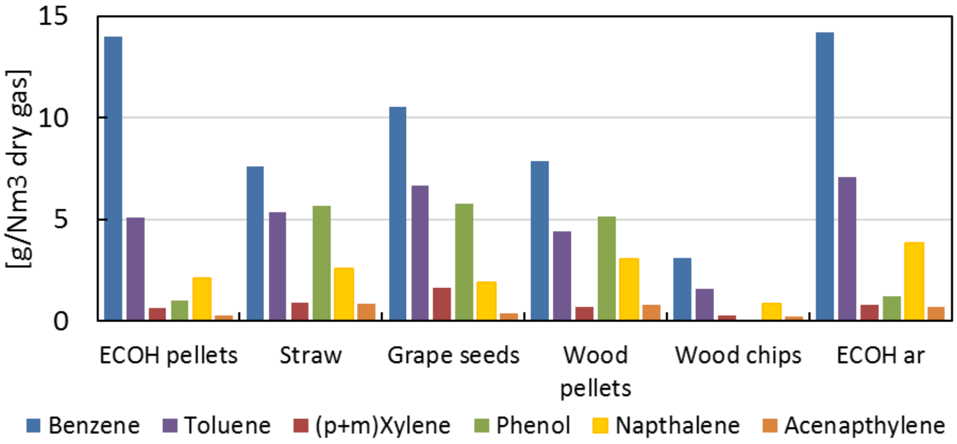

Figure 59 Major compounds emitted in the collected tar [g/Nm^3 dry gas] for the different biomasses tested

1.3 Combustion/calcination tests

The second stage of the enhanced gasification loop (i.e. combustion of the unconverted char and calcination of the $CaCO_3$ obtained at the gasifier outlet) has been also studied in the BFB reactor at ICB-CSIC (Figure 1). Two different chars have been used as fuel, namely char from grape seeds and from ECOH pellets collected from the SEG tests. To perform the combustion/calcination experiments described in this section the carbonated CO_2 sorbent collected from the corresponding SEG tests with such biomass feedstock was used. Moreover, the formation of polycyclic aromatic hydrocarbons (PAHs) generated in some of these combustion/calcination tests has been analyzed as explained in section 1.1.2.5. The experimental routine followed for each combustion/calcination test has been already described in section 1.1.3.2.

1.3.1 Grape seeds char

The combustion/calcination stage using unconverted grape seeds char as fuel has been studied modifying the char/carbonated sorbent mass ratio and the air excess as operating variables. Table 15 summarizes the experiments performed using grape seeds unconverted char as fuel. The air ratio given in this table corresponds to the ratio between the air flow rate used in the experiment and the stoichiometric air flow rate. In this table, the solid bed temperature reached in each case is given. The mass flow rate of char fed to the BFB reactor has been kept at around 1-1.1 kg/h for all the tests in Table 15, and the mass flow of carbonated CO_2 sorbent and the air flow rate have been modified for fulfilling the air excess and char/sorbent mass ratio indicated in this table.

Table 15 Experimental matrix of the combustion/calcination tests performed with char from grape seeds in the BFBR at ICB-CSIC

Char/sorbent mass ratio	Air ratio = 1.7	Air ratio = 1.5	Air ratio = 1.3
0.3			894ºC
0.2	848ºC	841ºC	856ºC

The char used in these combustion/calcination tests corresponds to the coarse fraction of the particles collected from the overflow in the SEG tests with grape seeds as a fuel explained in section 1.2.2. Composition of the char used in this case is included in Table 16. For these combustion/calcination experiments the carbonated CO_2 sorbent collected from these SEG tests using lime #2 as CO_2 sorbent was used. The composition of this carbonated CO_2 sorbent is indicated in Table 17. According to this composition, the $CaCO_3$ content of the carbonated CO_2 sorbent can be calculated, resulting in 0.24 mol_{CaCO3}/mol_{Ca}.

Table 16 Proximate and ultimate analysis of the grape seeds char used as fuel for the combustion/calcination tests in the BFBR at ICB-CSIC

%wt.	**PROXIMATE ANALYSIS**
% moisture	4.4
% ash	22.7
% volatile matter	10.1
% fixed carbon	62.8
	ULTIMATE ANALYSIS
% C	70.5
% H*	1.2
% N	0.96
% S	0.06

Table 17 Mass composition of the carbonated CO_2 sorbent used for the combustion/calcination tests in the BFBR at ICB-CSIC using grape seeds char as fuel

%wt.	
CaO	56.92
$CaCO_3$	31.37
CaS	0.18
C (char)	8.34

Flue gas composition, average solid bed temperature and combustion and calcination efficiencies obtained for these combustion/calcination experiments are compiled in Table 18. Char combustion efficiencies above 96 % are fulfilled in these experiments, increasing above 98 % when solid bed temperature goes beyond 850 ºC. Char fraction of the solids leaving the reactor through the overflow resulted around 1.2-1.4 % for the experiment with the lowest combustion efficiency of 96.6 % and it was less than 0.6 % for larger combustion efficiencies. Calcination efficiencies reached for these experiments resulted above 93.5 %, which makes the $CaCO_3$ content of the sorbent particles at the BFB reactor outlet to be around 0.02 mol_{CaCO3}/mol_{Ca}. As it can be appreciated from the flue gas composition, SO_2 was not detected in the flue gas since it has been retained completely by the CaO as $CaSO_4$, accounting between 0.4 and 1.1 %wt. in the outlet solids.

NOx (mostly NO_2) compounds measured in the flue gas come basically from the N contained in the fuel since the combustion temperatures reached were not as high as for favoring NOx formation from N_2 contained in the air. This NOx formation mechanism is dependent on the local fuel/air ratio as the volatile N-based compounds released during combustion could be oxidized into NOx if there is O_2 present or be reduced to N_2 when the O_2 content is limited. According to this behavior, it can be observed that the lowest NOx content of 792 ppm corresponded to the lowest air ratio used, whereas the largest amount of 1011 ppm was reached when increasing the air ratio and the lowest solid bed temperature was fulfilled. As appreciated in this table, the maximum NOx content was not reached operating with the maximum air ratio used (i.e. 1.7) as expected. The heterogeneity of the composition of the char used as fuel (since it was collected from different SEG experiments) can be the reason of this mismatch since the stoichiometric air flow rate considered for calculating the air ratio could have changed, as it was calculated using the composition in Table 16.

Table 18 Results obtained for the combustion/calcination tests using grape seeds char as fuel

No. experiment	**1**	**2**	**3**	**4**
Char/sorbent mass ratio [-]	*0.3*	*0.2*	*0.2*	*0.2*
Air ratio [-]	*1.3*	*1.3*	*1.5*	*1.7*
Average solid bed temperature [ºC]	894	856	841	848
Flue gas flow rate [Nm^3/min]	0.185	0.190	0.196	0.219
Flue gas composition (dry gas)				
O_2 [%vol]	3.76	3.51	2.29	4.19
CO [%vol.]	0.14	0.03	0.15	0.04
CO_2 [%vol.]	18.97	22.37	24.03	21.71
H_2 [%vol.]	0.03	0.00	0.01	0.01
N_2 [%vol.]	77.10	74.08	73.51	74.05
NOx [ppm]	868	792	1011	820
SO_2 [ppm]	0.0	0.0	0.00	0
Char conversion [%]	98.9	98.9	96.6	98.2
Calcination efficiency [%]	93.5	94.1	93.4	94.7

Aromatic emissions were measured for experiments No.1-3 at different conditions of char/sorbent and air ratio, which resulted in three different temperatures (841, 856 and 894 ºC). Results obtained for these combustion/calcination tests have been depicted on Figure 60. The same compounds that the ones determined in the experimental section 1.2.2.4 for the SEG experiments were analyzed. However, benzene, toluene and xylenes were not detected and most of the compounds determined corresponded to polycyclic aromatic hydrocarbons (PAHs) and water soluble compounds like phenol and phenol, 4-methyl. A maximum emission was found at the intermediate temperature (856 ºC) compared to the other temperatures of 841 and 894 ºC. Taking into account the main factors affecting the PAHs emissions in a fluidized bed combustion reactor, not only the combustion conditions and the feedstock influence these emissions but also the pyrolytic reactions between the radicals emitted and formed at the top of the combustion reactor [21]. On the one hand, the higher the combustion temperature, the higher the radicals emitted, the higher the outlet flow and the lower the residence time. On the other hand, the main pyrolytic reactions will take place at the top of the reactor where the temperature will be lower than the bed combustion temperature. This could explain that at the lowest temperature (841 ºC) and the highest temperature (894 ºC) with the highest flow speed, the total emissions are minimum. This trend was already reported for coal combustion in a fluidized bed reactor at different combustion temperatures [21].

Figure 60 (right) compares the emissions obtained for these three experiments as a function of the compounds emitted by rings number. Firstly, it is observed that independently of the solid bed temperature, the 3-rings compounds were the major pollutants emitted (42-48 %). One-ring compounds, associated with water soluble compounds like phenol and phenol, 4-methyl-, followed a decreasing trend with the solid bed temperature whereas 2-rings compounds (naphthalene) increased with the solid bed temperature. 3 and 4-rings compounds showed a maximum at 856 ºC as well as 5 and 6-rings compounds, although for these last ones the maximum was not so remarkable. The decreasing trend of 1-ring compounds with the temperature increase could be explained with the nature of the combustion char (grape seeds). Lignin is one of the components of this biomass and at higher temperatures, the water soluble compounds (1-ring) could breakdown into lighter compounds which would overcome recombination to form heavier aromatic compounds. In addition, as mentioned previously, the highest outlet flow and the highest amount of radicals emitted in addition to the increase of temperature will also influence on the PAHs emissions. Moreover, the increase of 2-rings compounds, naphthalene, with the increase of combustion temperature due to the decomposition of larger aromatic components could also corroborate this assumption.

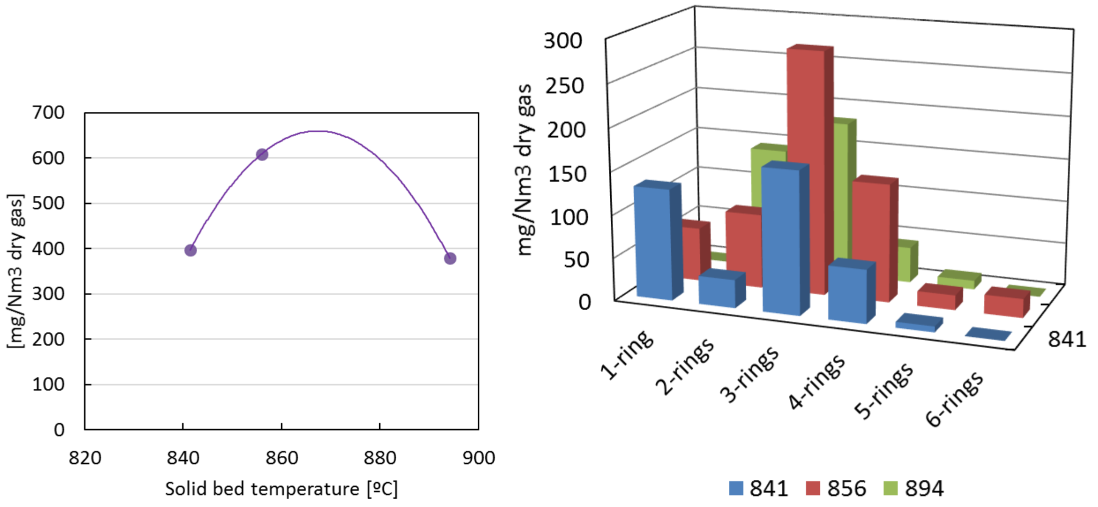

Figure 60 (left) collected tar (g/Nm3 dry gas) and (right) PAHs composition by rings number as a function of the solid bed temperature for the combustion/calcination tests with grape seeds char

Regarding the emissions of individual compounds, phenanthrene, napthalene and phenol were the major compounds emitted. Phenanthrene indicated a similar behaviour to the total compounds emitted with a maximum at the intermediate temperature. Other compounds following the same trend were acenapthylene, acenapthene, fluorene, anthracene, fluoranthene, pyrene, benzo(a)anthracene, chrysene, benzo(b)fluoranthene and benzo(a)pyrene. Phenol followed a decreasing trend with the increase of temperature whereas napthalene increased with the temperature (Figure 61).

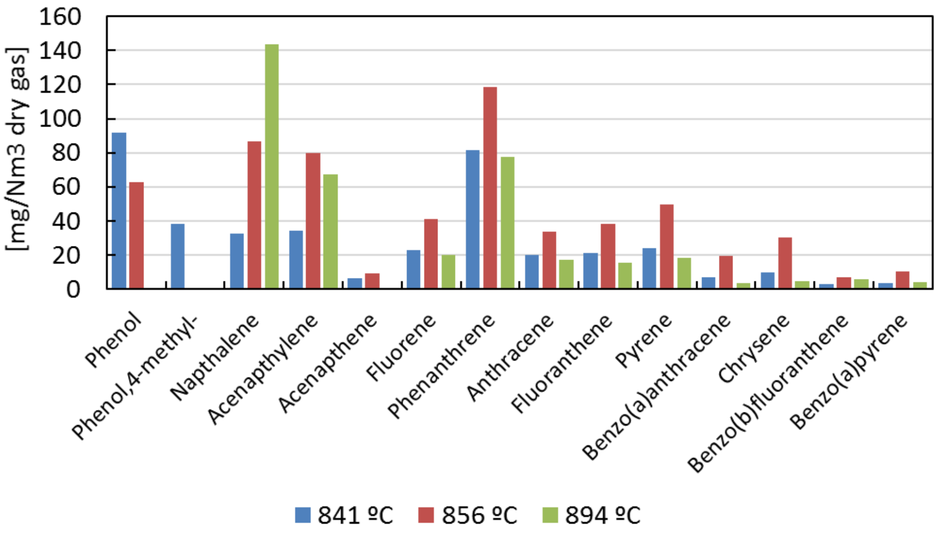

Figure 61 Major compounds as a function of the solid bed temperature for the combustion/calcination tests with grape seeds char

1.3.2 ECOH pellets char

The combustion/calcination stage using unconverted ECOH pellets char as fuel has been also studied. In this case, the char/carbonated sorbent mass ratio has been kept constant at 0.5 (i.e. the char and carbonated sorbent mass flows were kept constant at 2.5 and 5.1 kg/h, respectively) and the air excess has been modified as indicated in the experimental matrix shown in Table 19. The solid bed temperature reached in each case is indicated in this table, increasing as the air excess is decreased.

Table 19 Experimental matrix of the combustion/calcination tests performed with char from ECOH pellets in the BFBR at ICB-CSIC

Char/sorbent mass ratio	Air ratio = 1.9	Air ratio = 1.6
0.5	839ºC	847ºC

Similarly to the combustion/calcination experiments with grape seeds char, the char used in these tests corresponds to the coarse fraction of the particles collected from the overflow in the SEG tests with ECOH pellets as a fuel explained in section 1.2.3. Composition of the char used in this case is included in Table 20. For these experiments, the carbonated CO_2 sorbent collected from these SEG tests was also used. The composition of this carbonated CO_2 sorbent is indicated in Table 21. According to this composition, the $CaCO_3$ content of the carbonated CO_2 sorbent can be calculated, resulting in 0.23 mol_{CaCO3}/mol_{Ca}.

Table 20 Proximate and ultimate analysis of the ECOH pellets char used as fuel for the combustion/calcination tests in the BFBR at ICB-CSIC

%wt.	**PROXIMATE ANALYSIS**
% moisture	2.18
% ash	61.39
% volatile matter	14.26
% fixed carbon	22.17
	ULTIMATE ANALYSIS
% C	70.5
% H*	1.2
% N	0.96
% S	0.06

Table 21 Mass composition of the carbonated CO_2 sorbent used for the combustion/calcination tests in the BFBR at ICB-CSIC using ECOH pellets char as fuel

%wt.	
CaO	60.1
$CaCO_3$	31.6
CaS	0.20
C (char)	7.50

Flue gas composition, average solid bed temperature and combustion and calcination efficiencies obtained for these combustion/calcination experiments are compiled in Table 22. Char combustion efficiencies vary exclusively with the solid bed temperature, increasing from 95.5 to 96.1 % when the temperature rises from 839 ºC to 847 ºC. Both conversion values are anyway high, but slightly lower than the conversion values calculated for the grape seeds char in previous section. Figure 62 represents the char combustion efficiencies calculated for both chars as a function of the solid bed temperature. As it is noticed in this figure, char combustion efficiency for the ECOH pellet char falls below the conversion values obtained for the grape seeds char for a given temperature and for a lower air excess ratio (i.e. lower O_2 content in the flue gas).

Table 22 Results obtained for the combustion/calcination tests using ECOH pellets char as fuel

No. experiment	**1**	**2**
Char/sorbent mass ratio [-]	*0.5*	*0.5*
Air ratio [-]	*1.9*	*1.6*
Average solid bed temperature [ºC]	839	847
Flue gas flow rate [Nm^3/min]	0.185	0.162
Flue gas composition (dry gas)		
O_2 [%vol.]	6.28	3.80
CO [%vol.]	0.08	0.05
CO_2 [%vol.]	16.91	20.30
H_2 [%vol.]	0.10	0.06
N_2 [%vol.]	76.63	75.79
NOx [ppm]	734	830
SO_2 [ppm]	0	0
Char conversion [%]	95.5	96.1
Calcination efficiency [%]	94.1	91.2

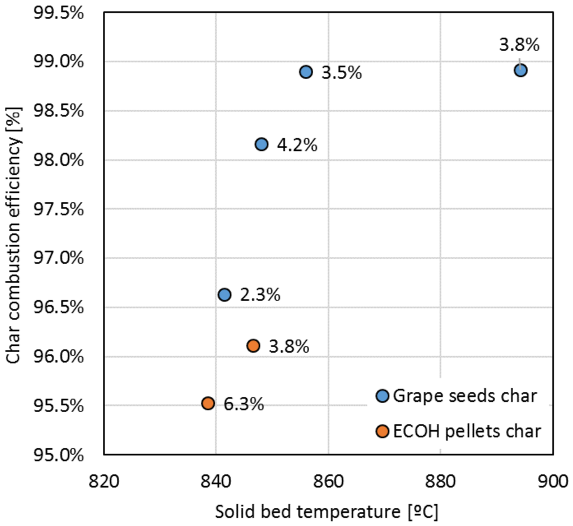

Figure 62 Char combustion efficiencies obtained for the combustion/calcination experiments with grape seeds and ECOH pellets chars as a function of the solid bed temperature. Numbers indicated in the chart correspond to the volume O_2 content in the flue gas

Calcination efficiencies reached for these experiments resulted 91-94 %, which makes the $CaCO_3$ content of the sorbent particles at the BFB reactor outlet to be around 0.02 mol_{CaCO3}/mol_{Ca}. As happened also with grape seeds char SO_2 was not detected in the flue gas since CaO resulting from $CaCO_3$ calcination is reacting with it to form $CaSO_4$, accounting around 1.2 %wt. in the outlet solids. As for NOx emissions, these resulted between 734 and 830 ppm.

Aromatic emissions were measured for experiment No.1 in Table 22, which resulted in a solid bed temperature of 839 ºC. Table 23 shows the results obtained for the PAHs emissions as well as the distribution by ring number and the individual composition. Only the detected compounds are mentioned in this table. The total emissions regarding polyaromatic compounds were of 427.3

mg/Nm^3 dry gas where the major compounds were phenanthrene (32 %), acenapthylene (13 %), phenol (11 %) and naphthalene (10 %) associated to 3, 3, 1 and 2-rings compounds, respectively.
In order to analyze the influence of the feeding material (i.e. grape seeds char or ECOH pellets char) on PAHs emissions, experiment No.1 with ECOH pellets char is compared to experiment No.3 performed with grape seeds char since both resulted in similar solid bed temperature (839-841 ºC), although the ratio char/sorbent was different. The total PAHs emissions with grape seeds char were 397.1 mg/Nm^3 dry gas, slightly inferior to the one obtained with ECOH char combustion. However, results expressed as mg/kg char showed that for the ECOH char the emissions were 1892.4 mg/kg char versus 3761.2 mg/kg char when the grape seeds char was burned. However, these differences should be related to the air excess used in these two experiments, which was larger for the ECOH char combustion than for grape seeds char combustion, improving in this was the combustion efficiency of these PAHs. The major compound emitted for the grape seeds char combustion was phenol (23%), followed by phenanthrene (21%), phenol, 4-methyl- (10%), acenapthylene (9%) and naphthalene (8%). Therefore, the nature of feedstock used is quite important in the compounds emitted during char combustion. Grape seeds, in addition to cellulose and hemicellulose, were also composed by lignin, which could release phenol and phenol, 4-methyl-. In the case of the ECOH char, these compounds only constituted the 11% of the total emitted PAHs, and it was only attributed to phenol.

Table 23 Individual compounds, total emitted and distribution by ring number for the ECOH char combustion [mg/Nm^3 dry gas] for experiment No.1 in Table 22

COMPOUND [mg/m^{3}N dry gas]	**COMB_D**
Phenol	47.2
Napthalene	44.1
Acenapthylene	56.9
Acenapthene	12.2
Fluorene	38.3
Phenanthrene	137.3
Anthracene	28.2
Fluoranthene	21.2
Pyrene	25.5
Benzo(a)anthracene	5.3
Chrysene	6.9
Benzo(b)fluoranthene	1.5
Benzo(a)pyrene	2.7
TOTAL [mg/Nm^{3}dry gas]	427.3
TOTAL [mg/Kg char]	1892.4
Ring number compounds [mg/m^{3}N dry gas]	
1-ring compounds	47.3
2-rings compounds	44.1
3-rings compounds	272.9
4-rings compounds	59.0
5-rings compounds	4.2
6-rings compounds	0.00

2 SEG validation in a lab-scale fluidized bed facility (USTUTT)

Pre-testing of fuels and sorbent prior to their use at the 200 kW$_{th}$ pilot scale facility have been conducted at the electrically heated 20 kW$_{th}$ dual fluidized bed (DFB) facility at USTUTT. The tests aimed mainly at the investigation of bed agglomeration phenomena as well as on dosability of fuels and sorbents under different operation conditions. This pre-testing was necessary for reducing the risk of shut down and damages at the pilot scale facility when using novel materials and operation conditions. Experiments have been conducted with wood pellets and pellets out of waste derived fuel that have been provided by Econward (ECO-pellets). Limestone with a nominal particle size distribution between 100 and 300 µm has been used as active bed material.

Experiments have been conducted under dual fluidized bed conditions as well as under semi-batch conditions for simplification of the experiments to reduce the required time and costs.

2.1 Description of the electrically heated 20 kW$_{th}$ dual fluidized bed facility at USTUTT

The facility consists of a bubbling and a circulating fluidized bed reactor that are connected to each other by loop seals (Figure 63). It is also possible to conduct semi-batch experiments by only using one of the reactors.
Tests with ECOH-pellets prior to the experiments in the pilot scale facility have been conducted in semi-batch mode by using the bubbling fluidized bed reactor as gasifier.

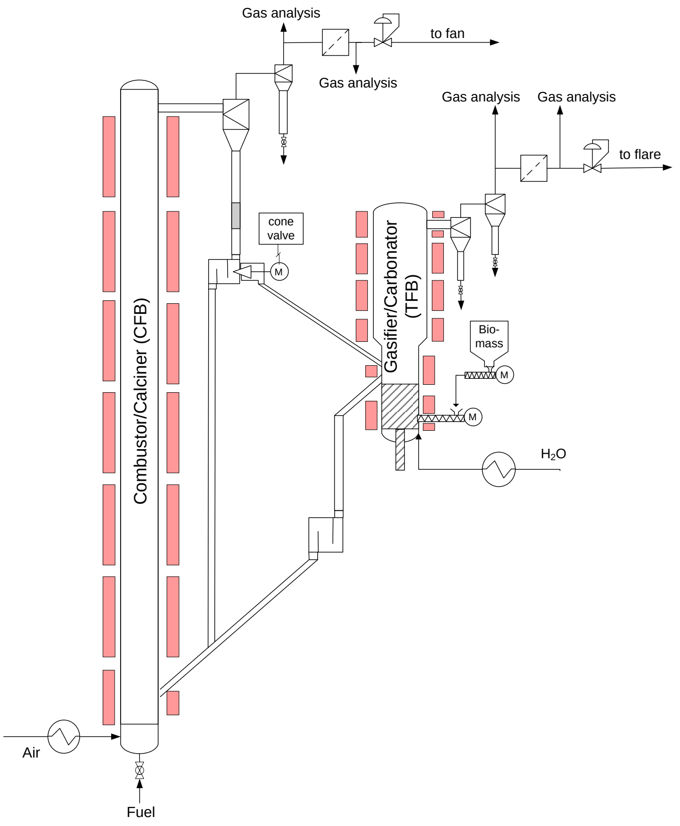

Figure 63. Scheme of the Gasifier of the 20 kW$_{th}$ test facility at USTUTT

Fuel is dosed to the gasifier by using a gravimetric dosing system. Steam is produced in a gravimetrically controlled steam generator and fed to the gasifier after passing the gas preheater. The maximum bed height of the gasifier is controlled via overflow, which enables having a constant bed inventory and a constant weight hourly space velocity (WHSV) when keeping the fuel feed constant. A cone valve regulates the mass flow between combustor and gasifier.

Both reactors are equipped with two cyclones and candle filters for reducing the particle concentration in the flue gas and syngas, respectively. The gas flows into both of the reactors as well as into the loop seals are controlled by mass flow controllers and are preheated before entering the respective reactor.

At the facility different gas measurement techniques such as NDIR, thermal conductivity, Micro-GC, standardized wet chemical tar measurement can be implemented before and/ or after the candle filters. Technical details of the facility are summarized in Table 24.

Table 24. Technical data of the 20 kW_{th} dual fluidized bed facility at USTUTT

	Combustor/ Calciner	**Gasifier/ Carbonator**
Reactor height	12.4 m	3.5 m
Reactor diameter	70 mm	150 mm
Fluidization velocity	4 – 6 m/s	0.2 – 1 m/s
Temperature	< 950 °C	< 950 °C
Regime	**CFB**	**BFB**

2.2 Experimental parameters and solids composition

All tests have been conducted with German limestone with a nominal particle size distribution between 100 and 300 µm as CO_2-active bed material. The composition of the limestone is given in Table 25.

Table 25. Chemical composition of the limestone used for the experiments (Limestone analysis is not normalized to 100%)

	x_{CaO}	x_{MgO}	x_{SiO2}	x_{Al2O3}	others	x_{CO2}[1]
	wt%, db					
German limestone	55.1	0.7	0.4	0.1	0.2	43.5

[1] Mass fraction of CO_2 that is released as CO_2 during calcination

Two different fuels have been used during the experiments. Wood pellets with Enplus A1 quality serving as reference fuel and pellets out of waste derived fuel from Econward. The composition of both fuels is shown in Table 26.

Table 26. Composition of ECO-pellets (04/17) used for the experiments and of Wood pellets as reference fuel

	H_u	γ_{H2O}	γ_{ash}	γ_V	γ_{FC}	γ_C	γ_H	γ_N	γ_S	γ_{Cl}
	J/g,ad	wt%,ad	wt%,db	wt%,daf basis						
ECO-pellets (04/17)	11138	1.92	40.5	88.2	11.8	52.8	6.8	2.3	0.4	1.0
Wood pellets	17358	6.0	0.2	82.7	17.3	50.8	6.1	0.2	0.1	0.02

Wood pellets as biomass of relatively high quality serve as reference fuel. They have a very low ash content of only 0.2 wt%,db and only minor contents of N, S, and Cl. In contrast to this, the ash content of the ECO-pellets is very high with a value of 40.5 wt%,db and also the contents of N, S, and Cl are much higher, compared to wood pellets. Due to the differences in the composition of wood pellets and ECO-pellets, it is possible to demonstrate the flexibility of the SEG process regarding fuel composition. The high ash content of the ECO-pellets offers the possibility to demonstrate the suitability of the SEG process also for ash rich biomasses/biogenic residues. This will increase the confidence in respect of fuel flexibility of the SEG/ FLEDGED process. The ECO-pellets have been dried to avoid the formation of mold during storage.

It must be noticed that the ash content of the batch of ECO-pellets (04/17) that has been used for the tests presented in this document was much higher compared to the batches that have been sent to USTUTT for the pilot scale tests later in the project with ash contents between 26 and 33 wt%,db.

2.2.1 DFB experiments with wood pellets

All experiments with wood pellets have been conducted in the 20 kW_{th} DFB facility using the bubbling fluidized bed as gasifier and the circulating fluidized bed reactor as combustor.

The influence of the gasification temperature on the syngas composition has been investigated for temperatures between 636 and 710 °C with a constant S/C molar ratio of 1.5. Gasification temperature has been increased by increasing the electrical heating power of the heating elements. During the experiments, the calcination temperature was kept constant at 896±2 °C.

2.2.2 Semi-batch experiments with pellets from Econward

The experiments with pellets made out of waste derived fuel from Econward have been conducted under semi-batch conditions using the bubbling fluidized bed (BFB) reactor of the 20 kW_{th} DFB facility as gasifier. The limestone was fully calcined prior to the experiments.

Gasification tests with ECO-pellets have been conducted at gasification temperatures between 604 and 754°C. The steam-to-carbon ratio has been kept constant at 1.5 mol_{H2O}/mol_{C}.

2.3 Results and discussion

2.3.1 DFB experiments with wood pellets

In Figure 64 the contents of H_2, CO, CO_2 and CH_4 are plotted for gasification temperatures between 636 and 710 °C. Within this temperature range the H_2 concentration decreases from 80 to 72 $vol\%_{wf}$ while CO_2 and CO concentrations are increasing from 1 to 10 $vol\%_{wf}$ and 5 to 8 $vol\%_{wf}$, respectively. The reason for these trends is the reduced CO_2 capture with higher gasification temperatures due to the $CaCO_3$/CaO equilibrium. The concentration of CH_4 decreases from 12 $vol\%_{wf}$ at 636 °C down to 8 $vol\%_{wf}$ at 710 °C.

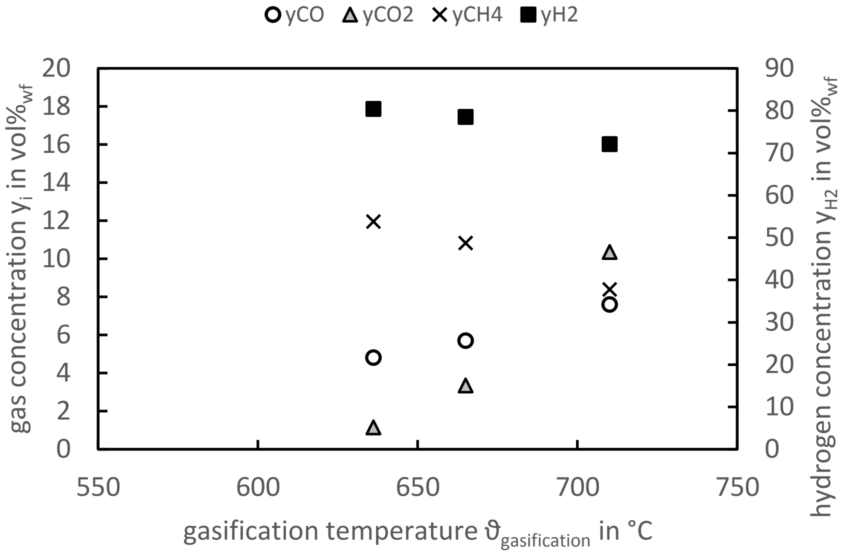

Figure 64. Gas concentrations at gasification temperatures between 636 °C and 710 °C

In Figure 65 the M-modules achieved from experiments in the 20 kW$_{th}$ DFB facility are compared to the results from tests in the 200 kW$_{th}$ DFB at IFK, University of Stuttgart. M-modules are calculated based on syngas compositions obtained from experiments at gasification temperatures between 636 °C and 710 °C in the 20 kW$_{th}$ DFB and between 600 °C and 774 °C in the 200 kW$_{th}$ DFB. During the gasification tests in the 20 kW$_{th}$ DFB, the M-module decreased from 13 at 636 °C down to 4 at 710 °C. The trend of the M-module achieved in the 20 kW$_{th}$ DFB matches the trend of the experimental results in the 200 kW$_{th}$ DFB. This shows that tests in the 20 kW$_{th}$ electrically heated DFB facility that were conducted prior to tests in the 200 kW$_{th}$ DFB system are comparable. It highlights that the facility is perfectly suitable to test difficult fuels prior to 200 kW$_{th}$ pilot scale testing to verify that they can be gasified successfully in the SEG process. The facility allows conducting pretesting of new and challenging fuels in the FLEDGED project, to avoid additional costs and for reducing the risk of a delay of pilot scale activities.

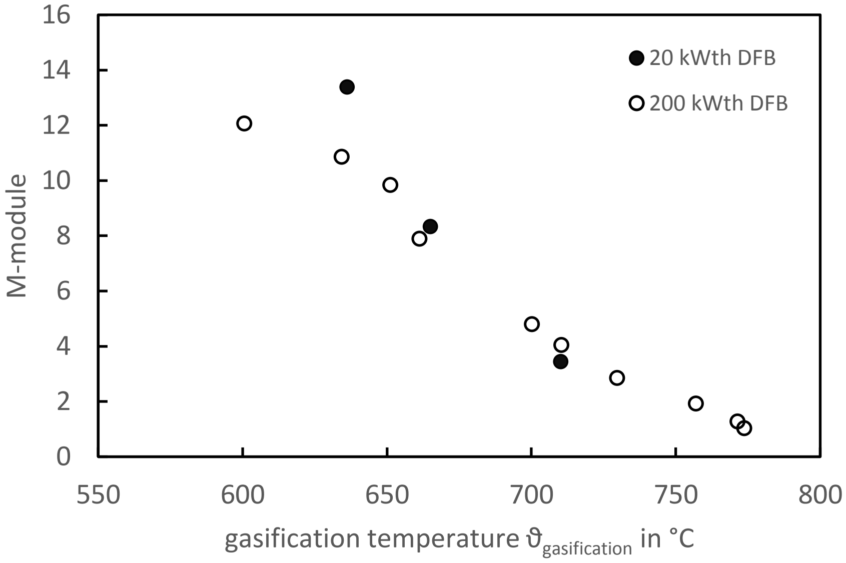

Figure 65: M-module calculated based on syngas compositions obtained with gasification temperatures between 636 °C and 710 °C in the 20 kW$_{th}$ DFB facility and between 600 °C and 774 °C in the 200 kW$_{th}$ DFB facility

2.3.2 Semi-batch experiments with pellets from Econward

During the operation of the BFB gasifier with ECO-pellets no bed agglomeration has been observed and no dosability problems occurred. It has also been possible to operate the facility with ECO-pellets during a whole day without mentionable problems. Therefore it is expected that the ECO-pellets are also suitable for gasification at larger scale.

In Figure 66, the trends of the gasification temperature and the S/C molar ratio are presented for an exemplary experiment. It can be seen that the gasification temperature and the S/C ratio were very stable during the experiment. In this case steady state conditions lasted for about 40 minutes.

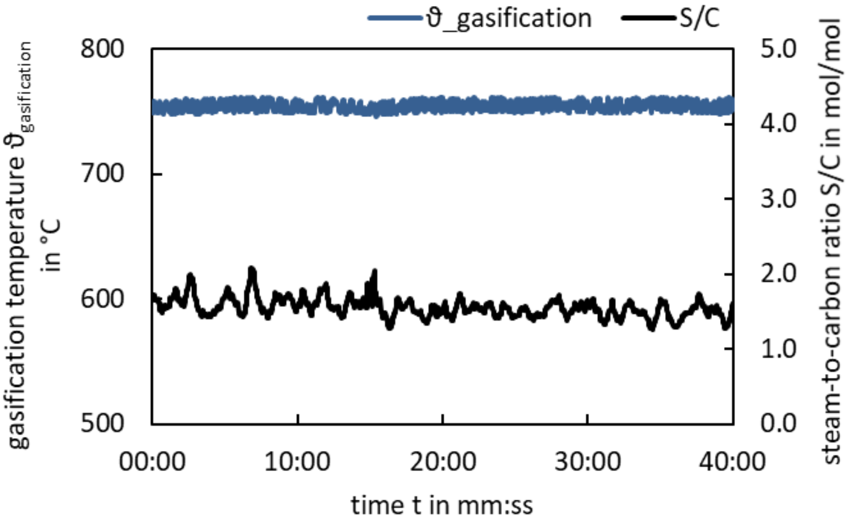

Figure 66 Trends of gasification temperature and S/C-ratio for an exemplary experiment

The respective trends of the H_2, CO, CO_2, CH_4 and C_xH_y contents in the syngas are plotted in Figure 67. The value of C_xH_y is the sum of the concentrations of C_2H_4, C_2H_6, C_3H_6, C_3H_8 and C_4H_{10}. It can be seen that as a result of the stable gasification temperature and S/C ratio also the syngas composition was very stable during the experiment.

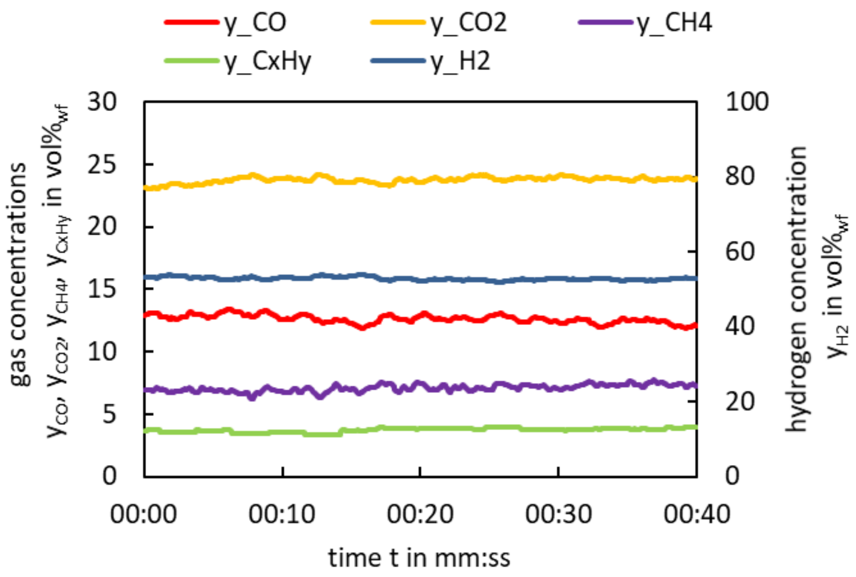

Figure 67 Syngas composition vs. time for an exemplary semi-batch SEG experiment at a gasification temperature of 754°C and a S/C molar ratio of 1.5

Figure 68 shows the syngas composition for gasification temperatures between 604 and 754°C. There is a strong influence of the gasification temperature on the syngas composition. The concentrations of H_2, CO and C_xH_y are almost constant until a gasification temperature of 660°C. Above that temperature the concentrations of H_2 and C_xH_y decrease while the concentration of CO increases. For the H_2 concentration values between 72 and 53 vol%$_{wf}$ were achieved. CO concentration reached values between 2 and 13 vol%$_{wf}$ and C_xH_y concentration decreased from 10 to 4 vol%$_{wf}$ in the investigated temperature range. The CH_4 concentration reaches 13 vol%$_{wf}$ at 604°C and decreases to a value of 7 vol%$_{wf}$ at 754°C. Due to the $CaO/CaCO_3$ equilibrium the CO_2 concentration increases strongly with increasing gasification temperature. The CO_2 concentration increases from 3 vol%$_{wf}$ at 604°C to 24 vol%$_{wf}$ at 754°C.

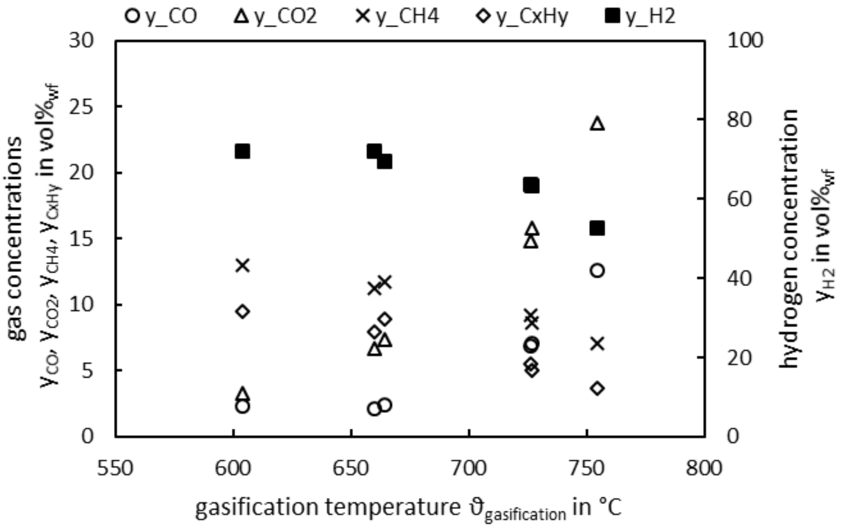

Figure 68 Syngas concentrations at gasification temperatures between 604 and 754°C for a S/C molar ratio of 1.5

The M-module ($M = (y_{H2} - y_{CO2})/(y_{CO} + y_{CO2})$) as well as the y_{CO2}/y_{CO}-ratio were calculated based on the syngas compositions presented in Figure 68. In Figure 69 the M-module and the y_{CO2}/y_{CO}-ratio are plotted versus the gasification temperatures. At 600°C the y_{CO2}/y_{CO}-ratio has a value of 1.5 and increases up to a value of 3.1 at 660°C. Above 660°C the y_{CO2}/y_{CO}-ratio decreases with increasing gasification temperature and reaches a value of 1.9 at 754°C.

At a temperature of 604°C the M-module has a value of 12.3 and decreases with increasing gasification temperature down to 0.8 at 754°C. According to the experimental results a gasification temperature of 727°C is necessary to achieve a M-module of 2 that is optimal for DME synthesis.

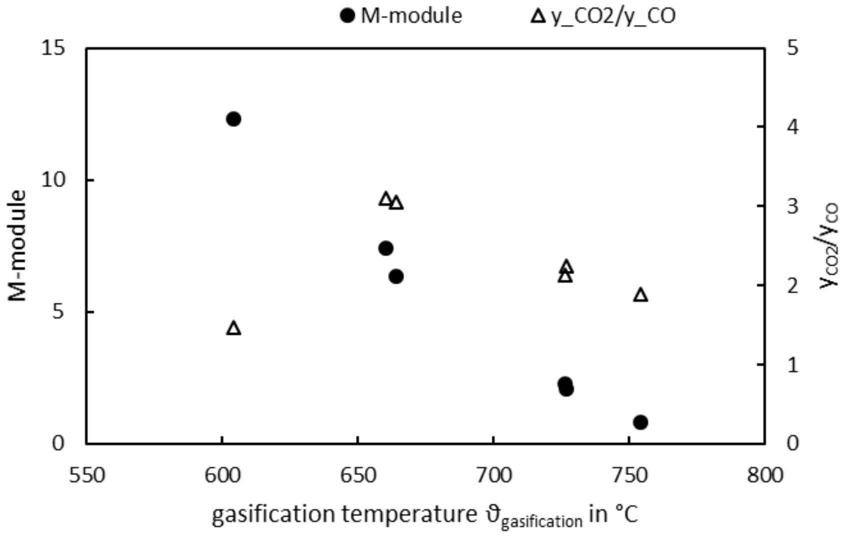

Figure 69 M-module and y_{CO2}/y_{CO}-ratio calculated based on syngas compositions obtained with gasification temperatures between 604 and 754°C for a S/C molar ratio of 1.5

3 Conclusions

In this document, all the results and conclusions obtained in the sorption enhanced gasification (SEG) experiments performed at the 30 kW_{th} BFB reactor at ICB-CSIC and at the 20 kW_{th} DFB facility at USTUTT have been reported.

Concerning the 30 kW_{th} BFB reactor at ICB-CSIC, SEG performance has been evaluated for 6 different biomass feedstocks. Special attention has been paid to study the influence of the main operating variables of this SEG process in the syngas yield and syngas composition as well as in solids conversion, with the aim of determining the suitability of modifying each variable depending on the desired effect.

As for the effect of the different variables, it was studied the influence of the gasification temperature, the steam-to-biomass ratio, the sorbent-to-biomass ratio and the activity of the CO_2 sorbent used. The main outcomes of these analyses have been:

- *Gasification temperature* has a great impact on the gas yield through char conversion, but also affects syngas composition. Depending on the reactivity of the biomass used, this variable would determine the M-module either by limiting the carbonation reaction and/or by improving char gasification reactions. Concerning light hydrocarbons content in the syngas and tar yield, both increase noticeably when reducing the temperature, affecting the gas conditioning for the subsequent synthesis process.
- *The steam-to-biomass (S/C) ratio* does not influence the permanent gas composition (i.e. M-module), but affects the content of light hydrocarbons in the syngas (C_2-C_4) as well as tar yield. When increasing the S/C ratio, the content of C_4 hydrocarbons in the syngas diminishes, increasing the content of C_3H_6, C_3H_8, C_2H_4 and C_2H_6. Moreover, the increase of C_2H_4 in the syngas, which is known to be a precursor of aromatic rings formation, promotes tar formation.
- *The sorbent-to-biomass (CaO/C) ratio* influences mainly the C_3-C_4 hydrocarbons content and the tar yield (due to the catalytic effect of CaO towards tar cracking). Moreover, the CaO/C ratio influences the M-module since its variation affects the amount of CO_2 separated and the solid residence time of char particles, and therefore their conversion. Increasing too much the CaO/C ratio reduces significantly the solid residence time of char particles in the gasifier and their conversion, which could limit the M-module fulfilled.

As for the performance of the different biomasses, the main outcomes of the study performed have been:

- For ECOH feedstocks and wood pellets/chips, char gasification kinetics are sufficiently fast as for not being the limiting factor of the M-module. Therefore, for these biomasses, CO_2 capture will determine the M-module reached. For reducing the M-module, CO_2 capture should be limited by raising the gasification temperature. Comparing these feedstocks, lignocellulosic biomasses (i.e. wood pellets and wood chips) resulted the most reactive and so needed a higher temperature to get the desired M-module around 2 through a limited CO_2 capture ratio by the equilibrium (i.e. around 715-720 ºC for wood-based biomass and higher for ECOH feedstock). Alternatively, CO_2 capture could be limited using a CO_2 sorbent with a lower CO_2 carrying capacity (as lime #1 in this document), which will allow reaching M-modules around 2 at a lower temperatures than using more reactive sorbents.
- Straw resulted in the lowest M-modules reached. For this biomass, reactivity of the char was the limiting factor. Therefore, the M-module of 2 is a compromise between having sufficient char reactivity and limited CaO conversion. As seen during SEG testing with straw (section

1.2.5.2), temperature needed for reaching an M-module was around 700 ºC, slightly lower than for the rest of the biomasses.

Finally, in the 30 kW_{th} BFB reactor at ICB-CSIC combustion/calcination tests have been also performed with the objective of assessing the performance in terms of gas emissions and combustion and calcination efficiencies. Experiments using unconverted char as a fuel from two different biomass feedstocks (i.e. grape seeds and ECOH pellets) have been performed. For each fuel, a parametric study has been carried out, comprising different fuel/sorbent ratios, different air excess and different temperatures. Gas contaminants (i.e. NOx, SO_2, PAHs) were analyzed for the experiments performed, and solid samples were taken for characterization so that calcination and combustion efficiencies could be calculated. For the experiments performed with grape seeds char as a fuel, char combustion efficiencies between 96.6 and 98.9 % were calculated for temperatures ranging from 841 ºC and 894 ºC, respectively. Calcination of the carbonated solids that resulted from the SEG tests was fulfilled with an efficiency above 93 %. Slightly lower char combustion efficiencies were calculated when using ECOH char as fuel, going from 95.5 to 96.1 % at temperatures around 840-850 ºC and different air excess ratios. No SO_2 was detected in the flue gas in any of the combustion/calcination test performed, indicating that CaO resulting from $CaCO_3$ calcination is reacting with it to form $CaSO_4$. $CaSO_4$ content in the outlet solids did not reached values higher than 1.1-1.2 %wt. in any of the experiments. Regarding NOx emissions, they came from the N contained in the fuel since the combustion temperatures reached were not as high as for favoring thermal NOx. Using grape seeds char, the lowest NOx content of 792 ppm corresponded to the lowest air ratio used, whereas the largest amount of 1011 ppm was reached when increasing the air ratio and the lowest solid bed temperature was fulfilled. When using ECOH char, NOx emissions resulted between 734 and 830 ppm for the highest and the lowest, respectively, air excess. Finally, the emission of polycyclic aromatic hydrocarbons (PAHs) was also evaluated for these combustion/calcination tests. For the grape seeds char, for which a broader experimental matrix was performed, a maximum PAHs emission value was found at the intermediate temperature (609 mg/Nm^3 dry gas at 856 ºC) compared to the other temperatures of 841 and 894 ºC (397 and 379 mg/Nm^3 dry gas, respectively). This trend is linked to the combustion conditions and the fuel, and has been already observed in the literature for coal combustion in a fluidized bed reactor at different combustion temperatures.

Concerning the experimental work performed in the 20 kW_{th} DFB facility at USTUTT, tests using wood pellets as fuel showed that the process can be operated stably in DFB mode and that the syngas composition can be adjusted flexibly by variation of the gasification temperature for fulfilling the requirements of the downstream DME synthesis process. Results achieved during the tests in the 20 kW_{th} electrically heated DFB facility are comparable to the results from first tests in the not electrically heated 200 kW_{th} pilot scale facility. This leads to the conclusion that the 20 kW_{th} facility is suitable for testing difficult novel fuels prior to their use in the 200 kW_{th} facility.

Semi-batch SEG tests have successfully been conducted in the bubbling fluidized bed reactor of the 20 kW_{th} DFB facility at USTUTT using ECOH pellets as biomass. It was possible to operate the facility with ECO-pellets without mentionable problems. During the experiments M-modules between 12.6 and 0.8 were achieved for gasification temperatures between 604 and 754 ºC. This shows that an adjustment of the syngas composition is possible for SEG with ECO-pellets. Due to the outcome of the experiments with ECOH pellets at the 20 kW_{th} facility, it was expected that ECOH pellets are also suitable for gasification at larger scale. In the meantime this has been proven during pilot scale tests with ECOH pellets as fuel.

Finally, in order to validate the results obtained in both gasification facilities, the following table shows the results obtained for two biomass feedstocks tested at ICB-CSIC and USTUTT facilities (i.e. wood chips/pellets and ECOH pellets) under similar conditions of gasifier temperature (i.e. 705-

710 ºC). As appreciated for the woody feedstocks, syngas composition obtained at the ICB-CSIC facility was practically the same concerning permanent gases as in the USTUTT facility operated in dual mode, despite of the differences in the S/C ratio. As for ECOH pellets, this biomass was tested only in semi-batch mode at the 20 kWth DFB facility at USTUTT, which would explain the small differences observed for permanent gas content. Based on this validation table, it can be confirmed that operation under high CaO/C ratios in the BFBR at ICB-CSIC is needed when results obtained in terms of gas composition want to be extrapolated to the performance of a dual fluidized bed system with a high temperature combustor/calciner connected to the gasifier.

Biomass used	*Wood chips (ICB-CSIC) and wood pellets (USTUTT)*		*ECOH pellets*	
Facility	*30 kWth BFBR at ICB-CSIC*	*20 kWth DFB at USTUTT*	*30 kWth BFBR at ICB-CSIC*	*20 kWth at USTUTT (semi-batch)*
Gasifier bed temperature	710ºC	710ºC	707-711ºC	709ºC
S/C ratio	3	1.3	1.3	1.5
Syngas composition [% dry basis and without N_2]				
H_2	72.7-74.3	72.1	60-64	65.1*
CO	8-8.8	7.6	5.4-5.8	5.9*
CO_2	7.6-8.9	10.3	10-11	13.6*
CH_4	6.9-9.3	8.4	11-11.6	9.5*
CxHy	2.1-2.8	No data available	6.9-7.7	5.9*

*extrapolated data (no measurement data at 709 ºC available)

Acknowledgments

This project has received funding from the European Union's Horizon 2020 research and innovation programme under grant agreement No 727600

http://ec.europa.eu

References

[1] Grasa G, Murillo R, Alonso M, Abanades JC. Application of the random pore model to the carbonation cyclic reaction. AIChE J 2009;55:1246–55. doi:10.1002/aic.11746.

[2] Grasa GS, Alonso M, Abanades JC. Sulfation of CaO particles in a carbonation/calcination loop to capture CO2. Ind Eng Chem Res 2008;47:1630–5. doi:10.1021/ie070937+.

[3] Neeft JPA. Rationale for setup of impinger train as used in the technical specification of sampling and analysis of tar and particles in the product gases of biomass gasification. Technical background document. 2005.

[4] Veksha A, Giannis A, Yuan G, Tng J, Chan WP, Chang VWC, et al. Distribution and modeling of tar compounds produced during downdraft gasification of municipal solid waste. Renew Energy 2019;136:1294–303. doi:10.1016/j.renene.2018.09.104.

[5] De Andrés JM, Roche E, Narros A, Rodríguez ME. Characterisation of tar from sewage sludge gasification. Influence of gasifying conditions: Temperature, throughput, steam and use of primary catalysts. Fuel 2016;180:116–26. doi:10.1016/j.fuel.2016.04.012.

[6] Van Paasen SVB, Kiel JHA. Tar formation in a fluidised bed gasifier. Impact of fuel properties and operating conditions. 2004.

[7] Florin NH, Harris AT. Enhanced hydrogen production from biomass with in situ carbon dioxide capture using calcium oxide sorbents. Chem Eng Sci 2008;63:287–316. doi:10.1016/j.ces.2007.09.011.

[8] Schildhauer TJ, Biollaz SMA, editors. Synthetic Natural Gas from Coal, Dry Biomass, and power-to-gas applications. Wiley; 2016.

[9] Barker R. The reversibility of the reaction CaCO3 ⇄ CaO+CO2. J Appl Chem Biotechnol 1973;23:733–42. doi:10.1002/jctb.5020231005.

[10] Tursun Y, Xu S, Wang G, Wang C, Xiao Y. Tar formation during co-gasification of biomass and coal under different gasification condition. J Anal Appl Pyrolysis 2015;111:191–9. doi:10.1016/j.jaap.2014.11.012.

[11] Hernández JJ, Ballesteros R, Aranda G. Characterisation of tars from biomass gasification: Effect of the operating conditions. Energy 2013;50:333–42. doi:10.1016/j.energy.2012.12.005.

[12] Berrueco C, Montané D, Matas Güell B, del Alamo G. Effect of temperature and dolomite on tar formation during gasification of torrefied biomass in a pressurized fluidized bed. Energy 2014;66:849–59. doi:10.1016/j.energy.2013.12.035.

[13] Mayerhofer M, Fendt S, Spliethoff H, Gaderer M. Fluidized bed gasification of biomass - In bed investigation of gas and tar formation. Fuel 2014;117:1248–55. doi:10.1016/j.fuel.2013.06.025.

[14] Kinoshita CM, Wang Y, Zhou J. Tar formation under different biomass gasification conditions. J Anal Appl Pyrolysis 1994;29:169–81. doi:10.1016/0165-2370(94)00796-9.

[15] Zhang Z. Tar Formation and Transformation in Steam Gasification of Biomass in a Dual Fluidised Bed Gasifier. University of Canterbury, 2017.

[16] Hosoya T, Kawamoto H, Saka S. Secondary reactions of lignin-derived primary tar components. J Anal Appl Pyrolysis 2008;83:78–87. doi:10.1016/j.jaap.2008.06.003.

[17] Wang S, Dai G, Yang H, Luo Z. Lignocellulosic biomass pyrolysis mechanism: A state-of-the-art review. Prog Energy Combust Sci 2017;62:33–86. doi:10.1016/j.pecs.2017.05.004.

[18] Collard FX, Blin J. A review on pyrolysis of biomass constituents: Mechanisms and composition of the products obtained from the conversion of cellulose, hemicelluloses and lignin. Renew Sustain Energy Rev 2014;38:594–608. doi:10.1016/j.rser.2014.06.013.

[19] Effendi A, Gerhauser H, Bridgwater A V. Production of renewable phenolic resins by thermochemical conversion of biomass: A review. Renew Sustain Energy Rev 2008;12:2092–116. doi:10.1016/j.rser.2007.04.008.

[20] Amen-Chen C, Pakdel H, Roy C. Production of monomeric phenols by thermochemical conversion of biomass: A review. Bioresour Technol 2001;79:277–99. doi:10.1016/S0960-

8524(00)00180-2.

[21] Mastral AM, Callén M, Murillo R. Assessment of PAH emissions as a function of coal combustion variables. Fuel 1996;75:1533–6. doi:10.1016/0016-2361(96)00120-2.